**Technical University of Crete**

**School of Production Engineering and Management**

# Integrating biomass-based Hybrid Renewable Energy Systems in the food production industry

Diploma Thesis

**Georgios Alexandros Argyropoulos**

Supervisor

Georgios Arampatzis, Associate Professor

**Chania, February 2023**

**Technical University of Crete**

**School of Production Engineering and Management**

# Integrating biomass-based Hybrid Renewable Energy Systems in the food production industry

Diploma Thesis

**Georgios Alexandros Argyropoulos**

Approved by the examination committee:

**Georgios Arampatzis**

Associate Professor

Technical University of Crete

School of Production Engineering and Management _____

**Michail Konsolakis**

Full Professor

Technical University of Crete

School of Production Engineering and Management _____

**Dimitrios Ipsakis**

Assistant Professor

Technical University of Crete

School of Production Engineering and Management

**Chania, February 2023**

# Acknowledgements

First of all, I would like to thank my family for their unending support and patience, and for having faith in me over all these years. I would also like to thank my professors, lecturers, and all of the people at the Technical University of Crete who taught me some very valuable academic and life lessons.

I would like to thank Professor Georgios Arampatzis for agreeing to supervise me during the development of this diploma thesis and for supporting me along the way.

This endeavour would not have been possible without the extreme patience and continuous support of Dr Nikolaos Sifakis to whom I would like to express my deepest gratitude and appreciation. He is an excellent guide and always freely shares his knowledge, tips, and tricks on important matters regarding this scholarly undertaking, in which he is very experienced. But above all, he has shown to be a kind and trustworthy person, and one who I would easily call a friend despite the short period of time for which we have known each other.

I am extremely grateful to all of my friends for the great and unforgettable times we had together in Chania and elsewhere, but also for the invaluable advice they have given me and the endless conversations that certainly gave me a lot of food for thought.

Last, but certainly not least, I would like to thank my girlfriend, who always supported me and put a smile on my face when it was most needed.

## Quote

*“Don't wish it was easier, wish you were better. Don't wish for less problems, wish for more skills. Don't wish for less challenge, wish for more wisdom”.*

*— Jim Rohn*

# Abstract

The energy crisis undergoing across the globe, has struck Europe in 2022, negatively affecting all European citizens' lives. The food industry is arguably of the highest importance for people's wellbeing. Thus, several actions should be taken to mitigate the crisis' impacting the industry. To this end, Hybrid Renewable Energy Systems (HRES) can be used to concurrently reduce energy costs and carbon footprint. This diploma thesis is a techno-economic analysis of the implementation of an HRES to enhance the environmental sustainability and reduce the energy cost for a poultry slaughterhouse and a feed production plant. To achieve these objectives, 15 distinct scenarios are simulated using the Hybrid Optimization of Multiple Energy Resources program and considering the real electrical energy needs of these plants. Three types of locally available biomass fuels are modelled, simulated, and evaluated.

The optimal scenario, based on the Net Present Cost metrics, suggests a 57% reduction in the Levelized Cost of Energy, and a 95% decrease in the carbon footprint, while the net energy purchased from the grid in negative. This noteworthy reduction in the electricity price, contributes towards the affordability of the final products, increasing the competitiveness of the business in the market. At the same time, the almost-eliminated carbon footprint, significantly promotes its sustainable aspect. Finally, the study's outcomes clearly show that the conflict between electricity cost and carbon footprint reduction is eliminated, leading to a sustainable and fruitful infrastructure. More biomass types are suggested to be evaluated, while the integration of energy storage systems could possibly increase the system's reliability and stability.

# Περίληψη

Η ενεργειακή κρίση που πλήττει τον πλανήτη, έπληξε την Ευρώπη το 2022, επηρεάζοντας αρνητικά τη ζωή όλων των Ευρωπαίων πολιτών. Η βιομηχανία τροφίμων είναι αναμφισβήτητα ύψιστης σημασίας για την ευημερία των ανθρώπων. Συνεπώς, θα πρέπει να ληφθούν διάφορα μέτρα για να μετριαστεί ο αντίκτυπος της κρίσης στη βιομηχανία αυτή. Για τον σκοπό αυτό, τα υβριδικά συστήματα ανανεώσιμων πηγών ενέργειας (ΥΣΑΠΕ) μπορούν να χρησιμοποιηθούν για την ταυτόχρονη μείωση του ενεργειακού κόστους και του αποτυπώματος άνθρακα.

Η παρούσα διπλωματική εργασία αποτελεί μια τεχνοοικονομική ανάλυση της εφαρμογής ενός υβριδικού συστήματος ανανεώσιμων πηγών ενέργειας για την ενίσχυση της περιβαλλοντικής βιωσιμότητας και τη μείωση του ενεργειακού κόστους σε ένα σφαγείο πουλερικών και μια μονάδα παραγωγής ζωοτροφών. Για την επίτευξη αυτών των στόχων, προσομοιώνονται 15 διαφορετικά σενάρια με τη χρήση του προγράμματος Hybrid Optimization of Multiple Energy Resources (HOMER PRO) και λαμβάνοντας υπόψη τις πραγματικές ανάγκες των εν λόγω εγκαταστάσεων σε ηλεκτρική ενέργεια. Τρεις τύποι τοπικά-διαθέσιμης βιομάζας μοντελοποιούνται, προσομοιώνονται και αξιολογούνται.

Το βέλτιστο σενάριο, με βάση το Καθαρό Παρόν Κόστος, υποδεικνύει μείωση κατά 57% του Κόστους Ενέργειας και μείωση κατά 95% του αποτυπώματος άνθρακα, ενώ η το ισοζύγιο ενέργειας που αγοράζεται από το δίκτυο είναι αρνητικό. Αυτή η αξιοσημείωτη μείωση της τιμής της ηλεκτρικής ενέργειας, συμβάλλει στην προσιτή τιμή των τελικών προϊόντων, αυξάνοντας την ανταγωνιστικότητα της επιχείρησης στην αγορά. Ταυτόχρονα, το σχεδόν μηδενικό αποτύπωμα άνθρακα, προάγει σημαντικά τη βιώσιμη πτυχή της επιχείρησης. Τέλος, τα αποτελέσματα της μελέτης δείχνουν σαφώς ότι η σύγκρουση μεταξύ του κόστους της ηλεκτρικής ενέργειας και της μείωσης του αποτυπώματος άνθρακα εξαλείφεται, οδηγώντας σε μια βιώσιμη και αποδοτική υποδομή. Προτείνεται η αξιολόγηση περισσότερων τύπων βιομάζας, ενώ η ενσωμάτωση συστημάτων αποθήκευσης ενέργειας θα μπορούσε ενδεχομένως να αυξήσει την αξιοπιστία και τη σταθερότητα του συστήματος.

# Table of Contents

# Table of Figures

# Table of Tables

# 1. Introduction

As concerns about climate change increase and its effects on everyday life are becoming more observable (Arias et al., 2021), people and industry are looking for ways to transition to a more sustainable way of living, conducting business, producing goods, and providing services (Z. Xu et al., 2020) to reduce Green House Gas (GHG) emissions which contribute to global warming (Kweku et al., 2018). This transition towards sustainability is even more important as the population and consequent energy demands grow (Anderson et al., 2020). In 2015, all United Nations Member States adopted the 2030 Agenda for Sustainable Development which has 17 goals. Goal number 13 is explicitly titled “Climate Action” and urges people to take action to combat climate change and its impacts (Z. Xu et al., 2020).

## 1.1. Introductory subjects

### 1.1.1. Climate Change

Scientists have been studying climate change for many decades and have collected increasingly more data regarding its cause and effect on the planet (Kweku et al., 2018). The most important aspect of climate change at the moment is global warming. Through geological studies, it has been found that Earth has been through warming phases and increased GHG concentrations before. However, the rate of global warming that is measured in the past few decades is unprecedented and the reason for that is the GHG emissions caused by human activities, according to Arias et al., 2021.

As a result of manmade activities that have sped up the natural process of climate change on Earth, global weather patterns have become increasingly unpredictable, giving rise to climate change, which has been gaining traction in recent years. This fast development has negative effects and upsets entire ecosystems, which have repercussions for human well-being. When compared to pre-industrial times, ambient temperatures rose by 1$^{o}$C globally in 2015 as a result of greenhouse gas emissions. By 2027, there is now a nearly 50% likelihood that temperatures will be higher than 1.5 °C. (Khandelwal et al., 2022)

While climate change is seen as a long-term change in climate, climate variability is the variation in weather patterns that occur over a short period of time at a particular region. (Kolawole et al., 2016) It should be highlighted that increased frequency and intensity of climatic extremes, which are characteristics that define climate variability, are generally accepted to be a result of climate change (Kandji et al., 2006).

Reduced health, changes in food availability and price, decreased labour, eroding cultural values, and social isolation are just a few examples of the social, cultural, and economic concerns brought on by climate change and variability (Sowah et al., 2020).

### 1.1.2. Energy Poverty

With the price of electricity rising rapidly over the last year in Europe (Figure 1) and around the globe, due to various causes, businesses and households are struggling to make ends meet, and thus for the first time since the International Energy Agency

(IEA) started tracking it, the total number of people worldwide without electricity access has started to rise (*World Energy Outlook 2022 – Analysis - IEA*, 2022).

According to (Pye et al., 2017), energy poverty is defined as a situation where individuals are not able to adequately heat their homes at affordable cost, as a result of rising energy prices, recessionary impacts on national and regional economies, and poor energy-efficient homes. According to this definition, microgrids that integrate renewable energy sources could provide energy independence and security, alleviating energy poverty (Akbari et al., 2022) and at the same time reduce overall $CO_2$ emissions substantially.

Universal access to energy resources is a problem in many developing nations. The bulk of the people in developing nations may not have easy access to electricity, which causes them to rely more on solid fuels, which not only harm the environment but also pose health risks. Additionally, people may not have enough money, which might make it more difficult for them to obtain modern energy sources.

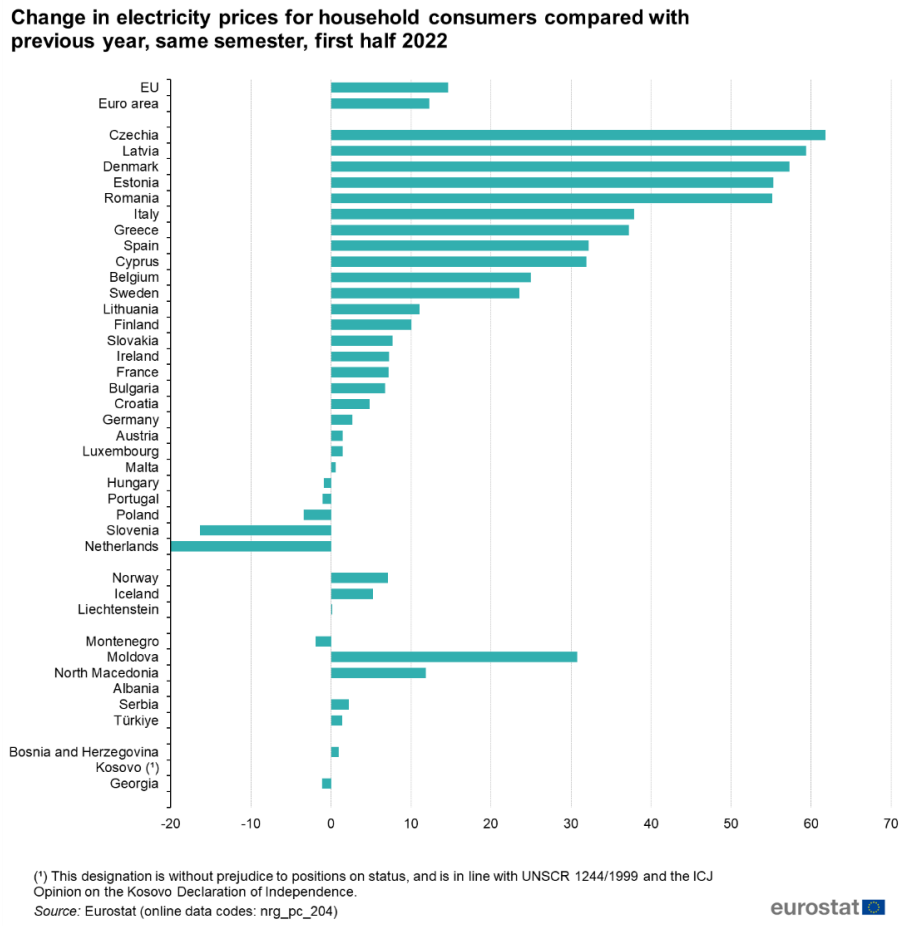


Figure 1: Change in electricity prices for household consumers compared with the previous year, same semester, first half of 2022

### 1.1.3. Sustainable development

In 1987, the World Commission on Environment and Development issued a report titled “Our Common Future” which defined Sustainable Development as “development that meets the needs of the present without compromising the ability of future

generations to meet their own needs". Although there are many ways to interpret the idea of sustainable development, at its core it refers to a method of growth that seeks to strike a balance between various, frequently incompatible needs and an awareness of the economic, environmental, and social constraints that our society is subject to.

In 2015 all United Nations (UN) member states, adopted the "2030 Agenda for sustainable development", which according to the UN, "provides a shared blueprint for peace and prosperity for people and the planet, now and into the future". At the core of this agenda are the 17 Sustainable Development Goals (SDGs). These goals build on decades of work by countries and the UN including but not limited to the Earth Summit in Rio de Janeiro, Brazil, in June 1992, Millennium Summit in September 2000 at UN Headquarters in New York, the Johannesburg Declaration on Sustainable Development and the Plan of Implementation, adopted at the World Summit on Sustainable Development in South Africa in 2002 and the 30-member Open Working Group to develop a proposal on the SDGs which was set up by the General Assembly in 2013 (Figure 2). (THE 17 GOALS | Sustainable Development).

In these 17 goals there is goal number 7 and 13 which are titled "Affordable and Clean Energy, ensure access to affordable, reliable, sustainable and modern energy for all" and "Climate Action, take urgent action to combat climate change and its impacts" respectively. These are the two goals this thesis will be focused around. However, because most of the 17 goals are linked to a certain degree, this thesis also contributes towards goal number 8 through the creation of employment opportunities, goal number 9 through the fostering of innovation and promotion of sustainability in industrialization, goal number 12 because of the improved sustainability of the production plants which will be the case studies of this thesis; and finally, goal number 15 through the protection of terrestrial ecosystems.


Figure 2: The UN 17 Sustainable Development Goals (SDGs) in the 2030 Agenda for Sustainable Development

### 1.1.4. Energy crisis – War – Energy independence

During the COVID-19 pandemic, oil prices fell dramatically due to several factors. One is the low demand for travelling and cargo shipments which was caused by many governments around the world enforcing lockdowns that forbade people from travelling abroad and often also locally. Another was the expectations the industry had about the stock market volatility; and finally, of critical importance was the Russia-Saudi Arabia oil price war combined with their guesswork about oil futures. These factors resulted in a remarkable event that occurred which was that crude oil prices dropped below zero in April 2020. Essentially, producers who did not have enough storage had to pay buyers as much as $37.63 per barrel to take their oil. (Le et al., 2021; *Too Much Oil: How a Barrel Came to Be Worth Less Than Nothing - The New York Times*, 2020)

However, towards the end of 2021, energy prices in Europe were on the rise again and soon surpassed the pre-COVID prices, in large part due to the Russian invasion of Ukraine that disrupted mostly natural gas imports from Russia to Europe, which is used for a large percentage of electricity production in the continent (*World Energy Outlook 2022 – Analysis - IEA*, 2022). This steep rise in electricity and fuel prices has caused social and economic turmoil that prompted a political response. In March 2022, the IEA proposed a 10-Point plan to reduce the European Union's reliance on Russian natural gas (IEA, 2022). European leaders have actively tried to reduce their countries' dependence on Russian natural gas (*EU Imports of Energy Products - Recent Developments - Statistics Explained*, 2022). However, this has been a slow process due to the large investments needed to transition to other, more sustainable, and independent energy sources. (*World Energy Outlook 2022 – Analysis - IEA*, 2022)

## 1.2. The agri-food sector

The agri-food sector consists of two big sectors in the economy. The first one is the agriculture sector which is the source of raw materials from plants and animals. The second one is the food sector which is the greatest recipient of products from the agriculture sector including crops and cattle and is responsible for their processing and distribution (Karwacka et al., 2020). Both sectors are considerable contributors to GHG emissions worldwide with an average percentage of 34% of total emissions globally (Crippa et al., 2021).

### 1.2.1. Energy consumption in the food industry

The global food industry consumes on average 200 EJ annually (FAO, 2017). The distribution of these demands for various production steps and countries can be seen in Figure 3.

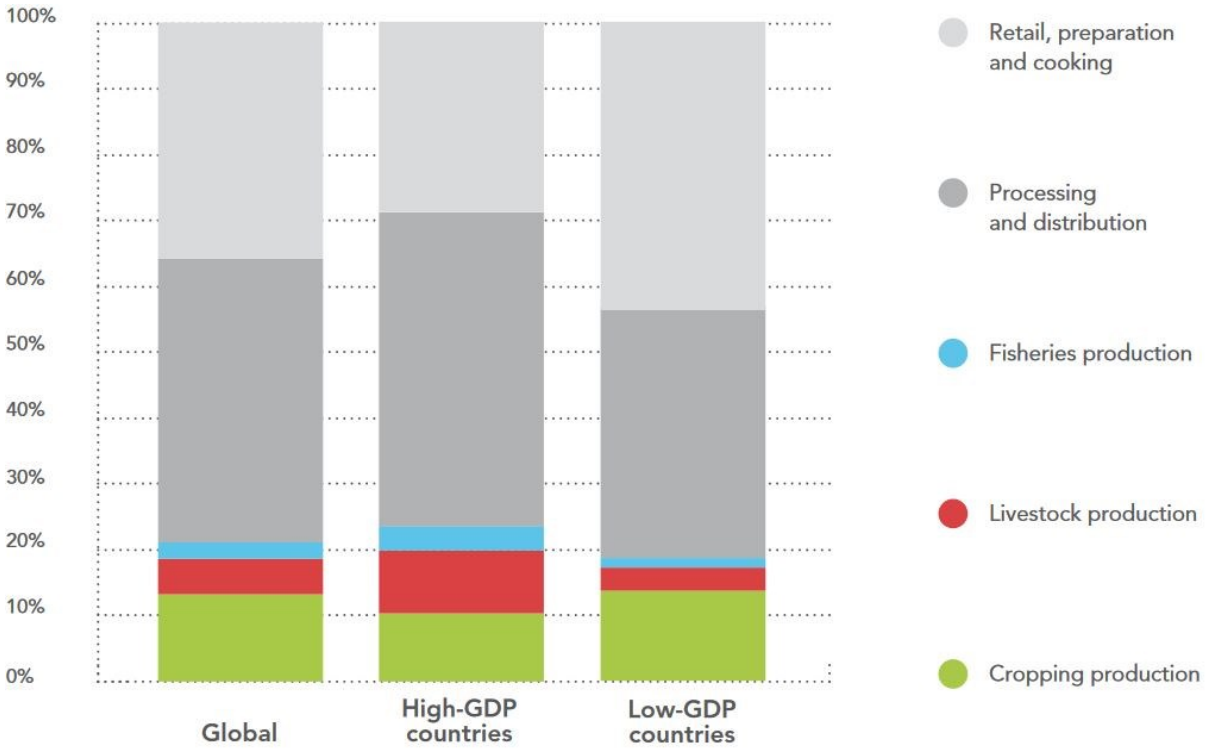


Figure 3: Indicative shares of final energy consumption for the food sector for high- and low-GDP countries

These demands are expected to rise further while the population grows, and poverty is eradicated. The reason for the connection between poverty eradication and rising energy demands in the food industry is the fact that first as people get wealthier, they tend to eat more meat which has a more energy-intensive production procedure (Bereżnicka & Pawlonka, 2018). Thermal energy is produced through electricity, the burning of fossil fuels, and the utilization of renewable resources like biomass.

Fossil fuels used in the food industry include mostly natural gas, diesel, and coal. According to the Department for Business, Energy and Industrial Strategy (2018), in the United Kingdom's food manufacturing sector, natural gas comprised 58%, while diesel and coal represented 6% of total consumed energy in 2017 (Department for

Business Energy and Industrial Strategy, 2018). This high reliance on fossil fuels for energy can have adverse effects on food security in times of fuel price spikes because this spike is directly seen in food prices, making it harder for low-income households to get the necessary food supplies (Taghizadeh-Hesary et al., 2019).

Biomass is a very diverse resource. The particular kind of biomass used, heavily depends on what is locally available. Transporting biomass over long distances makes its use rapidly uneconomical in large part due to its low energy density which is in the range of 1.4 to 10GJ/$m^3$ (Guerrero-Lemus & Martinez-Duart, 2012) when compared to diesel (33.7GJ/$m^3$). Diversifying aspects of utilizing biomass also include the different conversion and upgrading procedures that can be performed to improve characteristics such as particulate matter emissions, GHG emissions, and efficiency.

Other renewable heat sources also include solar collectors and geothermal energy which will be discussed further in this thesis.

### 1.2.2. Environmental concerns and objectives regarding the Green House Gas (GHG) emissions of the food sector

The energy demands, however, are not the only source of GHG emissions in the food industry. Methane is a GHG that is second in importance after $CO_2$ concerning its contribution to climate change. It has a 28 times greater global warming potential over a 100-year timescale and 84 times on a 20-year timescale when compared to $CO_2$ (*Methane Emissions*, 2022). Agricultural and food processing waste emits large amounts of methane when it is not treated properly. All organic matter that is left to decompose on fields or in landfills creates GHG emissions. Gases produced in anaerobic digestion tanks of sewage treatment plants that are not captured and utilized, also contribute to the greenhouse effect mostly through the emission of Methane ($CH_4$).

Meat production has been at the center of environmental concerns regarding the food sector due to its higher GHG emissions per kilo of produce. Total emissions from livestock globally amount to 14.7 Gigatonnes of $CO_2$ equivalent annually, which represents 28.1% of all anthropogenic GHG emissions according to Poore & Nemecek.

### 1.2.3. Efforts toward meeting environmental objectives in the food sector

The food manufacturing sector has already made significant changes to meet long-term reduction goals on energy and water use in response to environmental policies and growing social concerns (e.g. fuel switching, investing in new, energy-efficient equipment and technologies that have a low carbon footprint). Initiatives like the "Ambition 2025" pushed by the UK Food and Drink Federation have reduced $CO_2$ emissions from food production by 58% and water consumption by 39.4% in 2021 from the baseline of 1990.

Despite making up only about 16% of consumer-packaged goods products and generally being more expensive, the Sustainable Market Share Index published by New York University's Stern School of Business estimates that products marketed as sustainable are responsible for about 55% of the growth in consumer-packaged goods (CPG) from 2015 to 2019.

In Figure 4 it can be seen that the growth of sustainability-marketed products was 7.1 times faster than conventionally-marketed products, and 3.8 times faster than the overall CPG market.

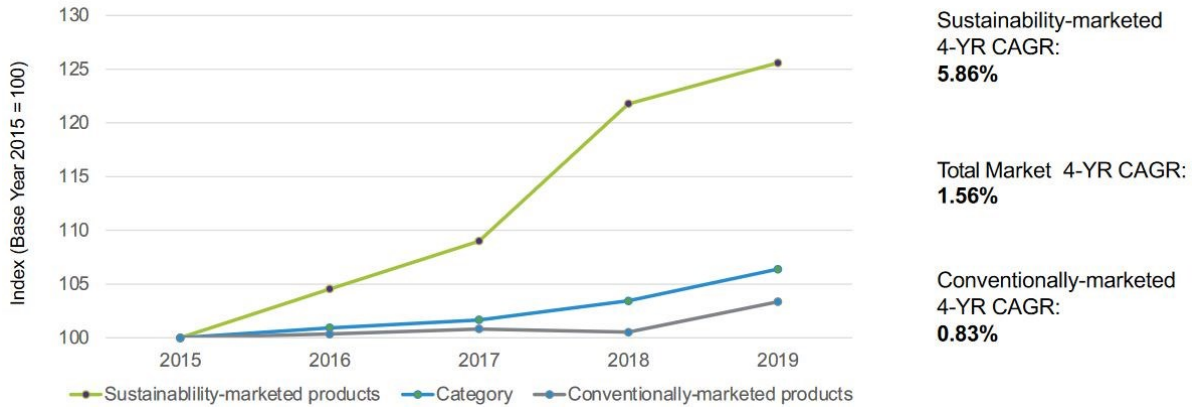


Figure 4: Sustainability-marketed products growth compared to conventionally-marketed products and the CPG market

### 1.2.4. Energy-demanding food sector industries

The food sector includes various types of industries with very different energy demands. Because of these big differences, it is worth analysing them and focusing emission reduction efforts on those industries with the highest demand.

One of the food industry's most energy-intensive subsectors is dairy processing (Briam et al., 2015). Concentrating raw milk and varied degrees of solid separation are common manufacturing processes for many dairy products. Thermal energy is often utilized for cleaning, evaporation, and pasteurization while electricity is typically used for driving pumps, refrigeration of products, separation, and control (T. Xu & Flapper, 2011).

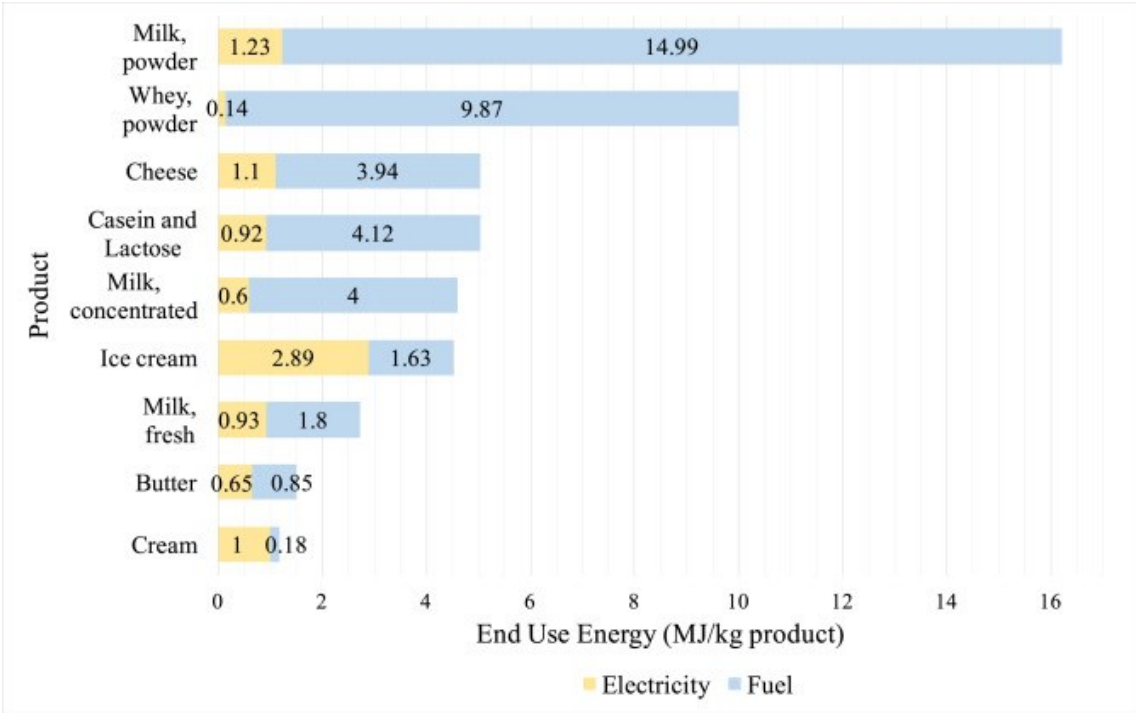


Figure 5: Average final electricity and fuel energy consumed to produce dairy products (Ladha-Sabur et al., 2019)

According to Ramírez et al., (2006), several meat industries use processes that consume significant amounts of power and fuels. For example, poultry slaughter requires more energy than other meats because of the removal of hair and feathers as well as singeing activities. The amount of energy used in slaughterhouses has increased due to a rise in the usage of automated equipment, hot water for cleaning, and temperature control.

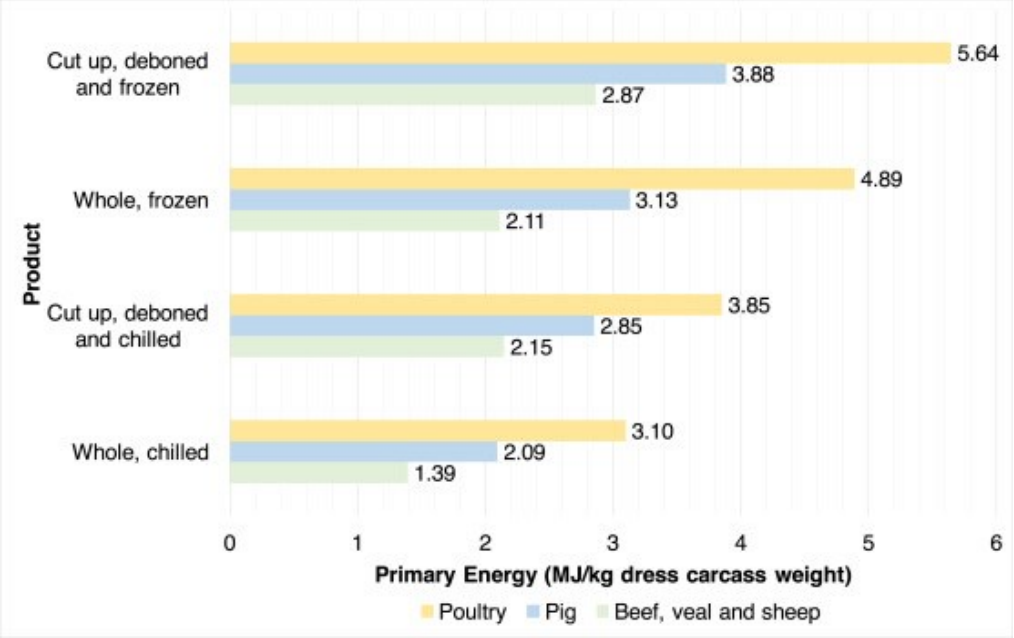


Figure 6: Average primary specific energy consumption values for meat processing (Ladha-Sabur et al., 2019)

This thesis is a case study on a poultry slaughterhouse and processing plant, and an organic feed production plant. For that reason, the energetic analysis, potential innovations, and opportunities will be focused on those parts of the food sector.

#### 1.1.1.1. The case of a poultry slaughterhouse and processing plants

Poultry slaughterhouses and processing plants are big consumers of energy in the food processing sector as seen in Figure 6. The process that demands the most thermal energy is scalding and defeathering (Jekayinfa, 2007). Water used for defeathering is at a lower temperature than water used for cleaning because of the needed antimicrobial effect in the latter. Electrical energy is mostly used to cool the work environment of the poultry processing facilities, chilling of the carcasses, cool, and refrigeration of the final products, and for other electric and electronic equipment used in the plant.

The slaughter and processing of poultry has some by-products that are worth analysing for their potential utilization for energy production or other purposes. These by-products are poultry blood and feathers. Poultry blood is mostly converted to low-value animal feed, and in Asian diets in the form of blood cubes, it is used as an inexpensive source of protein and iron (Wongngam et al., 2020). Feathers are sometimes unlawfully disposed of in landfills where they are unable to decompose due to their keratinous composition. Uses include gasification for energetic valorisation but also hydrolysation and mixing in feather meal with dried coagulated chicken blood which is then used as a form of protein for farm animals or as fertilizer (Campos et al., 2020; Hadas & Kautsky, 1994). The use of feather meal along with all other Processed Animal Proteins (PAPs) was banned from feed use for 20 years in the European Union.

The ban started in 2001 with Regulation (EC) No 999/2001 and was lifted for poultry and pigs in 2021 with Commission Regulation (EU) 2021/1372. PAPs from poultry are now allowed in pig feed production and vice versa. PAPs from poultry cannot be used in feed for poultry and the same is true for pigs.

#### 1.1.1.2. The case of feed production plants

Feed production plants have a very significant role in livestock production because they are responsible for mixing the correct ingredients in optimal amounts to reduce cost while maintaining the right nutrients in the final product. They constantly adjust their recipes according to the latest prices of all ingredients to ensure the lowest possible price for the final product. They use thermal energy in the form of steam and electrical energy for all the motors involved in the process. A typical feed processing system can be seen in Figure 7. Steam is only used in the Pellet Mill and has several important functions. These include the improved digestibility of the final product, elimination of pathogens, and reduced friction in the Pellet Mill which results in less energy demand.

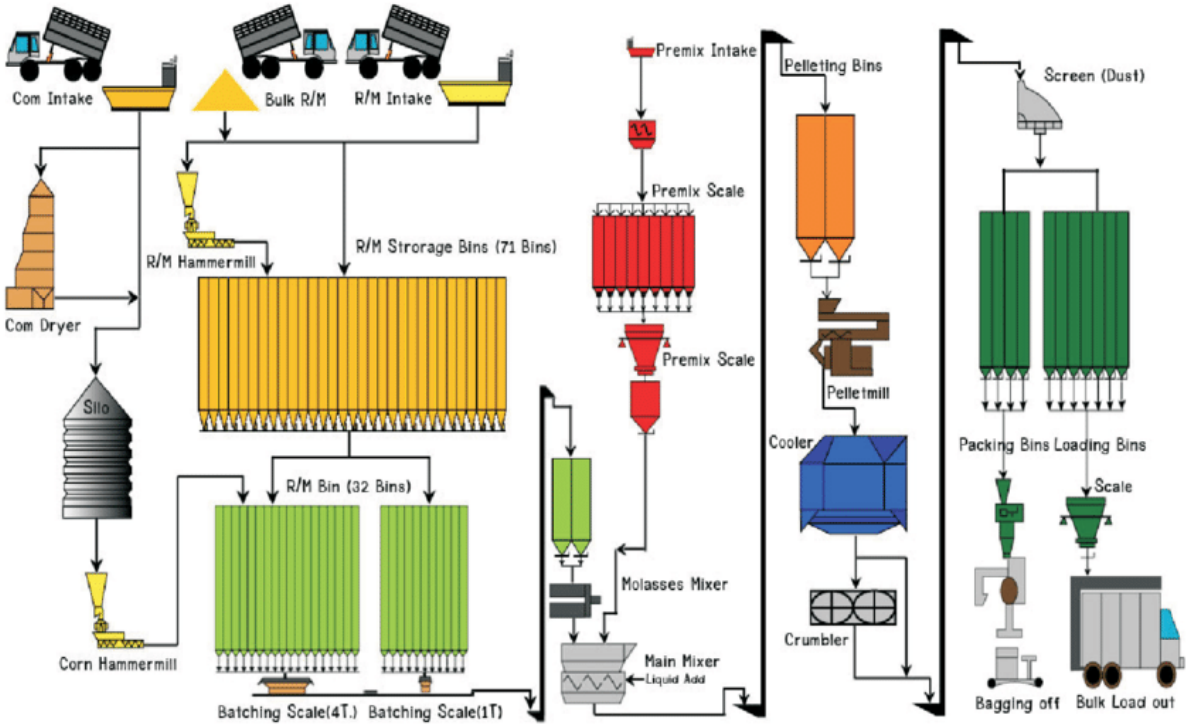


Figure 7: Typical feed processing system (Pathumnakul & Piewthongngam, 2010)

According to Bahnasawy et al., 2014, 80.76% of the energy used in rabbit feed manufacturing is consumed in the pelletizing process. In poultry feed, this rises to 83.26% and in feed, for large animals, it drops to 64.36%. Mccracken, (2002) stated that while greater use of steam in the Pellet Mill increased throughput, too much steam decreased the quality of the final product. The next biggest consumer of energy is grinding with a percentage of 5.17%, 5.8%, and 12.51% for rabbits, poultry, and feed for large animals, respectively.

#### 1.1.1.3. Food sector legislation regarding GHGs

The food sector is a large contributor to the total anthropogenic GHG emissions with approximately 30% in recent years (Crippa et al., 2021). The Effort Sharing Regulation (ESR) which provides annual emissions targets that refer to emissions from all effort-sharing sectors for all EU member countries, covers non-$CO_2$ greenhouse gas emissions from the EU agriculture sector. The European Green Deal states the European Union's commitment to transform its economy and be climate neutral by 2050. In 2021, the European Climate Law turns this deal into a legal commitment to reduce GHG emissions by at least 55% by 2030 compared to 1990 levels.

## 1.3. Hybrid Renewable Energy Systems (HRESs)

Renewable energy sources include solar, wind, geothermal, tidal or wave, and biomass (Mitigation of Climate Change 2022 Working Group III Contribution to the Sixth Assessment Report of the Intergovernmental Panel on Climate Change, 2022). The problem with most of these sources is that they are intermittent and thus cannot always provide stable and reliable energy. One way by which the stability and reliability of these sources may be increased is through their combination in systems called Hybrid Renewable Energy Systems (HRESs). When combined, these sources complement each other. For example, in the evening when the sun stops shining or if the weather is cloudy, solar sources will practically stop providing energy but at the same time, it may be windy which will result in wind sources picking up the slack. However, sometimes this complementarity is not enough to support the demands of the consumers in the grid, or it may be the case that none of these sources can provide energy. In that case, either Energy Storage Systems (ESSs) or the grid provide the required energy to meet the consumers' demand. HRESs are mainly divided into two categories: Off-grid/standalone and Grid-connected/Grid-tied systems.

### 1.3.1. Energy sources used in HRESs

#### 1.1.1.4. Biomass

As mentioned before, biomass is a very diverse renewable resource because it includes everything that is plant or animal based. Common types of biomass used to produce energy include:

1. Wood processing residues and wood such as wood pellets, lumber and furniture, wood chips, black liquor from pulp and paper mills, firewood and mill sawdust, and wastes
2. Organic materials in municipal solid waste such as cotton, food, wool products, yard waste, and some types of paper
3. Crops and waste materials from agricultural activities such as soybeans, corn, sugar cane, woody plants, switchgrass, algae, and crop and food processing residues.
4. Human sewage and animal manure produce biogas.

There are many ways of utilizing biomass resources for energy production. The traditional way includes the direct combustion of available material for heat that is mostly used for cooking and heating in low-income households. This way of converting

biomass to energy is much more inefficient than modern ways of conversion and often causes indoor pollution affecting mostly women, children, and the elderly(Mitigation of Climate Change 2022 Working Group III Contribution to the Sixth Assessment Report of the Intergovernmental Panel on Climate Change, 2022). Until the mid-nineteenth century, this was the only way that biomass was converted to energy, however, it is still commonly used for heating homes and industrial purposes mostly in rural areas.

Since the mid-nineteenth century, more efficient, modern, and environmentally friendly processes of converting biomass to energy have been developed, including thermochemical conversion to produce solid, gaseous, and liquid fuels, biological conversion to produce liquid and gaseous fuels, and chemical conversion to produce liquid fuels.

Thermochemical conversion includes the pyrolysis and gasification processes, which thermally decompose the biomass supply in heated, closed, and sometimes pressurized vessels called gasifiers. The main difference between the two is the amount of oxygen present and the process temperatures.

In the pyrolysis process, organic materials are heated to 400-500$^{o}$C in the almost complete absence of free oxygen and produce fuels like bio-oil, charcoal, renewable diesel, hydrogen, and methane. Bio-oil, produced by fast pyrolysis, can be processed further through hydrotreating to produce renewable gasoline, renewable diesel, and renewable jet fuel. This is accomplished using hydrogen under increased pressure and temperature in the presence of a catalyst.

In gasification, organic materials are heated to 800-900$^{o}$C while injecting steam and/or free oxygen in controlled quantities into the vessel to produce a hydrogen and carbon-monoxide-rich gas called synthesis gas or syngas. It is also called producer gas usually when it contains significant amounts of non-combustible gases such as carbon dioxide and nitrogen. Syngas can be utilized for heating, as fuel for diesel engines, and to generate electricity in conventional gas turbines. This gas can be treated even further by separating the hydrogen which can be burnt or used in fuel cells to generate electricity. Further treating syngas using the Fischer–Tropsch process can produce liquid fuels. Gasification of biomass can take place in vessels that use several different technologies such as bubbling fluidized bed, fixed bed, and circulating fluidized bed.

Animal fats, vegetable oils, and greases can be converted into Fatty Acid Methyl Esters (FAME) through a chemical conversion process known as transesterification, which are used to produce biodiesel.

Biological conversion processes include fermentation which converts biomass into ethanol and anaerobic digestion which produces biogas or renewable natural gas or biomethane. Biogas is produced in anaerobic digesters at dairy and livestock operations, sewage treatment plants, or municipal organic waste treatment plants. It also forms at solid waste landfills and may be captured using appropriate equipment (Caresana, 2011). If treated properly, biogas can have the same uses as fossil fuel

natural gas. Ethanol can be used as vehicle fuel. (*Biomass Explained - U.S. Energy Information Administration (EIA)*, 2022)

By using biomass materials that are by-products or wastes from other processes such as the organic section of municipal solid waste or sawdust from a furniture production plant, as raw materials for energy production or other processes, the conflict of food versus energy, landfilling, and pollution of the environment are reduced and at the same time, profitability in industries and sustainability of the use of materials is increased while expenses for societies and raw materials are decreased. This example is part of a circular economy and Industrial Symbiosis process which is a way of reaching the SDGs of the United Nations. An example of Industrial Symbiosis in the city of Lahti, Finland can be seen in Figure 8.

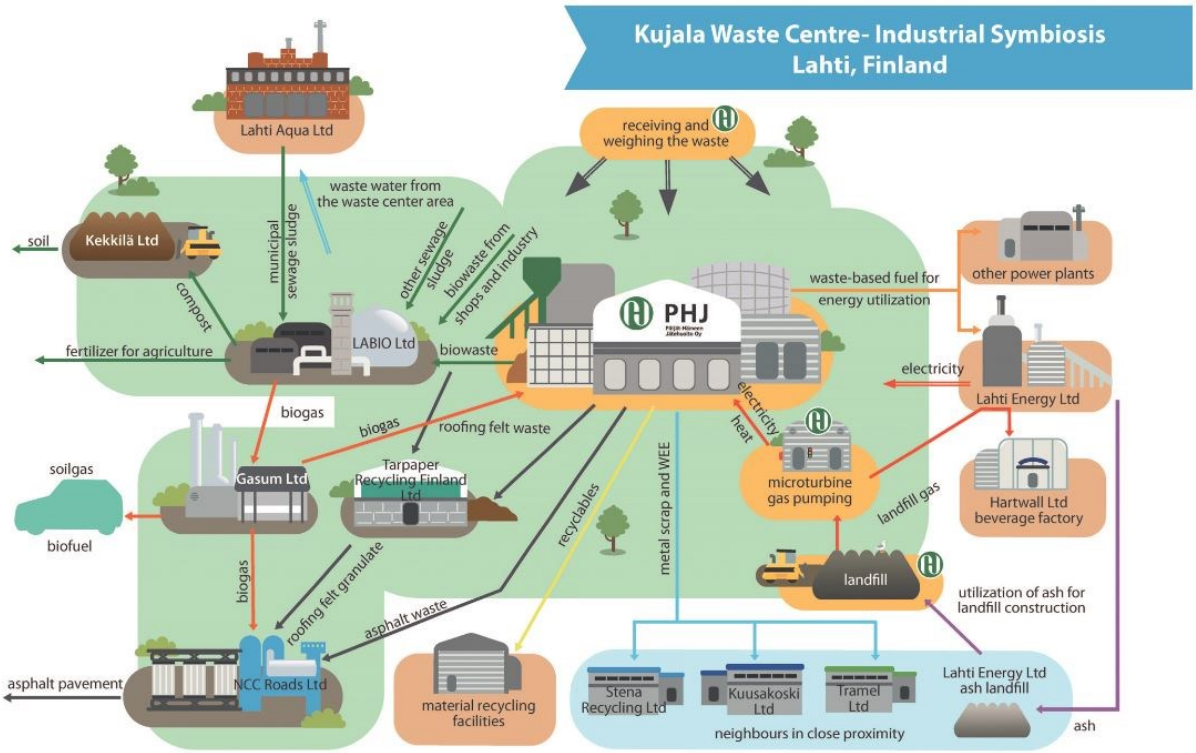


Figure 8: Kujala Waste Centre Flow-Chart. Designed by Anna Polkutie, Esa Ekholm and Hanna Bergman, supported by Lahti region. Source: City of Lahti, 2017 (*Industrial Symbiosis*, 2018)

#### 1.1.1.5. Photovoltaic systems (PV)

The most common way of utilizing solar power is using photovoltaic or PV systems. These are electric power systems that are designed to convert solar power into usable electric energy through photovoltaics. The components of these systems include the solar panels, inverter(s) to convert the panels' output from direct current to alternating current, cabling, mounting, and other electrical components to form a working system.

Photovoltaic systems convert solar radiation directly into electricity unlike other solar technologies such as Concentrated Solar Power (CSP) or thermal solar which are used for heating and cooling purposes. Their size can range from a few kilowatts on the rooftop of a house to fields of hundreds of megawatts. French physicist Alexandre

Edmond Becquerel made the first observation of the photovoltaic effect, which is the theory behind generating electricity from solar radiation, in 1839. A simple schematic of the photovoltaic phenomenon can be seen in Figure 9. When photons hit the semiconductor materials, a voltage difference is created between the P-Type semiconductor and the N-type semiconductor because electrons migrate over the P-N junction to the P-type semiconductor, and electron holes migrate to the N-type semiconductor creating a depletion region where charge carrier migration is no longer possible. The electric field is created around the depletion zone separating the static negative and positive charges. If an external circuit is connected at the top and bottom electrodes, an electric current will flow through it.

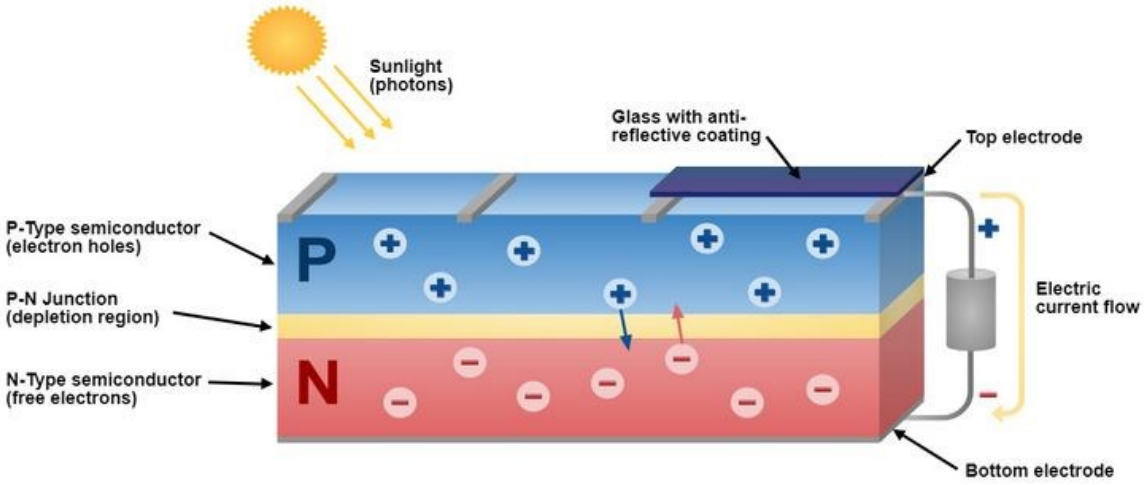


Figure 9: Simple schematic of a photovoltaic cell

The voltage created by a single cell is quite low and that is why cells are combined in panels. For large-scale applications, hundreds or even thousands of panels are connected to create solar fields (Figure 10).

Figure 10: Example of a solar park

Photovoltaic systems can be divided into two main categories: grid-connected and standalone. Grid-connected systems comprise the vast majority of the market. A big advantage over other energy sources is that their operation is completely silent and without any moving parts or environmental emissions. This reduces maintenance costs significantly and almost eliminates operational costs. Maintenance costs include the periodic cleaning of the panel's surface and the replacement of any faulty component of the system. They have developed into a mature technology and are currently used for mainstream electricity generation.

Due to their growth, the price per kW has declined rapidly, and due to technology advancements, their efficiency has increased leading some owners to earlier-than-planned replacement of the panels for economic reasons. Modern commercially available solar panels have efficiencies that are well over 20% (*Most Efficient Solar Panels 2022 — Clean Energy Reviews*, 2022).

There are some variations in the technology which include panels with combined heat and electricity generation using water tubes that run through the panel and solar trackers which track the movement of the sun and always keep the panels perpendicular to the sun's beams (Figure 11) (Amelia et al., 2019; Kalogirou & Tripanagnostopoulos, 2006).

Figure 11: Photovoltaic panels with dual-axis solar tracking system (What Is a Solar Tracker and Is It Worth the Investment? 2022)

#### 1.1.1.6. Wind Turbines

A wind turbine is a device that converts the kinetic energy of wind into electrical energy. There are two main types of turbines: Horizontal axis and vertical axis. Vertical axis turbines can further be separated into bladed and bladeless designs. Horizontal axis turbines are older and more commonly used. Most of the wind power globally today, is generated from big three-bladed horizontal axis wind turbines with their blades positioned upwind of the tower (Figure 12).

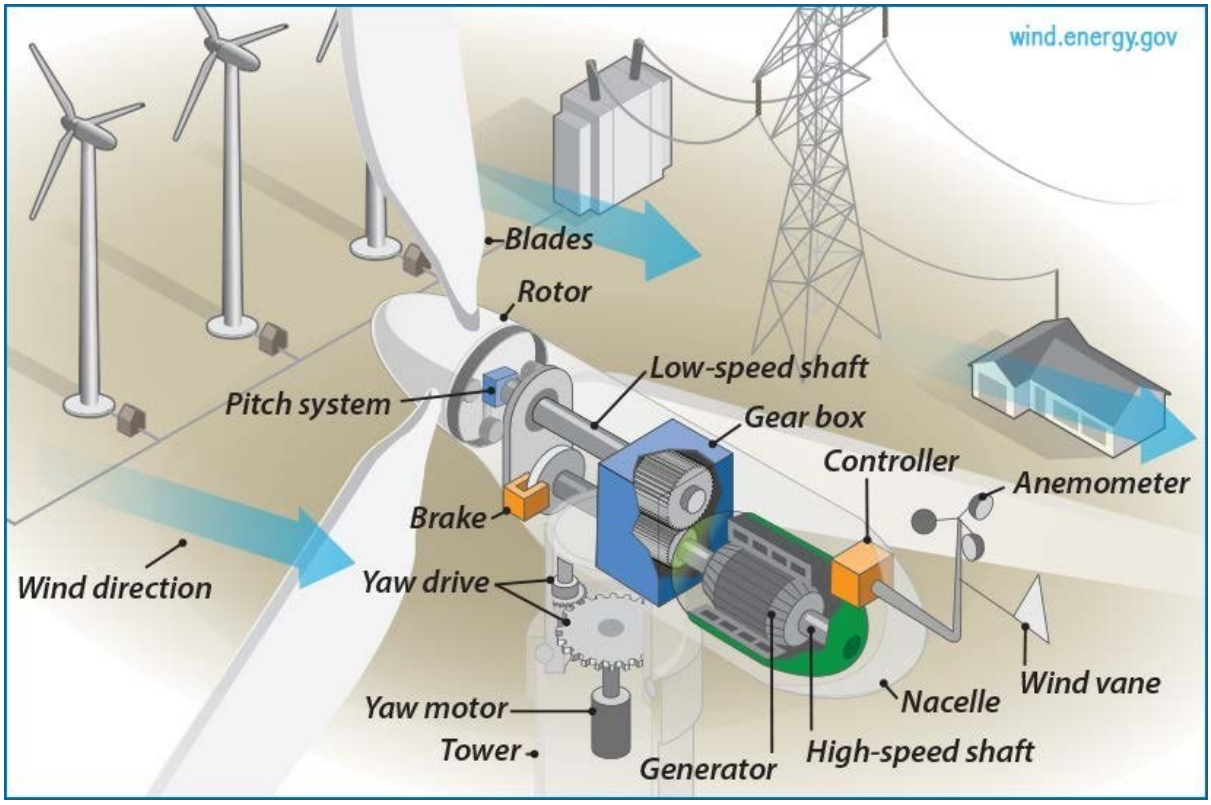


Figure 12: Schematic of a horizontal axis wind turbine

Conventional horizontal-axis wind turbines can be separated into three parts:

- The rotor, comprising about 23% of the total wind turbine cost, contains the blades that convert wind energy to low-speed rotational energy.
- The generator, control electronics, and some components for converting the low rotation speed of the blades into high rotation speed, which is needed to produce electricity, comprising about 34% of the total wind turbine cost.
- And the surrounding structure including the tower and rotor yaw mechanism comprises about 26% of the wind turbine cost.

A more detailed analysis of onshore wind turbine costs can be found in Figure 13.

As of 2021, the total global capacity reached 840 Gigawatt with 97.5 Gigawatt installed around the globe in 2021 which is another record annual installed capacity after the 2020 record of 92.7 Gigawatt (World Wind Energy Association, 2022).

In Figure 14 a part of the San Gorgonio Pass wind farm can be seen.

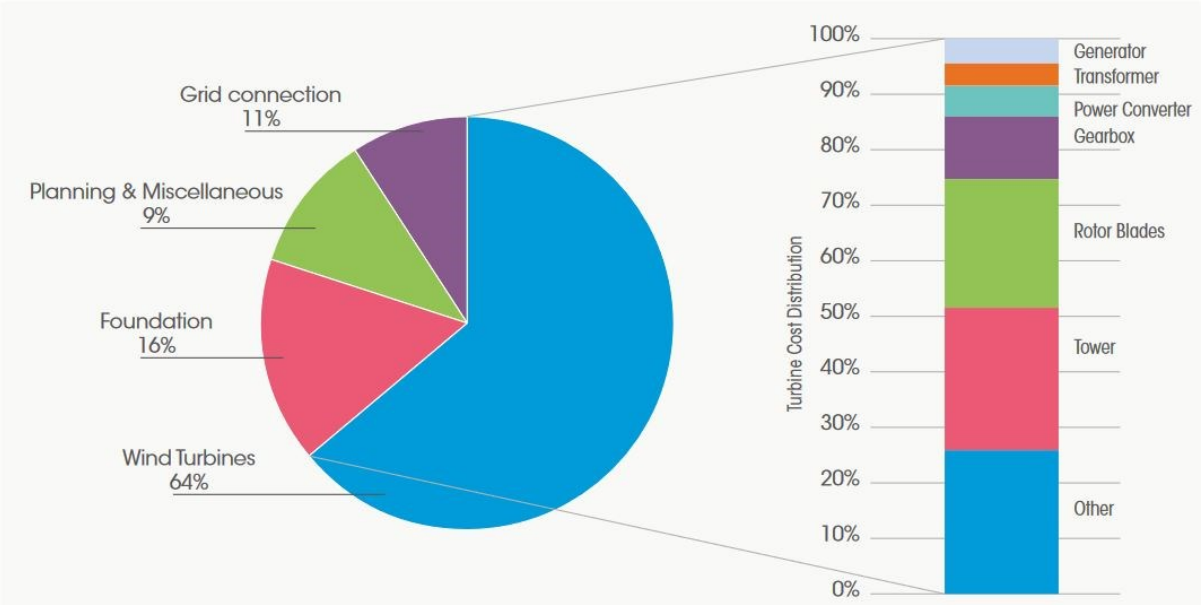


Figure 13: Capital cost breakdown for a typical onshore wind power system and turbine (Blanco, 2009; Renewable Energy Agency, 2012)

The maximal achievable extraction of wind power by a wind turbine is given by Betz's law as 59.3% of the rate at which the kinetic energy of the air reaches the effective disk area of the turbine. If the effective area of the disk is A, the air density is ρ, and the wind velocity is υ, the maximum theoretical power output P is calculated from the following equation (Grogg, 2005):

$$P = \frac{16}{27} * \frac{1}{2} * \rho v^3 A = \frac{8}{27} * \rho v^3 A$$

However, the overall efficiency of a wind turbine is reduced due to various factors including wind-to-rotor efficiency and gearbox, generator, and converter losses.

Figure 14: The San Gorgonio Pass wind farm in California (Eric Wilde, 2016)

#### 1.1.1.7. Wave/Tidal Turbines

A largely untapped renewable resource is marine or ocean energy. This can be extracted from waves, tides, and currents (IPCC, 2022). Wave energy converting (WEC) technologies are especially interesting as they can bring remarkable benefits to society. These include:

- It is a limitless and sustainable energy source that could make a substantial contribution to the mix of renewable energy. Combining renewable energy sources in hybrid systems is generally extremely advantageous because it enhances their accessibility and decreases the need for fossil fuels.
- Using wave energy for electricity would help countries become more energy self-sufficient and less reliant on importing energy from other nations.
- It will aid in the development of a new industry that offers jobs and innovation.
- Ocean waves can be used to generate electricity offshore, which eliminates the need for land and has no visual impact.

The majority of WECs, even those with distinct operating principles, are quite comparable from a general standpoint. Due to their shared environment and objective, the majority of them have the same fundamental sub-systems.

The principal sub-systems that constitute all WECs consist of:

- **The hydrodynamic subsystem** is the basic wave absorption mechanism that uses wave energy. It is coupled to the response and PTO subsystems against which it will actively transmit movements and forces, and it can have various forms which depend on the technology, such as an oscillating body, oscillating water column, and overtopping principle (Figure 15).
- The hydrodynamic subsystem's captured wave energy is transformed into electricity via the **power take-off subsystem**. PTO subsystems can be based on a variety of theories, with direct drive mechanical PTO, hydraulic PTO, linear

generators, air turbines, and low-head water turbines being some of the most popular.

- **The reaction subsystem** serves as a reaction point for the PTO and/or support for the hydrodynamic subsystem while keeping the WEC in place concerning the seabed (by using a mooring system, for example)
- As it handles the regulation of the WEC and its measurements, **the control and instrumentation subsystem** is the system's smart component. It is primarily made up of processors for automation and electromechanical operations, sensors and the data they collect, communication and data transfer, and the user interface.

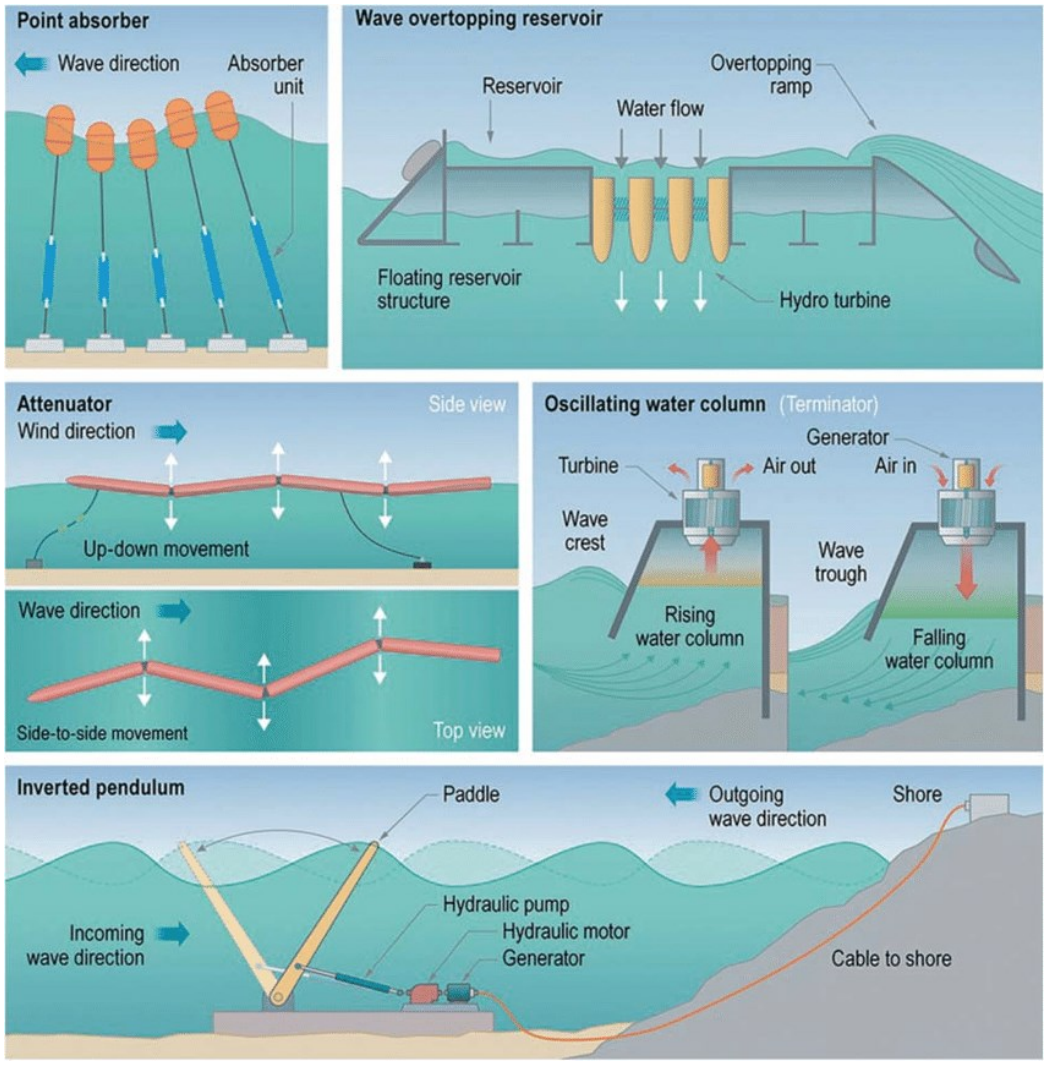


Figure 15: Common types of wave energy converters (Aydingakko et al., 2016)

WECs can be divided into different categories due to the range of ideas and concepts of harvesting wave energy.

A basic categorization is often made by using the terms attenuator, terminator, and point absorber.

Terminators are devices with large horizontal extensions parallel to the direction of wave propagation, while attenuators have large horizontal extensions orthogonal to

the direction of wave propagation. On the other hand, point absorbers come with elongations that are small compared to the prevailing waves' main wavelength.

Another way of categorizing WECs is by location, namely, offshore, near-shore, and onshore.

As of 2020 wave energy production capacity is only 524MW, and the generated energy in 2020 was 957GWh worldwide (Renewable Energy Agency, 2022).

#### 1.1.1.8. Concentrated Solar Power (CSP) systems

Concentrated solar power (CSP) is a renewable energy technology that uses mirrors to concentrate direct solar rays on a receiver filled with a fluid, usually thermal oil, or molten salts. The fluid in the receiver is called a Heat Transfer Fluid (HTF) and its purpose is to conduct heat to drive a steam turbine generator to produce electricity, akin to what one can find in a conventional thermal power plant.

Four CSP technologies exist today (Figure 16). These are:

1. Parabolic trough
2. Linear Fresnel reflector
3. Solar tower
4. Parabolic dish

The parabolic trough is the most used technology today with an 81% market share. (World Bank, 2021)

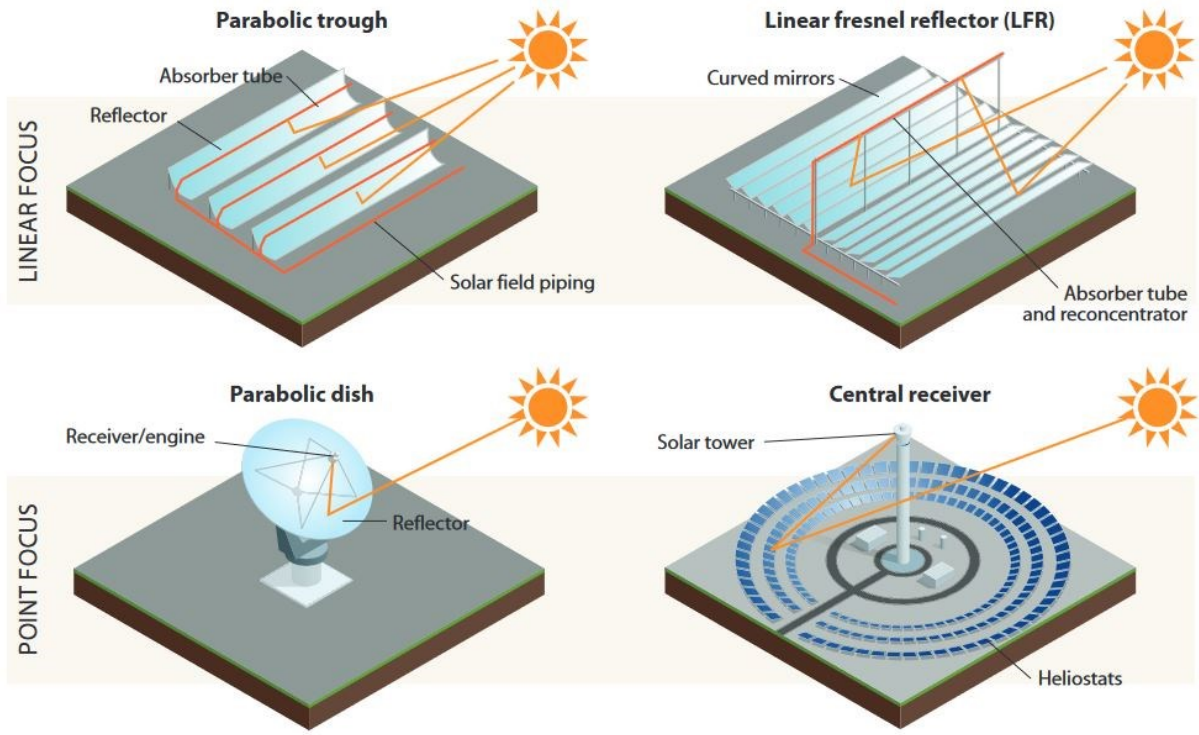


Figure 16: Four types of CSP technologies (World Bank, 2021)

In 2021 there were about 6 GW of operational CSP plants worldwide. These were mostly in Spain (2.3 GW), the United States (1.6 GW), Morocco (0.53 GW), China (0.5 GW), and South Africa (0.5 GW). (World Bank, 2021)

#### 1.1.1.9. Non-renewable energy production methods used as a backup

In HRESs it is often necessary to use backup energy production methods when energy storage or the grid are not available to ensure that the energy demands are met and blackouts are prevented. These methods usually include generators that are powered by diesel or natural gas.

### 1.3.2. Energy storage systems (ESSs) used in HRESs

Hybrid Renewable Energy Systems often integrate Energy Storage Systems because of the intermittent nature of most renewable energy sources. Due to their high cost, ESSs are usually deployed in Off-grid systems. The exception may be found in Pumped Hydro storage because it can store huge amounts of energy for long periods and thus can compensate the utility grid. However, pumped hydro can be implemented only in select areas with a suitable topography and requires a high capital investment. Different energy storage technologies with some characteristics in orders of magnitude are shown in Figure 17.

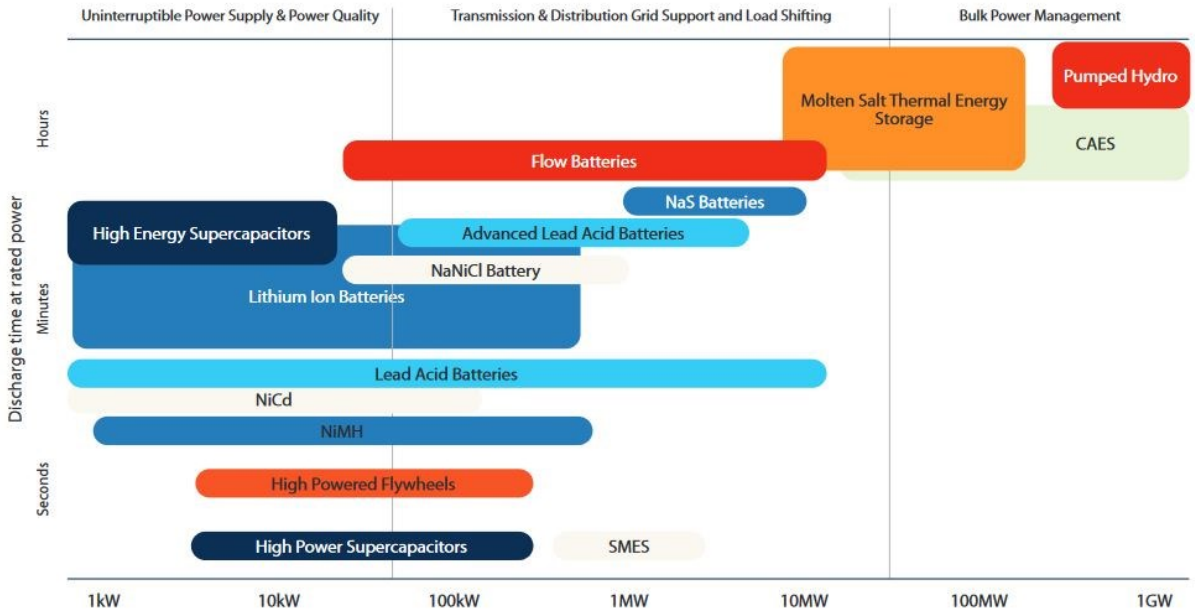


Source: Adapted from DOE/EPRI (2013).
Note: CAES = compressed air energy storage; GW = gigawatt; kW = kilowatt; MW = megawatt; NaNiCl = sodium nickel chloride; NaS = sodium sulfur; NiMH = nickel metal hydride; NiCd = nickel cadmium; SMES = superconducting magnetic energy storage.

Figure 17: Key characteristics of available energy storage technologies (World Bank, 2021)

#### 1.1.1.10. Batteries

Batteries are devices that store chemical energy and transform it into electrical energy through electrochemistry. They are systems called electrochemical cells. A battery can incorporate one or many electrochemical cells each comprising two electrodes, the anode, and the cathode, which are separated by an electrolyte. During chemical reactions between the anode and the electrolyte, electrons are released and at the same time, chemical reactions between the cathode and the electrolyte allow the cathode to accept electrons and which results in a stream from the anode to the cathode through an external circuit that is employed to perform tasks. Charged ions also move through the electrolyte solution that is in contact with both electrodes to balance the flow of electrons. These are called reduction-oxidation or redox reactions. Reduction happens at the cathode because it gains electrons and oxidation is what happens at the anode as it loses electrons. Different electrolytes and electrodes cause various chemical reactions that have an impact on the battery's operation, capacity for storing energy, and voltage. (*How a Battery Works - Curious*, 2016)

There are single use batteries and rechargeable batteries. In HRESs, only rechargeable batteries are considered for obvious reasons.

When choosing a battery, it's vital to take into account seven factors: durability, safety, affordability, energy density (Wh/kg), energy capacity (Ah), and voltage per cell.

The current options for ESSs include lead-acid, nickel-metal hydride (NiMH), and lithium-ion (Li-ion) according to (A. Chen & Sen, 2016).

#### 1.1.1.11. Hydrogen storage

Hydrogen storage is often used as an ESS (Kumar Singla et al., 2020). The process by which the energy is stored in Hydrogen is the following:

Excess energy produced by renewable sources in the HRES is used in an electrolyser which separates water into Oxygen and Hydrogen gas which is then stored separately in special high-pressure vessels. (T. Khan et al., 2022)

When the production of energy from the other sources in the system is not enough to meet demands, hydrogen is consumed in a Hydrogen fuel cell to produce electricity.

A hydrogen fuel cell is an electric power generation system that uses electrochemical processes at low temperatures to convert hydrogen into fuel and directly oxidize it to electricity. The hydrogen reacts with oxygen across an electrochemical cell to produce electricity, water, and small amounts of heat. The chemical reaction that governs this process can be seen below:

$$2H_2\ (g) + O_2(g) \rightarrow\ 2H_2O\ (g) + energy$$

There are many different types of fuel cells available on the market that can be used in all sorts of applications. Small fuel cells can power devices as small as a cell phone and large ones can provide electricity to power grids, act as a backup or emergency power sources in buildings and industry, or power a standalone microgrid of a remote community (*Use of Hydrogen - U.S. Energy Information Administration (EIA)*, 2022).

There are many different methods of storing Hydrogen. These include compressed hydrogen, physically adsorbed hydrogen, cryo-compressed hydrogen, metal hydrides, complex hydrides, and Liquid Organic Hydrogen Carriers (LOHC) or liquid organic hydrides. In Figure 18 a concept of these storage methods can be seen.

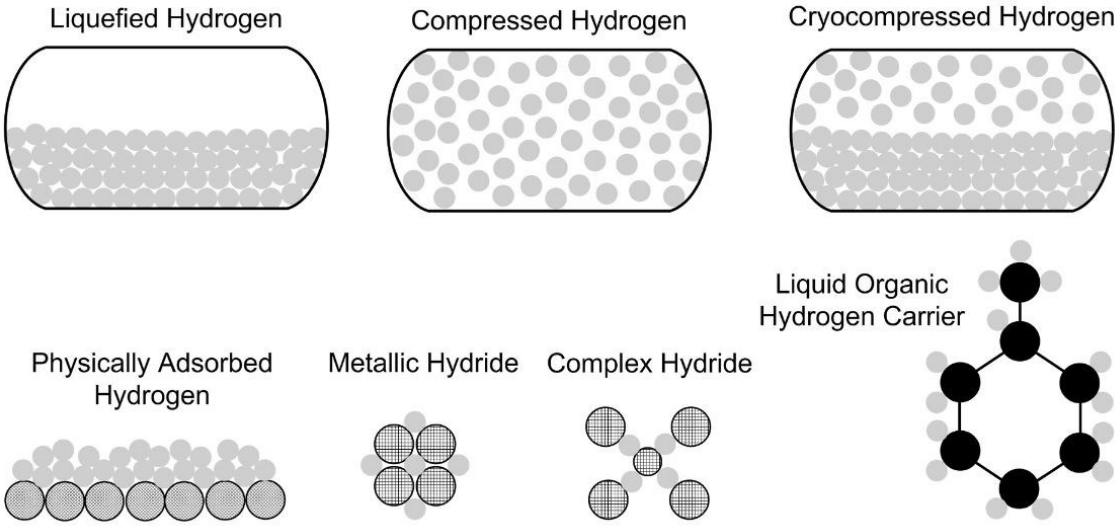


Figure 18: Concept of hydrogen storage methods (Usman, 2022)

Compressed Hydrogen is a well-established and the most widely used technology which is evolving its storage vessels to accommodate Hydrogen at higher pressure with a higher gravimetric energy density. (Usman, 2022)

#### 1.1.1.12. Other types of ESSs

Other less commonly used ESSs used in HRESs include Pumped Hydro Storage (Figure 19) (Akhtari & Baneshi, 2019; Amutha & Rajini, 2016; Baruah et al., 2021; M. Das et al., 2019; Kusakana, 2016; Tiwary et al., 2019) and Liquid Air Energy Storage (LAES) (Cao et al., 2022).

In Pumped Hydro Storage, energy is stored by pumping water to an upper reservoir with a considerable height difference from a lower reservoir. When energy is needed, water from the upper reservoir is allowed to flow to a lower reservoir through a turbine which generates electricity.

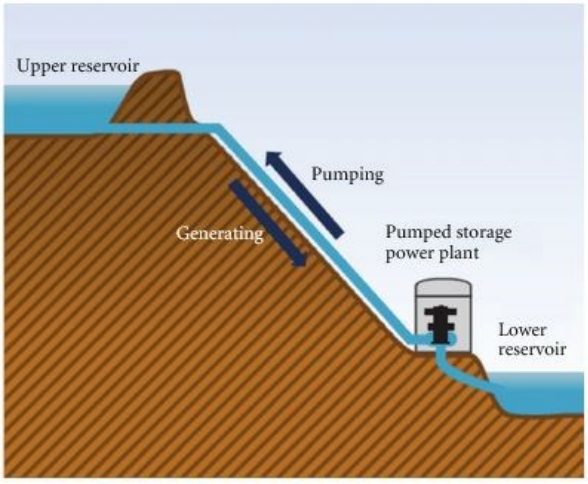


Figure 19: Simplified schematic of a Pumped Hydro Storage system (A. Kumar et al., 2011)

In Liquid Air Energy Storage, atmospheric air is cooled to its liquifying temperature and then stored in a pressurized tank. When energy is needed, the air is heated and released through a turbine to produce electricity. An example of such a system can be seen in Figure 20.

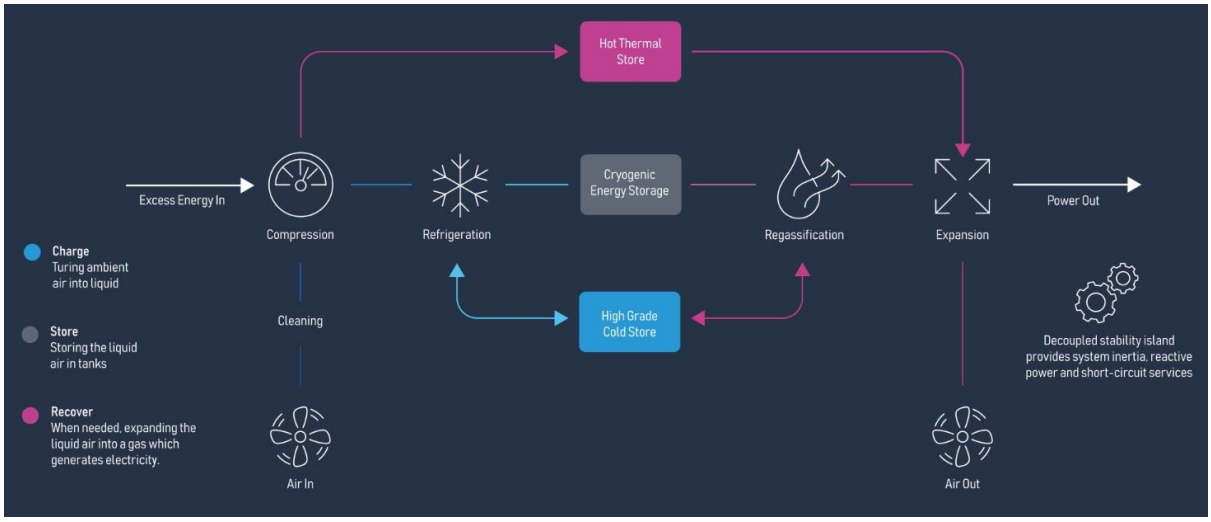


Figure 20: Liquid Air Energy Storage (LAES) system example, (*Technology | Highview Power*, 2022)

### 1.3.3. Electrical Grid

An electrical grid is essentially a network made of producers and consumers that are all synchronized. They are connected through lines that distribute and transmit electricity ranging from a few meters to thousands of kilometres. The synchronization aspect of an electricity grid refers to the fact that during operation of a grid, the electricity must be produced at the same moment that it is consumed. These grids are managed by one or more control centres to ensure their stable operation. The electricity that is transmitted through the lines can have different levels of voltage according to the application. In order to transmit electricity over long distances, high voltage is used in the range of 36kV or higher to reduce transmission losses. For shorter distance transmission, and the connection of some large consumers, medium voltage is used which is in the range of 1kV to 36kV. For household and small business consumers, medium voltage is converted to low voltage which is lower than 1kV. In Greece, low voltage is 220V for single phase systems and 400V for three phase systems.

The electricity grid is often also a part of HRESs and is mostly used as a backup energy source in various occasions such as meeting peak demand, or when meteorological conditions are unfavourable for renewable energy sources such as wind and solar (Chennaif et al., 2022). It also useful for absorbing excess electricity produced in a microgrid either in a paid form like a feed-in tariff that is pre-determined or in the form of a net-metering agreement.

#### 1.1.1.13. Net Metering/ Virtual Net metering

There are many different net metering schemes (Figure 21) used around the world depending on the unique circumstances in every country. In Greece, a simple mechanism of net-metering is used. According to this mechanism, consumers are billed only for the net amount of electricity they use which is measured using smart meters installed at the connection point of their renewable energy source to the grid (Poullikkas et al., 2013). At the moment, excess electricity that is injected into the grid

is credited to the customer's next electricity bill for a 36-month billing cycle. In the Net-metering scheme, the renewable energy sources must be connected to the same meter that the actual consumer is, which limits their deployment to the same location.

However, since March of 2019, Greek energy consumers can produce electricity from renewable resources, and connect the system to a different meter in a different location than that of consumption. This opens the possibility for consumers who did not have enough space available at their location, to still benefit from the production of their own energy.

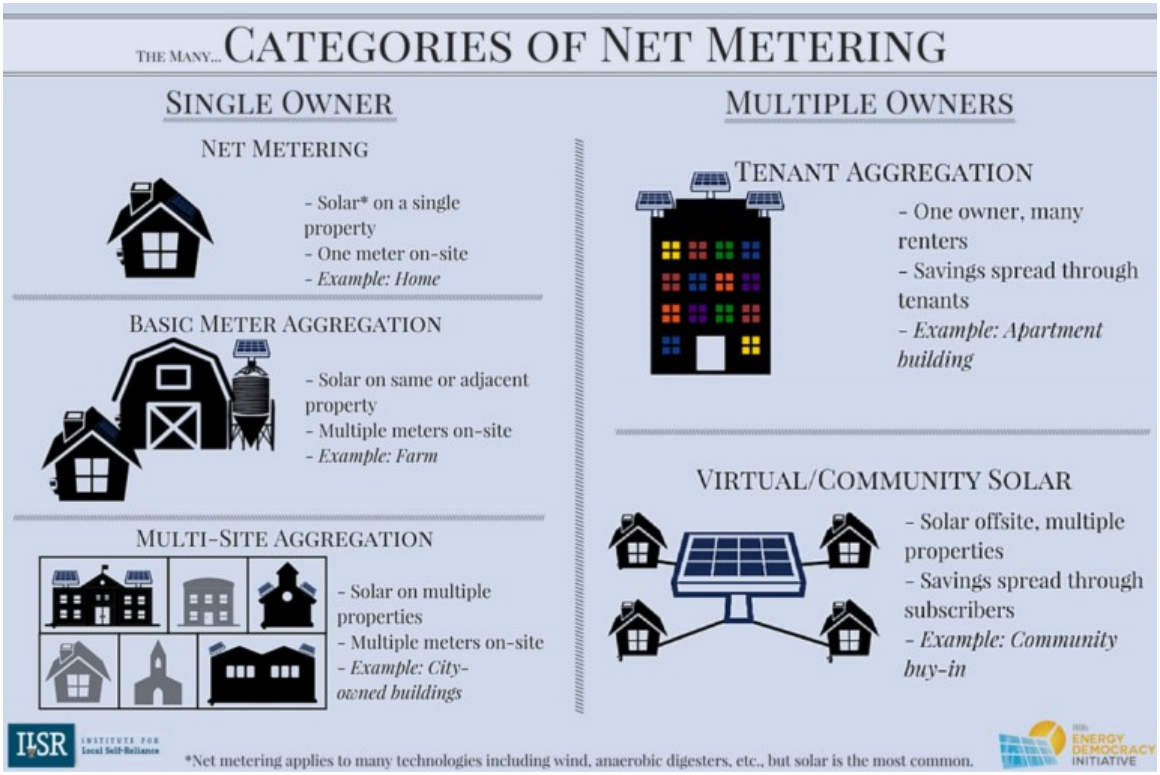


Figure 21: Different categories of net-metering (ILSR, 2015)

## 1.4. Scope of this study

The scope of this study is to analyse the electrical and thermal demands of a poultry slaughterhouse and an organic feed production plant and propose a Hybrid Renewable Energy System capable of meeting those demands at the lowest possible cost, lowest carbon footprint per kWh, highest profitability and highest return on investment percentage based on scenarios with different energy prices, discount rates and inflation rates. This study aims to investigate the use of extracted olive pomace, broiler feathers and their combination as fuels for electrical and thermal energy generation in a syngas generator combined with renewable energy sources such as wind and solar in all possible configurations. One of the aims of this study is to calculate the carbon footprint of each simulated configuration, using Lifecycle Analysis data for all components and their energy generation. Another scope of this study is to conduct a sensitivity analysis of the optimal configuration with regard to five important parameters of the system that could possibly change over time.

## 1.5. Novelty of this study

While reviewing the relevant literature on Hybrid Renewable Energy Systems, it was found that no studies have been done on their application on a poultry slaughterhouse or a feed production plant. Another observation is that minimal studies have focused on the use of extracted olive pomace (orujillo in Spanish) in gasification plants to produce thermal and electrical energy. Most of the studies that were reviewed used some kind of olive pomace straight from the olive mill in wet or dried form. The difference between extracted and wet or dry olive pomace is the oil content in the latter, which is significant (Yanık, 2017). Another fuel that will be considered for the gasifier is broiler feathers. There have been several studies on the gasification of broiler feathers but not in the context of an HRES. Most of the studies that investigated the gasification of feathers, referred and collected their data from a gasification facility in Poland which gasifies poultry feathers for heat production in a boiler. That facility does not generate electricity in a generator fuelled by syngas, unlike this study. Another innovation in this thesis is the use of Lifecycle Analysis (LCA) data in order to calculate the carbon footprint of the composition of each scenario that is simulated. The plant in Poland gasifies feathers with a small addition of wood pellets in order to stabilise the gasification process and provide some additional calorific value. There have not been any studies that combined olive pomace and feathers like this study does.

## 1.6. Structure of the following chapters

The structure of the next chapters is as follows:

In chapter 2, a literature review will be presented with all the relevant information regarding the deployment of HRESs around the world and a brief description of some studies will be given to convey their content.

In chapter 3 the poultry slaughterhouse and the feed production plant of this case study will be described along with the processes that occur there and the currently installed systems and methods that are used. Biomass waste that is produced in the plants but also other available biomass in the area will be listed and lastly, the used methodology for data collection and analysis will also be described.

In chapter 4, the results and findings of the simulated scenarios from the software will be presented and a discussion will be made on these results along with a sensitivity analysis of the optimal scenario.

Chapter 5 will state the conclusions, recommendations, and opportunities for further research in the future.

Chapter 6 is the bibliography used.

# 2. Literature Review

In reviewing the relevant literature, it was found that there has been extensive research on the topic of Hybrid Renewable Energy Systems (HRESs). A very common initial categorization made, is whether the system is connected to the local electricity grid or not. The former is called a Grid-connected (B. K. Das, Alotaibi, et al., 2021), Grid-tied (Fard et al., 2021), or Grid-integrated (Malik et al., 2022) system while the latter is

called an Off-Grid (Odou et al., 2020) or Standalone (Salameh et al., 2021) system. Through an extensive review of the relevant literature, it was found that Grid-connected systems are usually more cost effective due to the, still high, cost of ESSs used in off-grid configurations. The latter are usually more cost effective in the cases where long grid extensions need to be made, for example in remote villages or islands (Luta & Raji, 2018).

In this chapter a brief presentation of a several selected studies will be done. The scope of this presentation is to address the key points of every study and to provide the most important information, the methodology that was used as well as the conclusions drawn by the authors. Reference to each study will be limited to one paragraph. Every study that will be presented here has been approved and published in a scientific journal and has contributed to a better understanding of HRESs and their possible applications, advantages, and limitations.

Kumar & Channi studied the techno-economic and environmental viability of using the photovoltaic and biomass potential to power a rural village in India comprising of 770 households. To investigate this potential, they used version 3.14 of the HOMER Pro software. The optimal system design was selected with the Technique for Order Preference by Similarity to Ideal Solution (TOPSIS) considering the cost of energy generation, operating cost, generated energy, initial capital cost, net present cost, and the renewable fraction. A sensitivity analysis was performed considering the inflation and discount rate. They found that for a system comprising of photovoltaic arrays, a biomass generator, a converter, and lithium-ion batteries, the payback period of the photovoltaics was just 1.58 years with a usable lifetime of 25 years. (R. Kumar & Channi, 2022)

Seedahmed et al. made a techno-economic analysis for the electrification of a remote off-grid village in Saudi Arabia combined with a big commercial load using the HOMER software. The energy systems proposed were compared based on their levelized cost of energy (LCOE) and their gross present cost. A sensitivity analysis was done, by changing the size of the system components but also by tracking changes like the price of fuel, weather, and load demand of connected consumers. Through this analysis they concluded that the optimal system consisted of a wind turbine, a fuel cell, a battery and a diesel generator in a standalone configuration, which reduce the net present cost by 13.84% compared to the diesel generator based scenario. (Seedahmed et al., 2022)

Roy et al. investigated the possible implementation of an HRES to electrify and provide fresh water to an Off-Grid region of India which is currently powered by kerosene. The size optimization of the system was done using a non-dominated sorting genetic algorithm-II in MATLAB which minimized the damage to human health and the cost of energy while demand supply reliability is maintained through the index of Loss of Power Supply Probability (LPSP). An extensive analysis of the optimized systems was performed based on factors that include lifecycle emissions, ecosystem damage, human development index, job creation, carbon emission penalty, and cost of water. The proposed system used photovoltaics, biomass generators and a wind turbine with an electrolyser and fuel cell configuration for energy storage which prevents 75,832

kg of emissions per year, creates jobs for the community and improves the standard of living. (Roy et al., 2022)

Malik et al. studied a grid-connected hybrid system in the western Himalayan region of India that used the locally available renewable resources: solar, wind, and pine needles as biomass. They studied five configurations based on the aforementioned resources with or without integrating an ESS. The HOMER software was used to model the proposed configurations after analysing the alternatives. A sensitivity analysis was carried out to find the impact of factors such as solar radiation, real interest rate, life of the biomass gasifier, fuel price, and capacity shortage on system outputs to identify its critical parameters. This analysis found that the only parameter towards which the system was not sensitive was the price of fuel. The study concluded that the most cost-effective system was the grid-tied photovoltaic and biomass gasifier hybrid with a COE of \$0.099/kWh while saving an estimated 27.8Mt of $CO_2$ per year with respect to a pure diesel system. (Malik et al., 2022)

Buller et al. studied the case of optimizing the costs and energy supply of a wastewater treatment plant which uses a treatment process of high energy demand and already incorporated a photovoltaic array of 402kWp. Their study investigated the use of a biomass gasifier, photovoltaics, and the electricity grid as components in the hybrid system. To model this system and perform different simulations, the HOMER software was used. Results indicated that the grid connected solar/biomass gasifier system was more cost-effective than the Off-grid biomass gasifier having a COE of \$0.0298/kWh and \$0.0426/kWh respectively. The optimal system produced enough electricity to power the plant and 788,000 homes. The biomass gasifier used the anaerobic digestion of sewage sludge to produce biogas which was then consumed to produce electricity. (Buller et al., 2022)

Al-Najjar et al. studied the renewable resources in the city of Gaza and proposed an HRES with biomass and solar energy to provide sustainable electricity. Biomass was utilized through the incorporation of a biogas engine generator. The simulations were conducted using the HOMER Pro software for a daily average demand of 1,074kWh/day and peaks of 84.5$kW_p$. To evaluate the capacities of the system components, the authors presented a pre-mathematical model including different zones of load profile. This helped in achieving optimal contribution of biomass in the proposed model. The optimal solution resulted in a system with a minimum net present cost of \$2.3 million and a COE of \$0.438/kWh. (Al-Najjar et al., 2022)

Das et al. studied three electrochemical energy storage technologies as parts of different off-grid HRESs which comprised of various percentages of photovoltaics, micro gas turbine, and wind turbine capacities. These storage technologies include vanadium redox, lithium-ion and lead acid batteries. This was a case study on a community in Australia. They investigated all three technologies in two energy management strategies and optimized them by using a non-dominated sorting genetic algorithm II. The objectives of the algorithm were to minimize the cost of energy and the lifecycle emissions. Its constraint regarded reliability which is defined by the LPSP index. They found that the strategy of cyclic charging provided the lowest COE, but not the lowest lifecycle emissions which were provided by the load following strategy.

The technology with the lowest emissions over its lifecycle (46,258–104,664 kg CO2-eq per year) and COE (0.126–0.187$/kWh) was found to be the vanadium redox battery. (B. K. Das et al., 2022)

Bhatt et al. studied a microgrid that used second life batteries discarded by electric vehicles, for energy storage. In their study, they compared microgrids that consisted of floating photovoltaics, regular photovoltaics, biogas, and wind turbines which used new lithium-ion batteries and second life batteries to show the techno-economic viability of the latter. All models were simulated using the HOMER-Pro software which achieved the design of an optimal configuration for a research facility in Thailand. The factors that were considered for the selection of the optimal case included the minimization of COE and Net Present Cost (NPC). Results showed that the minimum COE and NPC were achieved with the grid-connected models. Therefore, the optimal grid-connected model was further analysed for its sensitivity towards various energy throughputs and cost multipliers of the second life batteries. It was shown that COE and NPC were reduced by 35% and 36% respectively, when second life instead of new lithium-ion batteries were used. (Bhatt et al., 2022)

Ji et al. studied the combination of rooftop photovoltaics and waste biomass for an application at a small neighbourhood scale in Beijing, China. The methodology used was that of a general optimization coupled with multi-perspective performance evaluation and the sensitivity analysis considered changes in energy policy, uncertainty in the economic landscape and demand response factors. Their results showed that using the rooftop photovoltaics and all of the available biomass could provide 73% of the local electrical load with an embodied $CO_2$ emission of 0.5416 kg/kWh and an LCOE of 0.103$/kWh. They concluded that the dispatchable rooftop PV production and the flexible shiftable load might assist in balancing energy demand and supply and reduce peak load and power supply costs, but demand response implementation has greater direct economic advantages than environmental benefits. (Ji et al., 2022)

Kirim et al. designed and studied modular HRESs that consisted of photovoltaics and biogas for the application of dairy cattle barns in Turkey. To assess the viability of different configurations, they looked at the factors of return on investment (ROI), annual worth, COE and NPC. Of interest to this study was also the contribution of electricity generation from these HRESs, to the country's gross domestic product (GDP), which was predicted using 13 independent variables. The best annual worth of various cattle barns was selected as an independent econometric variable. They calculated lasso, ridge, elastic net, and linear regression models and found that ridge regression produced the most confident results with the smallest root mean squared error value. Their results showed that the grid-tied biomass and photovoltaic HRESs are more economically viable when compared to off-grid biomass systems. Regarding the contribution to GDP, it was found that the total installed cost of photovoltaics was the most significant (97%). (Kirim et al., 2022)

Shezan et al. optimized standalone HRESs for two places in Bangladesh by comparing 5 separate load dispatch strategies. The optimization factors used, were the cost effectiveness and technical feasibility of the system while supporting a

growing load profile. The components used in the systems were photovoltaics, a wind turbine, a battery ESS, and a DG used as backup. The HOMER software was used to conduct the techno-economic analysis while MATLAB/Simulink was used to evaluate the different dispatch strategies. They found that for the HRES at hand, the best energy dispatch strategy is load following while the worst is CD if long-term operation is also considered. (Shezan et al., 2022)

Demirci et al. investigated the application and optimization of grid-tied and off-grid HRESs based on biomass, on a rural region with poultry farms in Turkey. The system's components include photovoltaics, wind turbines, but also a biomass generator that utilises the manure in the area. These were simulated using the HOMER-Pro software for their economic, technical, and environmental performance. An artificial neural network was used to conduct the sensitivity analyses with the parameters of inflation and load fluctuations. It was found that the photovoltaic/biomass system when connected to the grid, produced an 88.9% renewable fraction (RF). The results also showed that if an ESS was used, it increased the RF by approximately 10% and produced 16% less excess electricity. (Demirci et al., 2022)

Aziz et al. examined the best layout for an off-grid PV/diesel/battery HRES to power a remote region of Iraq. Using the MATLAB Link module in the HOMER program, a novel dispatch strategy with 12-hour foresight for the load and solar production was created. The technical, economic, and environmental performance of the suggested method is compared to the default cycle charging strategy in HOMER. They found that the suggested strategy, which has an NPC of $4.03 million, an RF of 41.3%, and $CO_2$ emissions of 851,377 kg per year, performs better than the cycle charging plan which has $4.19M, 33.9%, and 957.477 kg, respectively.(Aziz et al., 2022)

Hossein Jahangir et al. sought to evaluate the environmental and techno-economic viability of a standalone power plant to provide Tehran with the best planning for reliable electrification. This was done by generating a model in the HOMER software and performing a size optimization and sensitivity analysis of the proposed system to find the most cost-effective and environmentally friendly alternative for the city. The criteria used for choosing the best architecture were based on which option has the lowest NPC, COE, and carbon emission level. The results from HOMER showed that the photovoltaic, wind turbine, BG, and battery HRES was the best with an NPC of $113 million and a COE of $0.281/kWh.(Hossein Jahangir et al., 2022)

Hoseinzadeh & Astiaso Garcia conducted a case study on the Italian city of Catania that aimed to satisfy the need for 2 MW of energy. To that end, the HOMER software was used to simulate the economic and technical usage of solar panels, wind turbines, fuel cells, electrolysers, and hydrogen tanks. The authors pointed out that solar panels and wind turbines can complement one another for electricity generation in specific months of the year. They claimed that in comparison to wind turbines and fuel cells, photovoltaic panels are more efficient and contributed 72% of the total energy for the city. They conclude that a capital expenditure of 4.85 million euros, and an ROI of 2.59 million euros during the project's anticipated 25-year life, should be incurred to supply the aforementioned demands of the region. (Hoseinzadeh & Astiaso Garcia, 2022)

Qiblawey et al. conducted a thorough techno-economic analysis of expanding the RES usage in Tenerife and Gran Canaria islands. Electrical interconnection between the two islands was also looked at, and they found that, compared to the existing scenario, it would enhance the ideal aggregate RES penetration beyond 70%, reduce the COE by 30.3%, and $CO_2$ emissions by 70%. For all the scenarios that were investigated, they used the HOMER software and in order to rank, compare, and evaluate them, the parameter used was the COE. Without electrically interconnecting the islands they concluded that, compared to 18.8% and 15.5% at the time, the most inexpensive HRES penetration in each island would reach 60% which suggests that the intensity of $CO_2$ emissions might be reduced by 58%. Another effect was that the COE in Tenerife and Gran Canaria was reduced by an extra 23.0% and 25.3%, respectively. Their results also indicate a small increase in the optimum RES capacity if $CO_2$ emission fines are implemented.(Qiblawey et al., 2022)

Das, Hassan, et al. did a case study on a remote island in Bangladesh. The scope of the study was to design av HRES that included photovoltaics, a biogas generator, a wind turbine, and a vanadium redox flow battery for the provision of reliable electricity to the island. The system's components were scaled using two optimization algorithms which included the infeasibility driven evolutionary algorithm and the non-dominated sorting genetic algorithm II based on the lifecycle emissions and COE. To determine the best result, a fuzzy decision-making approach was used. They also compared the outcomes of the non-dominated sorting genetic algorithm with those of the HOMER software and the infeasibility driven evolutionary algorithm and concluded that the two algorithms yielded better results than the HOMER software when it comes to costs environmental aspects. (B. K. Das, Hassan, et al., 2021)

Wang et al. suggested the deployment of a grid-tied HRES for treating drinking water on a large scale. They developed a multi-objective nonlinear dynamic model with integer variables, in which trade-offs between four-dimensional benefits and system operations and configurations are simultaneously taken into account. The suggested model was converted into its equivalent single objective form using the ε-constraint technique and system planner attitude parameters, which was then solved by the LINGO program. The practicality of the proposed model was evaluated using a case study from China, where the ideal system design, the ideal self-sufficiency ratio, and the ideal energy balance are all attained. The effects of natural resource changes and power pricing techniques on the systems are also examined and contrasted. They concluded that with the achievable self-sufficiency ratio approaching 95%, installation of grid-tied HRESs comprising of photovoltaics, wind turbines and ESSs can assist power consumers in coping with the risks associated with future electricity price variability. (Wang et al., 2021)

Ribó-Pérez et al. suggested that biomass gasifiers have the potential to be a clean technology and provide reliability to energy systems, but their advantages are not as widely recognized as they should be. To support that suggestion, they pointed out that the HOMER software, which is widely used in designing and simulating microgrids, lacks a biomass gasifier module. They proposed a series of methods to incorporate the technical and economic characteristics to simulate an electric generator which uses syngas as fuel produced in a downdraft biomass gasification plant using the built-

in biogas power plant modules in HOMER. They presented the effectiveness of the method by two case studies of remote rural villages in Zambia and Honduras while also supporting the technological and financial feasibility of standalone photovoltaic/biomass HRESs. In both situations, the microgrid's ability to provide and distribute electricity had a lower LCOE than the alternative of connecting the villages to the electric grid. (Ribó-Pérez et al., 2021)

Baruah et al. studied the techno-economic viability of a standalone HRES for supplying power to a university campus in India. Solar energy, wind energy, syngas, biogas, and hydrokinetic energy were all taken into consideration for the system, with batteries serving as a backup. The HOMER-Pro software was utilised to model and simulate all scenarios based on hourly data input and they put various restrictions in place to constrain the component’s maximum installation capacity. They used the NPC, LCOE, battery storage, space needs, emissions, and employment potential as differentiating factors between the produced scenarios and used the Analytical Hierarchy Process (AHP) to determine the optimal solution. They concluded that the optimum HRES had an LCOE of $0.095/kWh and utilized photovoltaics, wind turbines, syngas, biogas, hydrokinetic and battery energy storage. They also conducted a sensitivity analysis to understand the behaviour of the system for a wider use in the area. (Baruah et al., 2021)

Eisapour et al. investigated and recommended a robust smart HRES to meet the electricity and heating needs of a university campus in Iran. To understand the campus's energy needs, main energy potentials, and geographic limitations, they conducted the necessary pre-assessments. They explored the viability of using a special integrated energy system to fulfil the load requirement of the campus using simulations, optimizations, and sensitivity analyses. Their results showed that the optimum energy system includes a micro gas turbine with a combined heat and power module, converters, thermal boilers, solar panels, a predictive controller, pumped hydro storage units, a COE of $0.09/kWh, and an NPC of $42.5 million. It also reduces the yearly $CO_2$ emissions of the campus by 8 Gt when compared to grid usage. An interesting finding that the authors reported was that LCOE and NPC were reduced by 15% and 6% respectively, when energy demand was reduced by 1% at certain times. (Eisapour et al., 2021)

Malik et al. conducted a case study of a standalone HRES with an environmental and techno-economic analysis. They produced simulations of HRESs that included and excluded ESSs in seven scenarios. The optimization and sensitivity analyses were done using the HOMER Software with the scaling criterion of total NPC. Their results showed that, with a contribution of 41% photovoltaics and 59% biomass, the photovoltaic, biomass gasifier and battery HRES was the most cost-effective design, with an estimated total NPC of $76,080 and COE of $0.185/kWh. Their sensitivity analysis showed that the most important factors of the system were solar radiation of the region, biomass gasifier lifetime, annual interest rate, annual capacity shortage, and biomass price. (Malik et al., 2021)

Fard et al. proposed an optimized way of managing energy to run a standalone HRES supporting a range of loads. The system that was presented included photovoltaics,

wind turbines, and an ESS with batteries and a fuel cell-reformer combination. The scope of this combination was to minimize the lifetime costs of the project. They investigated two technologies for hydrogen production in order to certify the benefits of the methodology proposed; and the model they built for each technology, links the variation between electricity and hydrogen to evaluate the best energy management approach. Their results show that the COE is reduced by 19% when municipal waste is used, coupled with a 27% decrease in fuel consumption. (Fard et al., 2021)

Ali et al. examined the techno-economic viability of prospective HRESs for the electrification of a rural community in Pakistan and in his paper provided a blueprint for other rural electrification projects. Initially, they did an extensive resource evaluation, and then with the HOMER Pro software, optimized the size of the system and evaluated the techno-economic viability for the supply of peak-load demand. Their results showed that a system utilizing photovoltaics as its primary energy source, batteries as storage, a diesel generator as backup, and a time-constrained availability of the national grid is the most practical solution given the lack of wind power and biomass resources in the area. They found that the LCOE of the grid-tied configurations was significantly lower than that of the standalone configurations with ranges of $0.072/kWh-$0.078/kWh and $0.145/kWh-$0.167/kWh, respectively. They concluded that the grid-tied system's LCOE was lower than the local government's tariff which made it an economically viable alternative. (Ali et al., 2021)

Singh & Basak investigated the problem of utilizing the excess rice straw that is produced by farmers. They presented a system which can use all this wasted biomass to produce energy and meet the electrical demands of 250 local village houses. Besides rice straw, the system also utilises photovoltaics, batteries, and the grid. The method by which the optimal size of the system was defined, was using the artificial bee colony algorithm. They also evaluated the proposal based on NPC, LCOE and annualized system cost. Their results indicated an LCOE of $0.089/kWh. (Singh & Basak, 2021)

Das, Alotaibi, et al. published a study in which they extensively examined the environmental and economic benefits of grid-tied and off-grid HRESs with various system configurations comprising of photovoltaics, wind turbines, batteries, and diesel generators for five distinct climatic zones. For their analyses they used the HOMER software. By incorporating the grid-connected alternative, a thorough techno-economic analysis of optimal hybrid systems is further investigated. They also explored the advantages of HRESs for the environment and investigated the sensitivity of various feed-in tariffs to the national grid. Furthermore, they examined the difficulties and possibilities of implementing such programs in standalone places. Their results showed that the COE of the grid-tied system with a feed-in tariff was $0.03/kWh (30%) lower than the cost per kWh of the grid, and that such a configuration could reduce annual $CO_2$ emissions by 45,582kg in comparison to the grid-only option. They found the same figure for the off-grid system to be 32,905kg annually. (B. K. Das, Alotaibi, et al., 2021)

Peláez-Peláez et al. investigated the use of an HRES that utilized technologies such as photovoltaics, a hydrogen fuel cell to produce heat and electricity, an electrolyser

to produce hydrogen and a tank to store it. A unique aspect of this study was that they used an absorption chiller along with a Heat Recovery Steam System to capture and use the heat produced by the fuel cell to satisfy the thermal demand. They used the HOMER software to optimize the NPC and COE of the system and found that the best system had a COE of $0.8399/kWh and NPC of $1,006,623 which deemed it economically unviable. (Peláez-Peláez et al., 2021)

As can be concluded by reviewing the relevant literature, many studies have been done on the use of HRESs for electrification purposes. These systems are applied to cases as small as a single household (Mokhtara et al., 2021) or even as large as cities (Yang et al., 2022). The components comprising them vary, but some are used in the vast majority. The most commonly used component for electricity generation is a photovoltaic due to the high availability of solar radiation in most study areas (Figure 22), its maturity, and its low installation, operation, and maintenance cost (Steffen et al., 2020). Another component that is used in almost all cases is an ESS. This is usually a battery or sometimes a hydrogen storage system with an electrolyser and fuel cell combination (Nasser et al., 2022; Peláez-Peláez et al., 2021; Singh et al., 2017). In a few studies, hydro storage has been examined (M. Das et al., 2019; Javed et al., 2021; Kusakana, 2016), but this is rare because of the special geological requirements and high cost associated with such ESSs (Hunt et al., 2020). An energy generating component that is also common but not as much as photovoltaics, is a wind turbine. One restriction this technology faces, is that the installation area needs to have an appropriate wind profile, otherwise it is deemed uneconomical. The presence of an appropriate wind profile is not as common as appropriate solar radiation which powers photovoltaics (Figure 23). Another disadvantage wind turbines have when compared to photovoltaics, is their large number of moving parts which need regular maintenance and thus increase costs (Steffen et al., 2020).

An energy generating component that has been examined less frequently than the two mentioned above is a biogas generator. This component uses biogas, syngas, or producer gas to power a motor coupled with an electric generator.

Biogas is produced through anaerobic digestion of organic matter (biomass) and has a high methane content. Syngas and producer gas are both produced through pyrolysis and gasification of biomass. Several studies have incorporated such technologies in their HRESs such as (Hossein Jahangir et al., 2022; Malik et al., 2022; Roy et al., 2022).

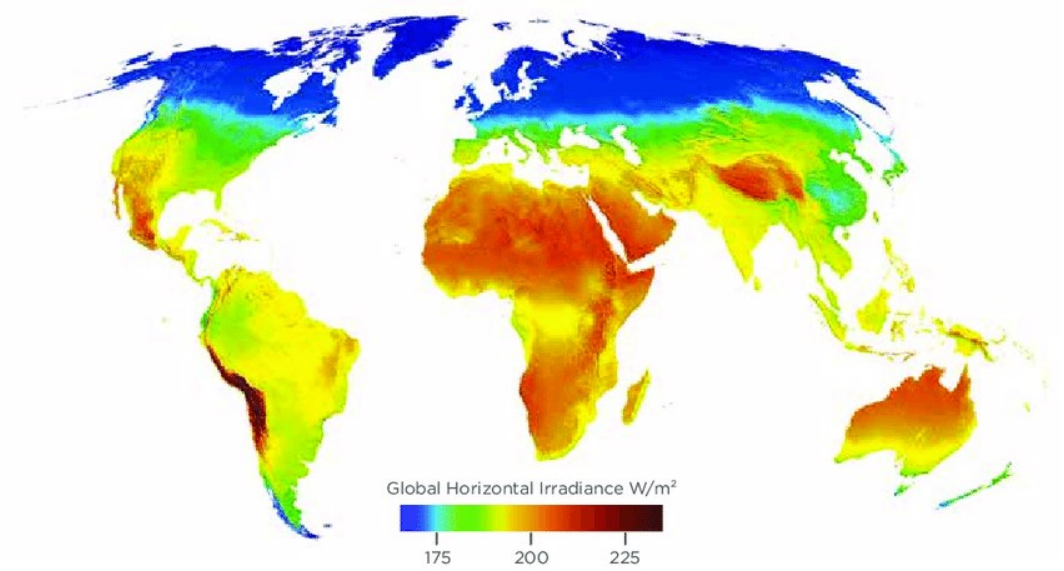


Figure 22: World solar potential (Commission on Geopolitics of Energy Transformation, 2019)

The type of biomass that is used for the production of these gases depends mostly on local availability. In the case study of this thesis, the biomass resources that are available are extracted olive pomace and broiler chicken feathers. In the relevant literature, very few studies were found that examined the gasification of extracted olive pomace (García-Ibañez et al., 2004; Gómez-Barea et al., 2005), but no studies that utilized this resource in an HRES. The gasification ratios reported in these studies range from 2.9 $Nm^3$/kgfuel-daf to 5.6 $Nm^3$/kgfuel-daf, when equivalence ratios were 0.41 and 0.73 respectively.

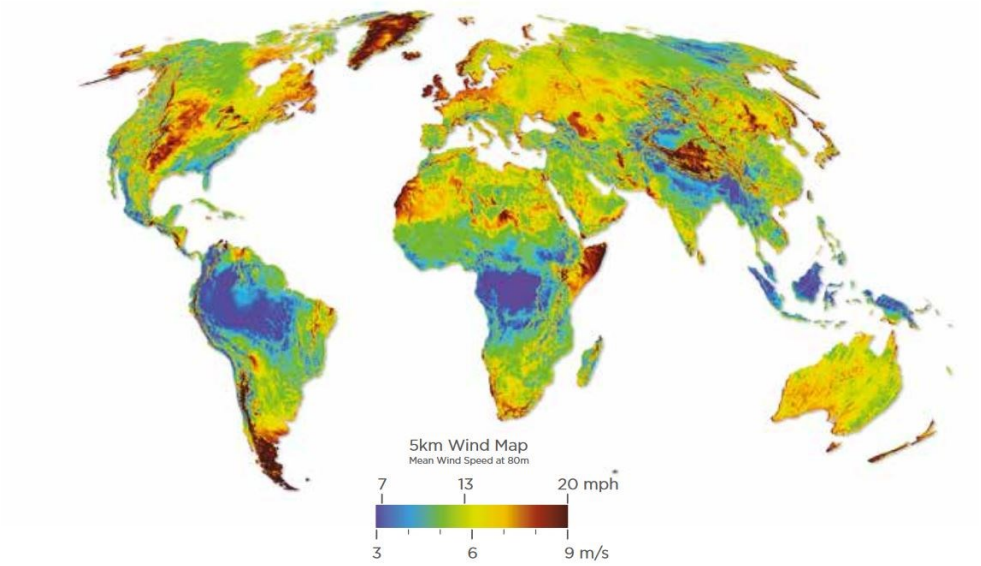


Figure 23: World wind potential (Commission on Geopolitics of Energy Transformation, 2019)

The gases produced had a maximum LHV of 3.8 MJ/Nm$^3$ (García-Ibañez et al., 2004). Studies have been done that examined the gasification of chicken feathers for energy production but again, not in the context of an HRES (Dudyński et al., 2012; Kwiatkowski et al., 2012, 2013; Mézes & Tamás, 2015). They found that syngas produced through feather gasification had an LHV of 1.96MJ/kg (Dudyński et al., 2012), with a gasification ratio of approximately 4.57. Problems that were found with the gasification of extracted olive pomace include the sintering or agglomeration of the bed material because of the high alkali content of this fuel, and a high dust content in the flue gases when a fluidised bed reactor was used. These problems were partially solved by using additives such as dolomite (Corella et al., 2004) or through leaching of the material before gasification to remove the alkali metals (Arvelakis et al., 2002). A problem that was identified in the gasification of feathers is the high sulphur content in the produced gas which requires cleaning with a scrubber before combustion to mitigate the negative effects of sulphur oxides on the environment (Dudyński et al., 2012).

There have been several studies that implemented an HRES to power an industrial consumer whether in a grid-connected or in an off-grid setting. In a grid-connected configuration, Wang et al. suggested a system consisting of photovoltaics, wind turbines, and a battery ESS which achieved a minimum LCOE of 0.3899CNY/kWh to power a drinking water treatment plant. As mentioned above, Buller et al. studied the implementation of a grid-connected and off-grid HRES with photovoltaics and a biomass gasifier, to power a wastewater treatment plant. The biomass used was sewage sludge from the same facility, and the gasification method was anaerobic digestion. They found an LCOE equal to $0.0298/kWh for the grid connected system and $0.0426/kWh for the off-grid configuration. In an off-grid configuration of photovoltaics, wind turbines, diesel generator and battery ESS, Diab et al. studied the powering of a factory and the town surrounding it in Egypt and their results showed an LCOE equal to $0.19/kWh.

Table 1: Literature regarding the use of HRESs

| Grid Type | No | Infrastructure (Load Type) | Location | Year | Data type | Baseline Load | Technical Components | | | | | Optimization Criterion | | |
|---|---|---|---|---|---|---|---|---|---|---|---|---|---|---|
| | | | | | | | PV | WT | BG | DG | ESS | Energy | Environmental | Economic |
| Off-grid | **1** | Community | Akita, Japan | 2022 | Hypothetical | High | - | X | X | - | X | - | - | COE=0.173 –0.435 USD/kWh) |
| Off-grid | **2** | Community | Uganda | 2020 | Hypothetical | High | X | - | - | X | X | - | - | 0.300$/kWh-0.879$/kWh |
| Grid-connected | **3** | Community | UK and Bulgaria | 2019 | Estimation | High | X | X | X | - | X | 83.5-85.2% | - | £0.222/kWh-£0.245kWh |
| Off-grid | **4** | Island | China | 2021 | Estimation | Medium | X | X | - | X | X | 100.0% | - | 0.243$/kWh |
| Grid-connected | **5** | Village | Himalaya | 2022 | Estimation | Low | X | X | X | - | X | 82% | Saves 27.8Mt CO2/yr | LCOE=0.099$/kWh |
| Grid-connected | **6** | Industry | Brazil | 2022 | Estimation | High | X | - | X | - | - | 100% | X | COE=0.0298USD/kWh (77% reduction) |
| Off-grid | **7** | Community | Barak, Libya | 2022 | Actual | High | X | X | - | - | X | 100% | - | COE=0.3€/kWh to 0.018€/kWh for RE-GES and 0.25€/kWh to 0.05€/kWh for RE-Battery. |
| Off-grid | **8** | Community | Nigeria | 2020 | Estimation | Low | X | X | - | X | X | 88.43-90.5% | 92.3% reduction | 79.8% reduction |
| Grid-connected and Off-grid | **9** | Community | Iran | 2020 | Estimation | High | X | X | X | - | X | 100.0% | 255,217–255,567kg/yr reduction | COE=$0.128/kWh-$0.223/kW h |
| Grid-connected and Off-grid | **10** | Community | India | 2020 | Estimation | Medium | X | X | X | - | X | 100.0% | 0.467kg/yr | COE=13.71Rs/Kwh |
| Grid-connected | **11** | Community | Beijing, China | 2022 | Estimation | High | X | - | X | X | X | 73% | Emissions=0.5416kg/kWh | LCOE=0.1030$/kWh |
| Grid-connected and Off-grid | **12** | Cattle barns | Turkey | 2022 | Estimation | Low | X | - | X | - | - | 100% | - | COE=0.0292$/kWh-0.0464$/kWh |

| | | | | | | | | | | | | | | |
|---|---|---|---|---|---|---|---|---|---|---|---|---|---|---|
| Off-grid | **13** | Community | Bangladesh | 2022 | Estimation | Low | X | X | - | X | X | - | X | LCOE=0.213$/kWh-0.6$/kWh |
| Grid-connected and Off-grid | **14** | Community | Turkey | 2022 | Estimation | High | X | X | X | X | X | X | X | X |
| Off-grid | **15** | Community | Iraq | 2022 | Estimation | High | X | - | - | X | X | 41.30% | 851,377kg/yr | 0.152$/kWh |
| Off-grid | **16** | City | Tehran, Iran | 2022 | Actual | High | X | X | X | - | X | 100% | 130 times reduced | 0.281$/kWh |
| Grid-connected | **17** | Power station | Ireland | 2022 | Actual | High | - | X | X | - | X | - | - | - |
| Grid-connected | **18** | City | Italy | 2022 | Estimation | High | X | X | - | - | X | X | 13kg/yr | 0.721€/kWh |
| Off-grid | **19** | City | Iran | 2019 | Estimation | High | X | X | - | X | | 18.3-41% | 1,714,716-2,449,769kgCO2/yr | COE=0.303$/kWh-0.336$/kWh |
| Grid-connected and Off-grid | **20** | Islands | Canary Islands | 2022 | Estimation | High | X | X | - | - | X | >41.2% | 58%-70% reduction | COE decreased by 23% and 25.3% |
| Off-grid | **21** | Hydrogen production plant | Egypt | 2022 | Estimation | Medium and High | X | X | - | - | - | 100% | - | 4.54$/kg - 7.48$/kg H2 |
| Grid-connected and Off-grid | **22** | Energy production plant | Oujda, Morocco | 2022 | Hypothetical | High | X | X | - | - | X | - | - | LCOE=0.11$/kWh-0.225$/kWh |
| Off-grid | **23** | Community | Uttarakhand, India | 2022 | Estimation | High | X | X | - | X | X | 93% | 90% reduction | LCOE=0.196$/kWh |
| Grid-connected | **24** | Village | Punjab, India | 2021 | Estimation | High | X | - | X | - | - | - | - | 4.67Rs/kWh |
| Off-grid | **25** | Island | Saint Martin, Bangladesh | 2021 | Estimation | High | X | X | X | - | X | 100% | 16,302 kg CO2-eq/yr | COE=0.195$/kWh |
| Grid-connected | **26** | Industry | Huili county, China | 2021 | Actual | Low | X | X | - | - | X | 95% | 71.18% decrease | LCOE=0.3899CNB/kWh-0.5531CNB/kWh |
| Grid-connected | **27** | Port | Crete, Greece | 2021 | Actual | High | X | X | - | X | X | 100% | 100% decrease | LCOE=0.08€/kWh-0.129€/kWh |
| Off-grid | **28** | Community | Honduras and Zambia | 2021 | Estimation | Low-Medium | X | - | X | - | X | 100% | - | 0.06USD/kWh |
| Off-grid | **29** | Community | Australia | 2021 | Estimation | High | X | X | - | X | X | - | 18,043–23,902 kgCO2/yr | COE=0.255$/kWh-0.406$/kWh |

| | | | | | | | | | | | | | | |
|---|---|---|---|---|---|---|---|---|---|---|---|---|---|---|
| Grid-connected | **30** | University Campus | Nigeria | 2022 | Actual | High | X | X | - | X | X | 51.3% | 5,192,407kgCO2/yr | COE=0.09478$/kWh-0.11$/kWh |
| Off-grid | **31** | Academic township | Sikkim, India | 2021 | Actual | High | X | X | X | - | X | 100% | 990,301 kgs of. CO2, 3,644 kgs of CO and 1,764 kgs of NOx | LCOE=0.095$/kWh |
| Off-grid | **32** | University Campus | Iran | 2021 | Estimation | High | X | X | X | X | X | - | 8Gt CO2 emission reduction | LCOE=0.09$/kWh |
| Off-grid | **33** | Community | India | 2021 | Estimation | Low | X | X | X | X | X | 100% | 27.8 Mt CO2/year reduction | 0.185€/kWh |
| Grid-connected | **34** | Not specified | Not specified | 2021 | Hypothetical | Unclear | X | X | - | - | X | X | X | X |
| Grid-connected | **35** | University Campus | Cyprus | 2021 | Actual | High | X | X | - | - | X | 99.59% | - | 0.1626 $/kWh |
| Grid-connected and Off-grid | **36** | Community | Pakistan | 2021 | Actual daily, Estimated hourly | High | X | - | - | X | X | - | - | 0.072$/kWh-0.078$/kWh |
| Grid-connected | **37** | Village | India | 2021 | Estimation | High | X | - | X | - | X | 100% | - | LCOE=0.089 $/kWh |
| Grid-connected | **38** | Energy production plant | Jordan | 2021 | Hypothetical | High | - | X | - | - | X | 100% | - | LCOE=0.13-0.15$/kWh |
| Grid-connected and Off-grid | **39** | Villages | Bangladesh | 2021 | Estimation | High | X | X | - | X | X | 68-100% | 45,582kg-CO2/yr reduction | LCOE=0.07$/kWh |
| Grid-connected and Off-grid | **40** | Villages | India | 2016 | Hypothetical | High | X | - | - | - | X | 100% | X | 0.135$/kWh |
| Grid-connected and Off-grid | **41** | Irrigation system and RO desalination plant | Egypt | 2019 | Estimation | Low | X | - | - | X | X | 100.0% | 86,511 kg/year reduction | COE=0.059$/kWh |
| Grid-connected | **42** | House | Sidhwanbet, Punjab, India | 2022 | Estimation | Low | X | - | X | X | X | 100% | 99.90% | COE=0.362$/kwh |
| Off-grid | **43** | Industry | Makkah, Saudi Arabia | 2021 | Actual | High | - | X | - | X | X | 60.50% | 64.20% | NPC reduction: 13.84% |
| Off-grid | **44** | Village | West Bengal, India | 2022 | Estimation | High | X | X | X | - | X | 100% | 57.37% | LCOE=0.1967$/kWh |
| Grid-connected and Off-grid | **45** | Village | India | 2017 | Estimation | Medium | X | - | X | X | X | 89%-100% | - | COE=0.145$/kWh |

| | | | | | | | | | | | | | | |
|---|---|---|---|---|---|---|---|---|---|---|---|---|---|---|
| Grid-connected and Off-grid | **46** | Village | India | 2018 | Estimation | High | X | - | - | X | X | - | - | COE=5.41INR/kWh |
| Grid-connected and Off-grid | **47** | Village | India | 2016 | Estimation | Medium | X | X | - | X | X | 100% | 0kg | 0.111$/kWh |
| Off-grid | **48** | Community | South Africa | 2016 | Estimation | Low | X | X | - | X | X | - | - | - |
| Off-grid | **49** | Town and factory | Egypt | 2016 | Estimation | High | X | X | - | X | X | 73% | 113,987.71kg/yr | 0.19$/kWh |
| Grid-connected | **50** | City | Canada | 2019 | Actual | High | X | X | X | - | X | 100% | 3.9-4.6GHG CO2eq tonne/yr | 0.385USD/kWh |
| Off-grid | **51** | House | Saudi Arabia | 2021 | Estimation | Low | X | X | - | - | X | 100.0% | 0kg/yr | LCOE=0.4381$/kWh-0.5646$/kWh |
| Off-grid | **52** | Airport and Sea Water Reverse Osmosis plant | Egypt | 2021 | Estimation | High | X | X | - | X | X | 11.2% | 59.5% reduction | 0.089 $/kWh |
| Grid-connected and Off-grid | **53** | Village | South Africa | 2018 | Estimation | High | X | X | - | - | - | 100% | - | 7.54-21.02USD/kWh |
| Off-grid | **54** | Village | Benin | 2020 | Estimation | High | X | - | - | X | X | 97% | 97% CO2 reduction | 0.207$/kWh |
| Off-grid | **55** | Sea Water Reverse Osmosis plant | Iran | 2018 | Estimation | Medium | X | - | - | X | X | - | 37,940kg emission reduction | 0.3975 $/kWh-0.5975 $/kWh |
| Grid-connected | **56** | Residential Building | China | 2020 | Estimation | High | X | X | - | - | X | 81.3% | - | 0.2230 $/kWh |
| Off-grid | **57** | House | Pakistan | 2019 | Estimation | Low | - | X | - | X | X | 100% | 100% reduction | COE=0.309$/kWh |
| Off-grid | **58** | House | Turkey | 2018 | Hypothetical | Medium | X | X | - | X | X | 95-100% | - | COE=0.186$/kWh |
| Off-grid | **59** | Charging station | Spain | 2018 | Hypothetical | High | X | - | - | - | X | 100% | 100% reduction | 0.25-0.4€/kWh |
| Grid-connected | **60** | Community | Ghaza | 2022 | Estimation | High | X | - | X | X | X | 64.30% | 6.4 times less CO2 | NPC=$2.3M. COE=$0.438/kWh |
| Off-grid | **61** | Community | Western Australia | 2022 | Estimation | High | X | X | X | - | X | 95% | Lifetime emissions= 46,258–104,664 kg CO2-eq/yr | COE=0.126–0.187$/kWh |
| Grid-connected and Off-grid | **62** | Research facility | Thailand | 2022 | Actual | High | X | X | X | - | X | 100% | Net-zero emissions | NPC=4,136,254$ COE=0.0411$/kWh |

| | | | | | | | | | | | | | | |
|---|---|---|---|---|---|---|---|---|---|---|---|---|---|---|
| Off-grid | **63** | Villages | Colombia | 2016 | Estimation | Medium and High | X | X | - | X | X | X | X | X |
| Grid-connected | **64** | Laboratory | USA | 2017 | Actual | High | X | - | - | X | X | - | 5,925,155 kg reduction of CO2 | X |
| Off-grid | **65** | Town | Yemen | 2017 | Estimation | High | X | X | - | X | X | 64% | 100% reduction | 0.137-0.188$/kWh |
| Off-grid | **66** | Telecommunication applications | India | 2017 | Actual | Low | X | X | - | X | X | X | - | 0.164-0.271$/kWh |
| Off-grid | **67** | Community | East Malaysia | 2017 | Estimation | Medium | X | - | - | X | X | 100% | 100% reduction | 0.323-0.638$/kWh |
| Off-grid | **68** | Radio transmitter station | India | 2019 | Actual | High | X | - | X | - | X | 100.0% | - | LCOE=0.4864$/kWh |
| Off-grid | **69** | Household | Nigeria | 2019 | Estimation | Low | X | X | - | X | X | 63-100% | 84.98-91.53% reduction | 0.459-0.562USD/kWh |
| Off-grid | **70** | Island | Malaysia | 2017 | Estimation | - | X | X | - | X | X | 41.6% | 2,571,131kg/yr | 0.279$/kWh |
| Off-grid | **71** | House | Saudi Arabia | 2017 | Hypothetical | Low | X | X | - | - | X | 100% | 0kg/yr | 0.609-1.615$/kWh |
| Off-grid | **72** | Community | Bangladesh | 2021 | Estimation | High | X | X | | X | X | 89% | 40,239CO2eq/yr | COE=0.234 $/kWh |
| Off-grid | **73** | Research facility | India | 2017 | Estimation | Medium | X | - | - | - | X | 100% | 0kg/yr | 0.203$/kWh |
| Off-grid | **74** | Village | Algeria | 2017 | Estimation | High | X | X | - | X | X | 96% | 593,125tons/yr reduction | 0.176$/kWh |
| Off-grid | **75** | Island | South Korea | 2016 | Estimation | High | X | X | - | - | X | 100% | - | 0.326$/kWh |
| Off-grid | **76** | House | Iran | 2016 | Estimation | Low | X | X | - | - | X | - | - | 0.783-1.443$/kWh |
| Off-grid | **77** | Island | Maldives | 2021 | Estimation | High | X | X | - | X | X | 96.0% | 96% reduction | 0.23$/kWh |
| Off-grid | **78** | House | Algeria | 2021 | Estimation | Low | X | X | - | X | X | 100.0% | 0kg/yr | 0.21$/kWh |
| Off-grid | **79** | Community | Iceland | 2015 | Unknown | High | - | X | - | X | - | 40-89% | Diesel consumption information | 0.295$/kWh |
| Grid-connected and Off-grid | **80** | Island | Turkey | 2015 | Estimation | High | X | X | - | - | - | 68% | 0.389kgCO2/kWh reduction | 0.836-1.016$/kWh |
| Grid-connected and Off-grid | **81** | Island | South Korea | 2014 | Estimation | High | X | X | - | X | X | - | - | 0.230-0.273$/kWh |
| Off-grid | **82** | Sea Water Reverse Osmosis plant | Egypt | 2020 | Estimation | High | X | X | - | X | X | 74% | 81.5% CO2 reduction | 62% lower COE compared to DG |
| Off-grid | **83** | Sea Water Reverse Osmosis plant | Egypt | 2020 | Estimation | High | X | X | - | X | X | 93.1% | 94% reduction | 0.107$/kWh |

| | | | | | | | | | | | | | | |
|---|---|---|---|---|---|---|---|---|---|---|---|---|---|---|
| Off-grid | **84** | Sea Water Reverse Osmosis plant | Canary Archipelago | 2019 | Estimation | Medium | X | X | - | X | X | 92-96% | 80,029.88-84,872.15kg/yr emissions | 0.404 $/kWh-0.478$/kWh |
| Grid-connected and Off-grid | **85** | Hotel | Turkey | 2013 | Actual | High | X | X | - | - | X | 74% | - | - |
| Off-grid | **86** | Island | Malaysia | 2013 | Estimation | High | X | X | - | X | X | 100% | 100% reduction | 0.821-1.230$/kWh |
| Off-grid | **87** | Village | Ethiopia | 2019 | Estimation | Medium | X | X | - | X | X | 94% | 37.3 tons CO2 reduction | 0.207$/kWh |
| Off-grid | **88** | Village | Algeria | 2019 | Estimation | Medium | X | - | - | X | X | 93% | 1,994.5kg/yr CO2 emissions | COE=0.37$/kWh |
| Off-grid | **89** | Industrial Park | China | 2020 | Actual | High | X | X | - | - | X | 100% | 0kg/yr | LCOE=0.226$/kWh |
| Off-grid | **90** | Residential | Spain | 2021 | Estimation | Medium | X | - | - | - | X | 100% | 0kg/yr | COE=$0.8399/kWh |
| Off-grid | **91** | City | UAE | 2021 | Actual | High | X | - | - | X | X | 68.1% | 83.2% reduction | LCOE=0.346$/kWh |
| Grid-connected | **92** | Town | Pakistan | 2018 | Estimation | High | X | X | X | - | - | 87.7% | 19,976.607kg/yr reduction | LCOE=0.05744 $/kWh |
| Off-grid | **93** | Research facility | Brazil | 2013 | Estimation | Low | X | - | - | - | X | 100% | - | 0.657-1.351$/kWh |
| Grid-connected and Off-grid | **94** | Community | China | 2020 | Estimation | High | X | X | X | - | X | 100% | 133,970kg reduced CO2 emissions | COE=$0.201/kWh |
| Off-grid | **95** | University Campus | Turkey | 2012 | Estimation | High | X | - | - | X | X | 38% | 72,857kgCO2/yr | 0.256-1.051$/kWh |
| Off-grid | **96** | City | Pakistan | 2022 | Actual | High | X | X | - | - | X | 100.0% | - | LCOE=0.117$/kWh-0.133 $/kWh |
| Grid-connected | **97** | City | China | 2022 | Estimation | High | X | X | - | - | X | - | - | LCOE= 0.1$/kWh-0.2618$/kWh |
| Grid-connected and Off-grid | **98** | Village | China | 2022 | Estimation | High | X | X | X | - | X | 100.0% | 120,284kg/yr reduction | COE=0.084$/kWh-0.131$/kWh |
| Off-grid | **99** | Laboratory | Greece | 2011 | Actual | Medium | X | - | - | X | X | 100% | 0kg/yr | 0.650-1.920€/kWh |
| Off-grid | **100** | University Campus | Turkey | 2011 | Actual | High | X | X | - | - | X | 25% | 117,755kgCO2/yr | 3.391-3.847$/kWh |

A topic that has extensively been researched is the implementation of an HRES for the electrification of rural communities either in cases where there was no electricity at all, or in cases where there was a grid, but the production of energy was very expensive and/or polluting because of the sole use of diesel generators (Table 1). HRESs are also used for the electrification of remote and off-grid islands. Such a study was done by P. Das et al., in 2021, where they studied the application of an HRES on an off-grid island in Bangladesh. The proposed system consisted of photovoltaics, wind turbines, a diesel generator and batteries and had an LCOE of $0.234/kWh. The excess energy of the system would be used to produce drinking water in a seawater desalination facility. The novelty of their study was that they also calculated that their system would create 1.64 new jobs. Along the same lines, Odou et al. studied an HRES consisting of photovoltaics, a diesel generator, and batteries for the electrification of a remote off-grid village in Benin. They found that with the addition of the diesel generator to the system, battery capacity could be reduced by 70% compared to the photovoltaics and battery system. They also found that the $CO_2$ emissions were reduced by 97% when compared to the diesel generator-only system. Gebrehiwot et al. also studied the electrification of a rural village. Their case study was a remote, off-grid village in Ethiopia with an estimated daily peak demand of 19.6kW. The proposed system utilises photovoltaics, wind turbines, batteries, and a diesel generator and has an LCOE of $0.207/kWh and an NPC of $82,734.

When it comes to biomass utilisation in the context of an HRES, Li et al. studied a village in China and proposed the use of biogas produced from the anaerobic digestion of manure, which was available in the village. The system they proposed also utilised photovoltaics, wind turbines and batteries. They studied both grid-connected and off-grid scenarios. They found that in the off-grid scenarios, the optimal configuration had a COE of $0.131/kWh and an NPC equal to $420,486. In the grid-connected case they found the optimal system to have a COE of $0.084/kWh and an NPC equal to $369,461.

Also utilising manure for biogas production, Ahmad et al. studied the implementation of a grid-connected HRES that utilised photovoltaics, wind turbines and a generator running on biogas, to power a town called Kallar Kahar in Pakistan. They calculated an optimal LCOE equal to $0.05744/kWh and a system cost of $180.2 million for 73.6MW peak load. Murugaperumal et al. studied the electrification of a rural village in India using an HRES that utilizes photovoltaics, wind turbines, batteries, and a biogas generator that uses biogas produced through the anaerobic digestion of rice husks and manure. They explored the possibility of a standalone and grid-connected system and concluded that the standalone configuration was optimal with an LCOE of 13.71Rs/kWh and NPC of 1.21 million Rs. Jahangir & Cheraghi explored the technoeconomic and environmental parameters of implementing an HRES to provide electricity in an off-grid setting to a village in Iran. Their optimal system comprises of photovoltaics, batteries and a biogas generator that uses biogas produced through anaerobic digestion of local agricultural and animal wastes. This configuration had a minimum LCOE equal to $0.128/kWh.

# 3. Methodology

In this chapter of the thesis, the collection methods for the data that was used in the analysis will be presented. Furthermore, the details of the case study will be laid out and the methods of analysis will be explained. More specifically, the data that was collected includes:

- Hourly electricity demand in kWh.
- Hourly electricity rates in €/kWh.
- Total consumption of olive pomace in kg.

## 3.1. Selection of the test site for the case study

The test site that was selected for this case study, is a poultry slaughterhouse and a compound feed production plant in Laconia, Greece. This test site was selected because the author has personal experience from working in the slaughterhouse and thus has a good understanding of the processes that take place there. Regarding the compound feed production plant, his personal knowledge was not as extensive, but any information required, was provided by the plant owner and operator.

## 3.2. Case study description

In this case study, there are two production plants that together form the load profile that is considered. The first one is a poultry slaughterhouse combined with a poultry processing plant. The second one is a compound feed production plant. The processes and operations that take place in both plants will be described in the next chapters.

## 3.3. General information about the area of the case study

The two production plants are stationed at a distance of 100m from one another and approximately 20km to the south of Sparta, which is the capital of the region of Laconia (Figure 24). The climate of this area is Mediterranean with mild winters and hot summers. Snow is rare at low altitudes but very common on the two mountains, Parnonas and Taygetos that are on the east and west side of it respectively.

Figure 24: Laconia within Greece

The population of Laconia is 84,469 as of 2021 and its area is 3,639km$^2$.

### 3.3.1. Poultry slaughterhouse and processing plant

The poultry slaughterhouse that will be studied in this thesis, slaughters organic broiler chickens that are approximately 90 days old. This is worth mentioning because the energy requirements are slightly different than the case of conventionally grown chicken that are approximately 35-40 days old. This difference is mainly found in the defeathering process because the 90 days old chicken require slightly higher temperature and longer time in the hot water bath before the defeathering machine.

The whole process starts the day before the actual slaughter takes place. 15 hours before the scheduled slaughter time, a boiler that uses exhausted olive pomace (or diesel as backup) is fired up to start heating the water required for defeathering. The hot water bath has a capacity of 6m$^3$ and must be maintained at a constant temperature of 55.5$^o$C when chickens are passing through it. When it is almost dark, workers go into the barn, catch the chickens, and put them in special crates so they can be transported to the slaughterhouse. The next morning, a visual inspection of all the machinery is done. If everything is ready, the chain is started and the stunning and killing machines are turned on. Chickens are first stunned using electricity and water and then a cut is made near the base of the head to exsanguinate them. After exsanguination, chickens are dead and the carcasses are put through the hot water bath to loosen the feathers for the defeathering machine. The defeathering machine used in this facility, has 12 electrical motors that turn rubber fingers at a fast rate. These fingers stick to the feathers and thus remove them from the skin. After defeathering, cleaning takes place, and the head from most chickens is removed,

apart from some roosters that are sold with the head and feet still attached. After this, a circular cut is made around the cloaca, to separate the intestines from the rest of the body. Afterwards, a straight cut is made from the cloaca towards the chest, the intestines are removed and a general inspection of the carcass in conducted. Then, the oesophagus and lungs are removed, and the carcass is cleaned internally. After this, the feet are removed, and the carcass is submerged on the far end of the chiller. This is a large semi-circular tank with water at a temperature of 0.5$^{o}$C and a large metal screw that slowly pushes the carcasses through the cold water to the other side. After about 20 minutes in the cold water, carcasses have reached almost 12$^{o}$C and are ready to be sorted and processed according to customer orders. When the carcass is cut according to the customers' orders, it is packaged, weighed, and refrigerated (0-4$^{o}$C) or frozen (-18$^{o}$C).

A general flow chart of the above process can be seen in Figure 25. The colouring represents intensity of energy usage. Green is for low intensity, yellow for medium and red for high intensity.

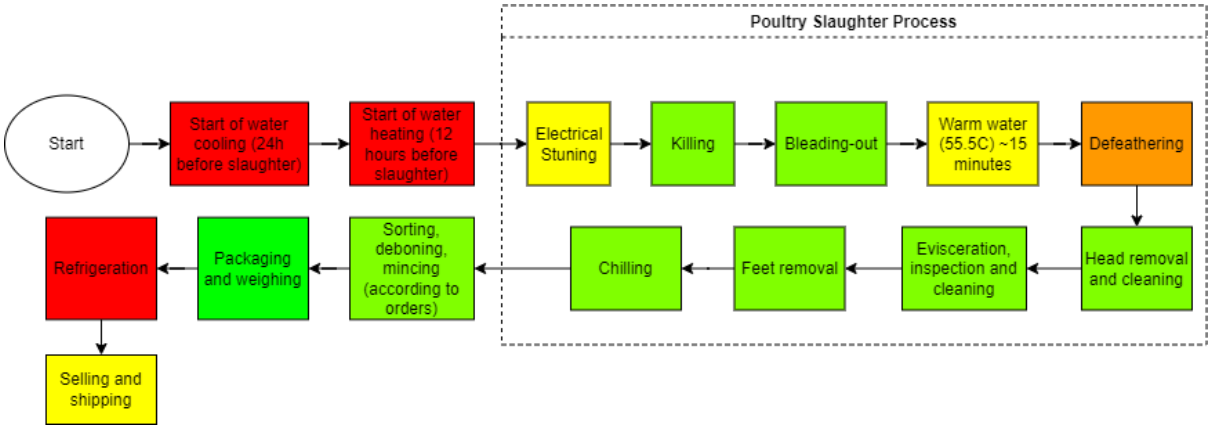


Figure 25: Poultry slaughterhouse process chart flow

### 3.3.2. Compound feed production plant

The compound feed production plant (Figure 26) produces compound feed for a variety of production animals such as broiler chickens, laying hens, pigs, sheep, and cows.

Figure 26: Compound feed production plant of the case study

This feed is sold in the form of pellets (Figure 27) for large animals such as cows or sheep, or in the form of crumbs for poultry (Figure 28).

Figure 27: Compound feed pellets

It is also possible to produce feed that is just mixed ingredients (Figure 29).

Figure 28: Compound feed crumbled (Gantz Andrea, 2022)

In the case of producing feed by just mixing ingredients, no steam is used and thus, no thermal load occurs. In this case, the electrical load is also lower because the pelleting press is not used.

Figure 29: Mixed, non-pelletized feed (pelletizermill.com, 2023)

## 3.4. Load profile

These facilities each have a distinct electrical and thermal load profile. However, accurate data on the thermal load was not available and therefore it is estimated.

### 3.4.1. Electrical Load

The electrical load profile available, was a combination of the demands of the slaughterhouse and the feed production plant. There are no available distinct

measurements for the two facilities. However, due to the known operating hours of the feed production plant (Monday to Friday 08:00-16:00) and the knowledge of the author regarding the processes that take place there, it is safe to attribute any electrical load outside of the aforementioned operating hours, to the slaughterhouse.

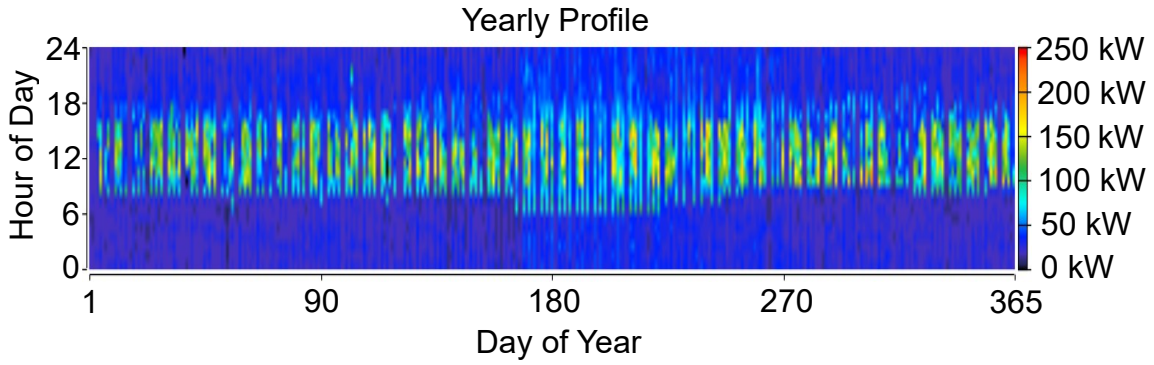


Figure 30: Electrical load profile for 2021

Hourly electrical load data for these two facilities combined, was obtained from the electricity provider. This data starts at the 1st of August 2020 and spans until the 31st of October 2022. The data that was used, was from the 1st of January 2021 00:00, up until the 31st of December 2021, 23:00. In Figure 30, a heat map of the electrical load throughout the year can be seen.

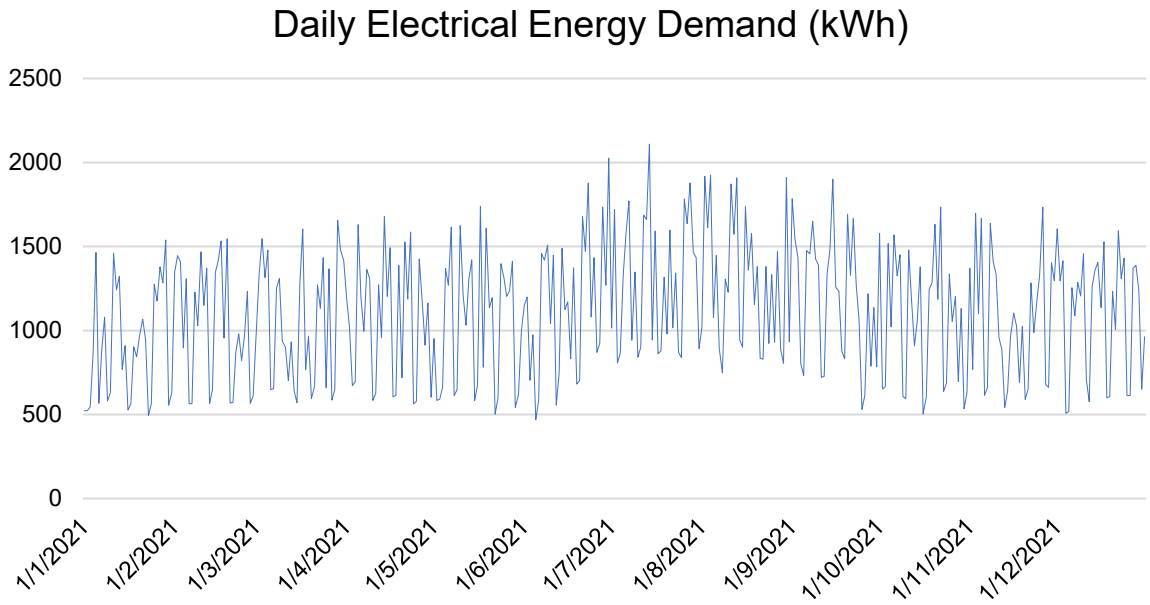


Figure 31: Daily electrical energy demand

It is worth noting that this industry is connected to the medium voltage distribution network and owns one AC/AC 20000V/400V transformer for the slaughterhouse and feed production plant.

Figure 31 makes it clear that, during the summer months there is an increase in the electrical energy demand. This can be attributed to the increased cooling needs of the

poultry processing plant due to the high ambient temperatures that the study area experiences during that season.

The mean daily electrical load profile of 2021 is depicted in Figure 32.

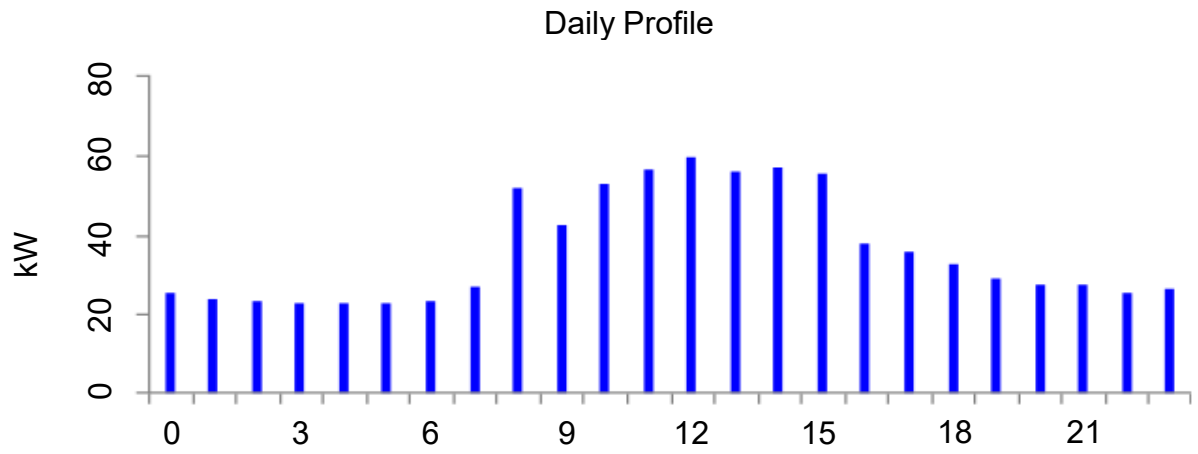


Figure 32: Daily Profile of electric load

The chart of the daily electric load profile depicts a substantial use of electricity even during nighttime hours. This is in large part due to the constant need for refrigeration in order to keep the products at the right temperatures in the poultry processing plant.

The seasonal electrical load profile of 2021 is depicted in Figure 33.

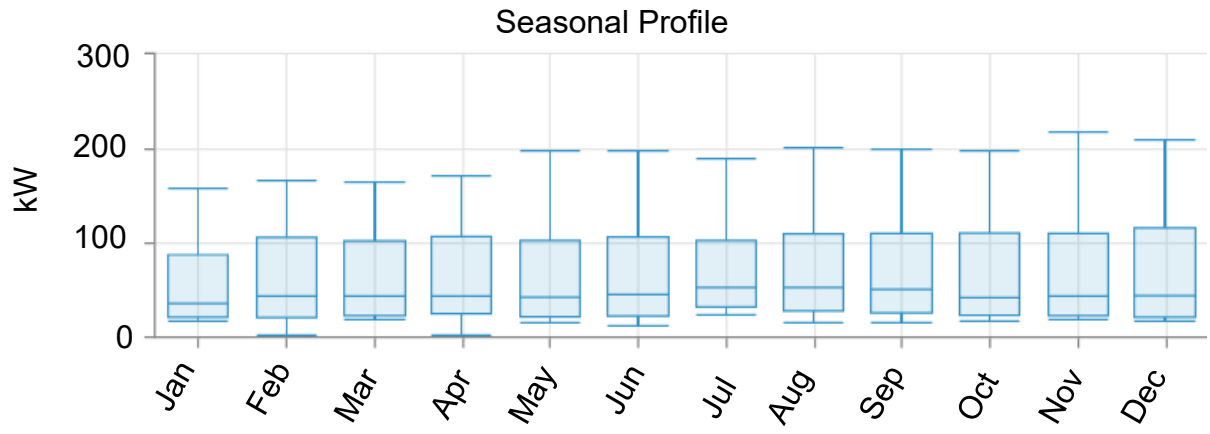


Figure 33: Seasonal Profile of electric load

A slight drop in electricity consumption is observed in January, February, and March which is mostly due to the lower ambient temperature, which results in reduced refrigeration needs.

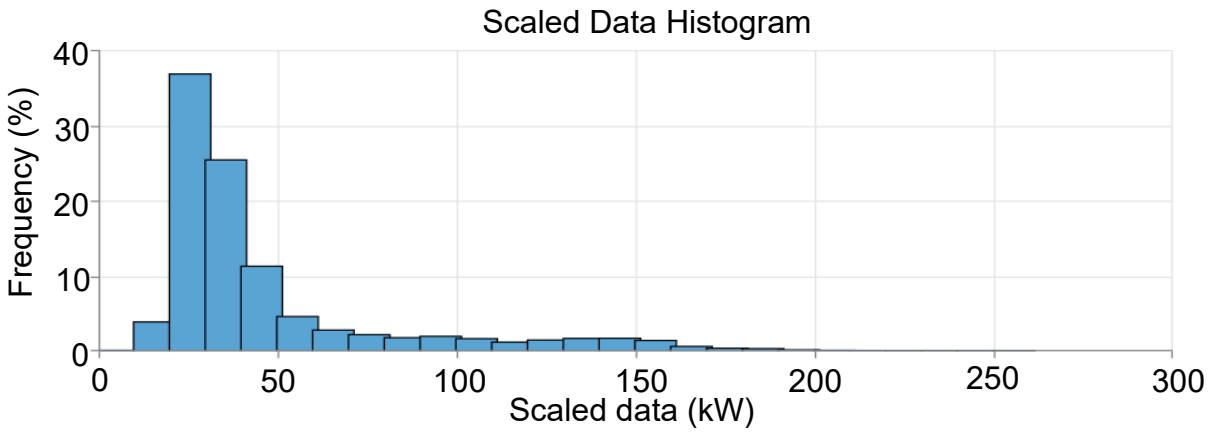


Figure 34: Load frequency histogram of the selected industry from the year 2021

The load frequency histogram that can be observed in Figure 34, shows that electric loads of less than 50kW are the most frequent. This is due to the fact that the 10-50 kW range is the load that the cooling systems induce on the system. This is present at all times. However, at times when the rest of the poultry house is not operating, (approximately 16 hours per day), this load is the only one present one making it the most commonly occurring value range for the electric load.

### 3.4.2. Thermal Load

The thermal load was not available in hourly timestep data. The data that was available was purchased quantities of extracted olive pomace and the date of purchase from January 2021 up until August 2022. From personal knowledge and after consulting the plant owner, a load profile was created for a typical week and then differentiated for the whole year according to the ambient temperature and a small random variability factor. This estimated profile can be seen in Figure 35 and Figure 37.

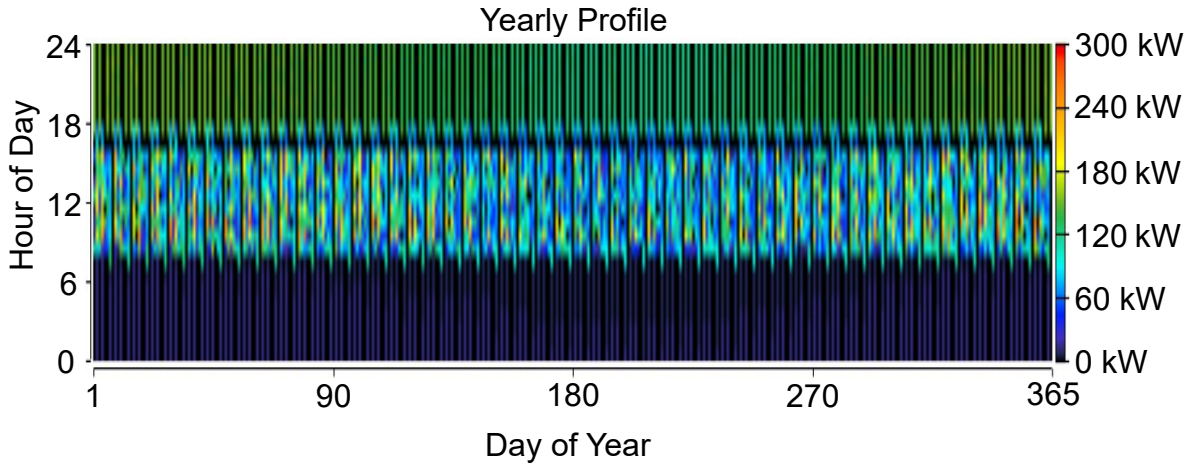


Figure 35: Thermal load estimated profile for one year

At the moment all the thermal energy in both plants is produced by underfeed screw biomass boilers (

Figure 36, Figure 38) that use extracted olive pomace as their primary fuel but have the capacity to use diesel if for whatever reason the extracted olive pomace is unavailable.


Figure 36: Type of underfeed screw biomass hot water boiler operating in the poultry slaughterhouse. (schmid-energy.ch, 2023)

1. Fuel inlet via stoker screw
2. Cast burner pan with primary air feed
3. Combustion chamber
4. Secondary air
5. Burnout grate
6. Automatic discharge of the grate ash
7. Ash container for grate ash
8. Radiation roof (variable for varying moisture content of fuel)
9. 3-pass heat exchanger
10. Front door with automatic fire tube cleaning system of fire tubes
11. Flue gas cleaning using multi-cyclone with automatic discharge of ash particles
12. Tank for ash particles
13. Flue gas fan (optionally to right, left or at rear)
14. Operating and inspection door to combustion chamber

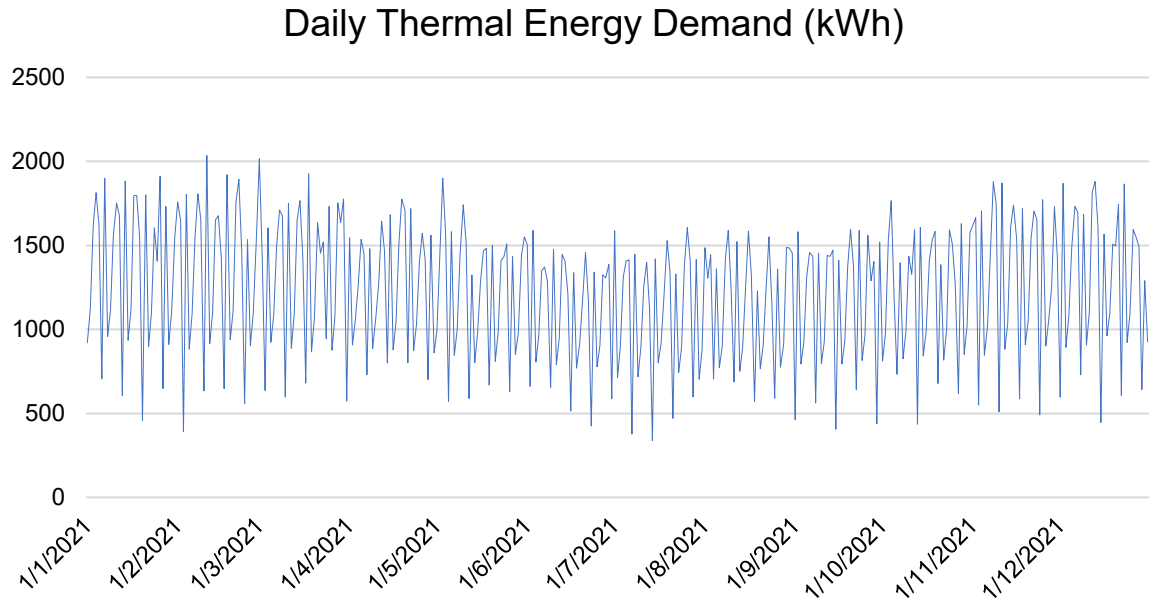


Figure 37: Daily thermal energy demand

The boiler that operates at the compound feed production plant is designed differently because its purpose is the generation of heat to vaporize water and create steam, instead of just warm water.


Figure 38: Type of underfeed screw biomass steam boiler operating at the compound feed production plant (hurstboiler.com, 2023)

## 3.5. Availability assessment of renewable resources

The study area has a latitude equal to 36.95 and a longitude equal to 22.4816. The meteorological data that was used, included:

- Wind speed at a height of 10m (m/s),
- All Sky Surface Shortwave Downward Irradiance (Wh/$m^2$),
- Temperature at 2m ($^oC$).

The data was obtained from the POWER Project's Hourly 2.0.0 version on 2022/12/01. (*POWER | Data Access Viewer*, 2022) The period for which this data was downloaded, spans from the 31st of December 2011 until the 31st of December 2021. The reasons behind the selection of this period are the following:

- Over the span of 10 years, any extreme single-year events will not skew the average very much,
- It is the most recent decade, and as such, has the highest chance of being representative of the years to come,

The data from the POWER Project starts on 1AM of the selected date, while the HOMER software assumes that the first value corresponds to midnight. To compensate for this difference, the starting date for the downloaded data is set to one day before the actual date from which data will be used. If this adjustment was not made, real-time electrical load data and meteorological data would have a 1-hour difference throughout the year resulting in errors when estimating the contribution of photovoltaics in real-time electricity production.

The data that was directly available in HOMER, was monthly averages, with the most recent being December 2013 for wind and temperature data, and June 2005 for solar data. This was deemed unsatisfactory because it does not consider the last 8 years, and hourly adjustments for photovoltaics cannot be made. Another issue with the wind data available in HOMER, was that it represented values at the height of 50m, instead of 10m that was appropriate for the available wind turbine.

The hourly values of all meteorological data that were obtained from the POWER Project, were processed as follows:

- First of all, in 2012, 2016 and 2020 the values on the 28th of February, were replaced by the average values for the 28th and 29th of February of the same year.
- Then, the 29th of February was deleted, to create a constant number of hourly values for each year (8760).
- After this, 8760 values were created, one for every hour of the year, and were calculated as the average of all years for that hour.

These calculated averages were imported to the HOMER software for all simulations.

In Figure 39, the average wind speed at the study area is plotted, and in Figure 40, the monthly average temperature can be seen.

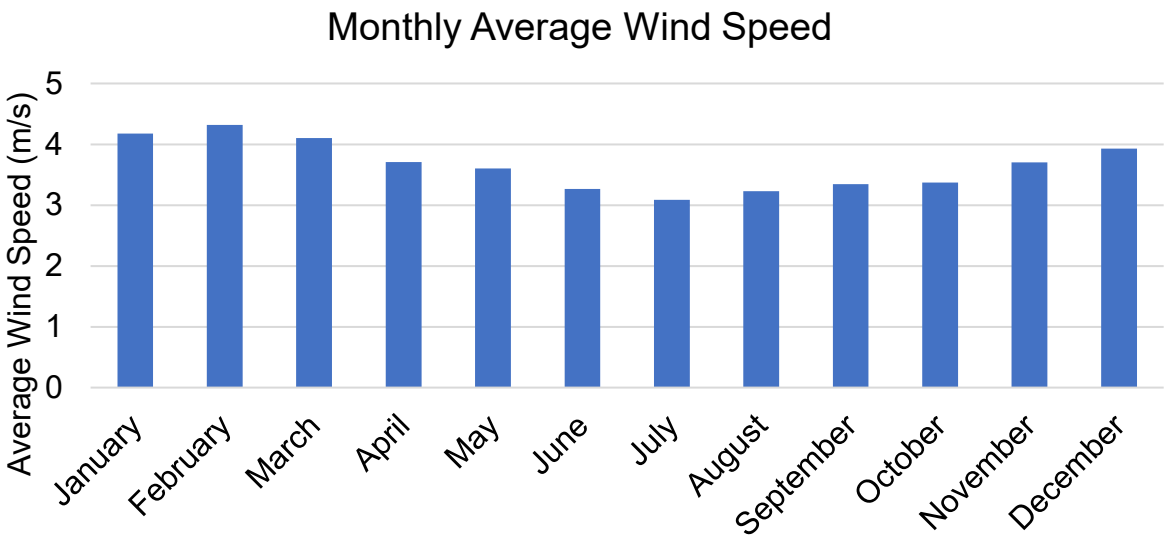


Figure 39: Monthly average wind speed at the test site

The plots of Figure 39, Figure 40, and Figure 41 were all created with the data obtained from the NASA POWER Project for that particular area.

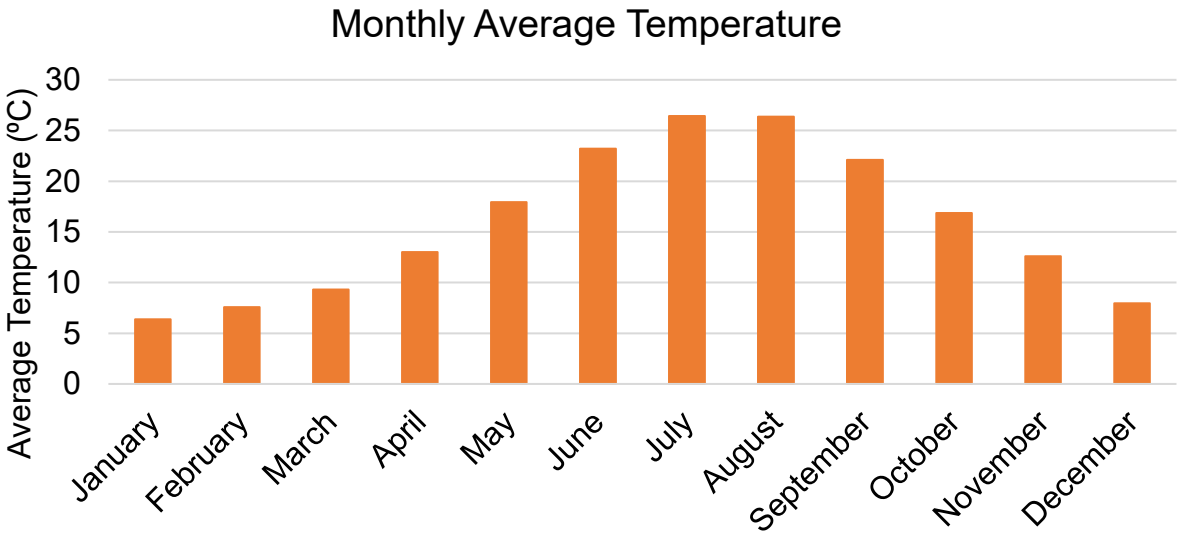


Figure 40: Monthly average temperature at the test site

Upon analysing the meteorological data, it was found that:

- Wind speed never exceeds 8m/s, with an annual average of 3.65m/s,
- The annual average solar radiation is 5.04kWh/m$^2$/day,
- And the annual average temperature is 15.86$^o$C.

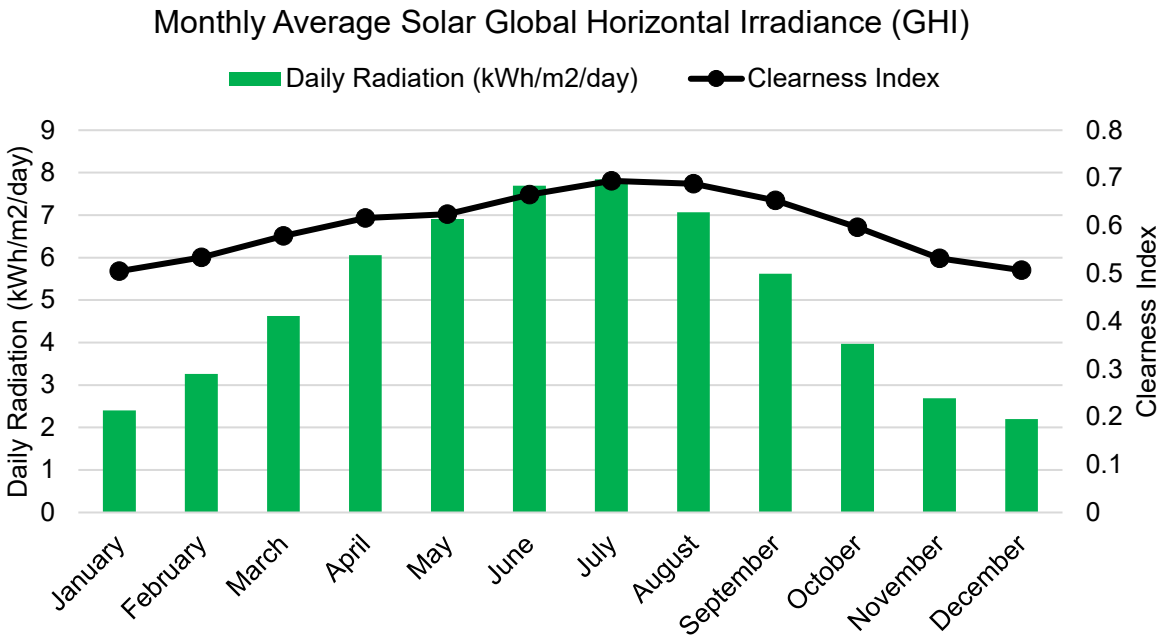


Figure 41: Monthly average solar Global Horizontal Irradiation (GHI) and Clearness Index at the test site

## 3.6. Simulated scenarios

Four distinct scenarios were simulated with the HOMER software. Three scenarios include the same components (Figure 42) but their difference can be found in the biomass resource that is used for the Syngas Generator.

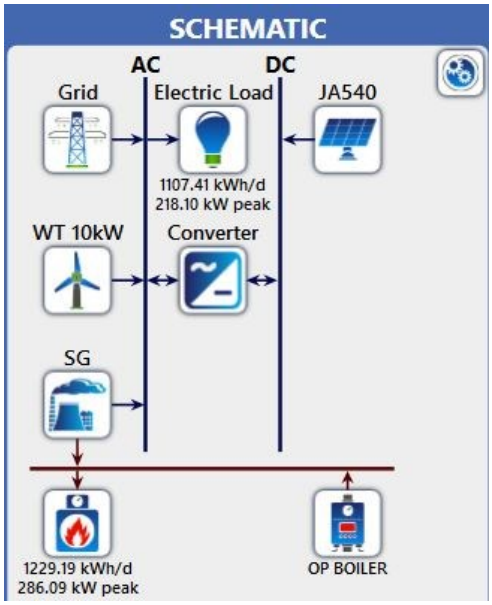


Figure 42: HOMER schematic with photovoltaics (JA540), wind turbines (WT 10kW) and syngas generator (SG)

In the first scenario, the biomass that was available for gasification, was extracted olive pomace (Figure 43 (right)), in the second it was broiler feathers (Figure 43 (left)), and in the third it was a combination of extracted olive pomace and broiler feathers at a ratio of 9:1 by weight, respectively.

Figure 43: Broiler feathers (left)(alamy.com, 2019) and extracted olive pomace (right) (messinialive.gr, 2019)

In these scenarios, the number of 10kW wind turbines was constrained to 6, because in Greece, the HEDNO (Hellenic Electricity Distribution Network Operator) only allows up to 60kW of installed wind turbines when combining other renewable energy technologies in the context of a net-metering agreement. For this reason, a fourth

scenario was created that only incorporates wind turbines without restrictions on their number.

Something worth noting is the fact that, according to HEDNO, combinations of renewable energy resources in the context of a net-metering agreement, are only allowed to users that are connected to the medium voltage distribution system (20,000V). In low voltage connections (400V), combinations are not allowed.

### 3.6.1. Extracted olive pomace

The dry and nitrogen-free gas yield from the gasification of extracted olive pomace is 1.47Nm$^3$ per kg of dry-ash-free (d.a.f.) biomass (Campoy et al., 2014). With an average of 50% nitrogen in the syngas that is produced, gasification ratio is equal to 2.94Nm$^3$ per kg d.a.f. biomass (Bain & Broer, 2011). The density of syngas is 0.95kg/m$^3$ (Singh Brar et al., 2013). Through the combination of this information, it is concluded that the gasification ratio is **2.793kg syngas per kg of d.a.f. biomass**.

The LHV of the produced syngas is 3.30MJ/Nm$^3$. With a density of 0.95kg/m$^3$, syngas has an LHV of **3.47MJ/kg**. The carbon content of d.a.f. extracted olive pomace is **53.3%w/w** (Campoy et al., 2014).

The average market price of this biomass type is €100 per ton at the moment, in the study area. However, since this also includes 8% moisture and 14.2% ash on dry basis, the d.a.f. price is calculated as:

$$\frac{\frac{€100}{0{,}92}}{0{,}858} = €\mathbf{126{,}68}/\boldsymbol{ton} \quad (1)$$

The available biomass per day was set to 10 tonnes, to allow simulations to use as much as profitable.

The fuel curve of the Biogas Generator was adjusted according to the following information:

According to a supplier of biomass gasifiers (Karouzos, 2022) that was contacted about this, the average consumption of extracted olive pomace per kWh is 1.1kg. Using the above-mentioned gasification ratio, the gasifier will consume:

$$1.1\frac{kg_{OP}}{kWh} * 2.793\frac{kg_{syngas}}{kg_{OP}} = \mathbf{3.0723}\frac{\boldsymbol{kg_{syngas}}}{\boldsymbol{kWh}} \quad (2)$$

### 3.6.2. Feathers

According to Dudyński et al., the syngas that is produced from the gasification of feathers has an LHV of **1.96MJ/kg**. The gasification ratio that was calculated from data provided in the same paper, is **4.56kg$_{syngas}$/kg$_{feathers}$**. This applies for feathers that have a moisture content of 51.6%. This moisture content is achieved after pressing feathers from the slaughterhouse that have 70% moisture, in a screw press. Further drying is achieved with the heat generated from the gasifier, and final drying takes

place inside the gasification chamber. The feather gasification plant that they studied is in Poland, and it does not use pure feathers as biomass, but also uses a small amount of wood pellets to increase the heating value and stabilize the gasification process. This is necessary because sometimes feathers may be half frozen due to extremely low ambient temperatures. The ratio of feathers to pellets they used was 15:1 in weight. The carbon content of d.a.f. feathers was found to be 61.77%. When accounting for the moisture content of 51.6% and the ash content of 0.7%, actual carbon content is calculated as follows:

$$61.77\% * \frac{100 - (51.6 + 0.7)}{100} = \mathbf{29.46\%} \quad (3)$$

According to the slaughterhouse owner, the average feather quantity is 450kg per week which can be converted into a daily quantity of approximately 65kg.

$$\frac{450kg}{7days} \approx 65kg/day = \mathbf{0.065tonnes/day} \quad (4)$$

According to the supplier of biomass gasifiers (Karouzos, 2022) that was contacted about this, the average consumption of feathers with the above characteristics per kWh is 1.3kg. Using the above-mentioned gasification ratio, the gasifier will consume:

$$1.3\frac{kg_{biomass}}{kWh} * 4.56\frac{kg_{syngas}}{kg_{biomass}} = \mathbf{5.928}\ \frac{\boldsymbol{kg_{syngas}}}{\boldsymbol{kWh}} \quad (5)$$

### 3.6.3. Combination of feathers and extracted olive pomace

In this scenario, extracted olive pomace and broiler feathers are combined in a weight ratio of 9:1, respectively. All the data is combined according to this ratio as follows:

$$LHV_{OP-F} = 0.9 * 3.47MJ/kg + 0.1 * 1.96MJ/kg = \mathbf{3.319MJ/kg} \quad (6)$$

$$Gasification\ Ratio = 0.9 * 2.793\frac{kg_{syngas}}{kg_{OP}} + 0.1 * 4.56\frac{kg_{syngas}}{kg_{Feathers}} \approx \mathbf{2.97}\frac{\boldsymbol{kg_{syngas}}}{\boldsymbol{kg_{OP-F}}} \quad (7)$$

$$Carbon\ content = 0.9 * 53.3\% + 0.1 * 29.46\% = \mathbf{50.916\%} \quad (8)$$

The daily available biomass quantity is limited by the available feather quantity. Adhering to this constraint, availability is calculated as:

$$Daily\ available\ biomass\ quantity = 10 * 0.065 = \mathbf{0.65tonnes/day} \quad (9)$$

The density of syngas is kept constant at **0.95kg/m$^3$**.

## 3.7. Boiler component

In all scenarios that were simulated, a boiler with 85% efficiency was added to supply the additional required heat that was not generated by the syngas generator. For the simulation to be as close to reality as possible, the fuel used in HOMER would have to be extracted olive pomace. Unfortunately, in HOMER, it is not possible to use the biomass as resource for multiple fuels. And since it is already being used as a resource to generate syngas, it could not be used for the boiler.

To overcome this problem, the extracted olive pomace was simulated as a conventional fuel with a density of 650kg/m$^3$, lower heating value of 17.30MJ/kg, carbon content of 41.75%, sulphur content of 0.13% and a price of €0.1/kg. In order to calculate the real percentage of energy that was generated from renewable sources in each simulation's results, the energy consumed in the boiler will also be counted as renewable.

## 3.8. Conceptualization of scenarios

To determine the scenarios that are to be simulated, categorizations are made according to the type of biomass that is used in the syngas generator (OP for Olive Pomace, OP-F for the combination of Olive Pomace and Feathers at a weight ratio of 9:1, and F for Feathers) but also according to the components that comprise the system (Grid, PV for photovoltaics, SG for Syngas Generator, WT for Wind Turbines, and the Boiler). The aim is to find the combination of components and their capacity in kW that is the most economically profitable according to the calculation of its Net Present Cost (NPC) for the project's lifetime of 25 years.

In total, according to the above mentioned categorizations, there are 15 scenarios simulated excluding the Base case where there is only the Grid and the Boiler. In Table 2 all scenarios with their components are presented.

All scenarios include the Grid as a component. There are 12 scenarios in which a Syngas Generator is simulated. The distinction that is made between these 12 scenarios is the fuel that is used to produce the syngas. In four of these scenarios the fuel that is used is pure extracted olive pomace that is bought in bulk from suppliers in the area. In another four, the fuel that is used is pure broiler feathers which are a by-product of the slaughterhouse operations; and in the remaining four scenarios, the fuel that is used, is a combination of extracted olive pomace and broiler feathers in a weight ratio of 9:1 respectively. In the three scenarios where there is no Syngas Generator simulated, the components are combined as follows: In the first one, only the PV component is simulated, in the second one, a combination of PV and WT is simulated, and in the third one, only WTs are simulated. In all scenarios, the legislative constraints were taken into account.

Table 2: Combinations of Components and SG fuels for the simulated scenarios

| Case No | SG Fuel | Grid | SG | PV | WT | Boiler |
|---|---|---|---|---|---|---|
| 0 | - | ✓ | × | × | × | ✓ |
| 1 | OP-F | ✓ | ✓ | ✓ | × | ✓ |
| 2 | OP-F | ✓ | ✓ | ✓ | ✓ | ✓ |
| 3 | - | ✓ | × | ✓ | × | ✓ |
| 4 | - | ✓ | × | ✓ | ✓ | ✓ |
| 5 | OP-F | ✓ | ✓ | × | ✓ | ✓ |
| 6 | OP-F | ✓ | ✓ | × | × | ✓ |
| 7 | - | ✓ | × | × | ✓ | ✓ |
| 8 | F | ✓ | ✓ | ✓ | × | ✓ |
| 9 | F | ✓ | ✓ | ✓ | ✓ | ✓ |
| 10 | F | ✓ | ✓ | × | ✓ | ✓ |
| 11 | F | ✓ | ✓ | × | × | ✓ |

| | | | | | | |
|---|---|---|---|---|---|---|
| 12 | OP | ✓ | ✓ | ✓ | × | ✓ |
| 13 | OP | ✓ | ✓ | ✓ | ✓ | ✓ |
| 14 | OP | ✓ | ✓ | × | × | ✓ |
| 15 | OP | ✓ | ✓ | × | ✓ | ✓ |

In Table 3, most of the technoeconomic characteristics of the simulated components are presented.

Table 3: Technoeconomic characteristics of the simulated components

| **Syngas Generator (AC)** | | | |
|---|---|---|---|
| Capital cost | Cap (kW) | Capital (€) | Cost (€/kW) |
| | 20 | 88000 | 4400 |
| | 25 | 110000 | 4400 |
| | 30 | 132000 | 4400 |
| | 35 | 154000 | 4400 |
| | 40 | 172000 | 4400 |
| | | | |
| O&M Cost (€/op. hr) | Cap (kW) | Capital (€/hr) | Cost (€/kW/hr) |
| | 20 | 1.2 | 0.06 |
| | 25 | 1.5 | 0.06 |
| | 30 | 1.8 | 0.06 |
| | 35 | 2.1 | 0.06 |
| | 40 | 2.4 | 0.06 |
| | | | |
| Fuel Curve | Output (kW) | Fuel Consumption (kg/hr) | |
| | 1 | 3.0723 | |
| | 20 | 61.446 | |
| | 40 | 122.892 | |
| | 60 | 184.338 | |
| | | | |
| Minimum Load Ratio (%) | 25 | | |
| CHP Heat Recovery Ratio (%) | 25 | | |
| Lifetime (hours): | 220,000 | | |
| Minimum runtime (minutes): | 30 | | |
| Maintenance schedule: Every 200 operating hours, 6 hours downtime with €20 cost | | | |
| | | | |
| **Photovoltaic Array JAM72S30 530-555/MR** | | | |
| Capital cost | Cap (kW) | Capital (€) | Cost (€/kW) |
| | 1 | 2240 | 2240 |
| | 5 | 8000 | 1600 |
| | 10 | 14400 | 1440 |
| | 50 | 64000 | 1280 |
| | 100 | 120000 | 1200 |
| | 200 | 216000 | 1080 |
| | 400 | 400000 | 1000 |
| | | | |
| O&M Cost (€/yr) | Cap (kW) | Capital (€/yr) | |

| | | | |
|---|---|---|---|
| | 1 | 50 | |
| | 5 | 70 | |
| | 10 | 100 | |
| | 50 | 200 | |
| | 100 | 350 | |
| | 200 | 600 | |
| | 400 | 1000 | |
| | | | |
| Lifetime (years) | 25 | | |
| Derating Factor (%) | 80 | | |
| Temperature coefficient: | -0.35 | | |
| Operating Temperature (°C) | 45 | | |
| Efficiency (%) | 20.9 | | |
| | | | |
| **Converter** | | | |
| Lifetime (years) | 25 | | |
| Efficiency (%) | 98 | | |
| | | | |
| **Olive Pomace Boiler** | | | |
| Efficiency (%) | 85 | | |
| | | | |
| **Wind Turbine** | | | |
| Rated Capacity (kW) | 10 | | |
| Cost (€/piece) | 17,050 | | |
| Lifetime (years) | 25 | | |
| Hub height (m) | 10 | | |
| Availability Losses (%) | 0.5 | | |
| Power Curve | Wind Speed (m/s) | | Power Output (kW) |
| | 3 | | 0 |
| | 3.5 | | 0.233 |
| | 4 | | 0.6998 |
| | 4.5 | | 1.2205 |
| | 5 | | 2.0775 |
| | 5.5 | | 3.1274 |
| | 6 | | 4.2227 |
| | 6.5 | | 5.2849 |
| | 7 | | 6.2045 |
| | 7.5 | | 7.0121 |
| | 8 | | 7.6875 |
| | 8.5 | | 8.3492 |
| | 9 | | 8.905 |
| | 9.5 | | 9.326 |
| | 10 | | 9.503 |
| | 10.5 | | 9.498 |
| | 11 | | 9.432 |
| | 12 | | 8.838 |

| | | | |
|---|---|---|---|
| | 13 | | 7.974 |
| | 14 | | 7.197 |
| | 15 | | 6.6 |
| | 16 | | 6.3 |
| | 17 | | 6.2 |
| | 18 | | 6.2 |

## 3.9. Calculation of the carbon footprint of each scenario.

To calculate the carbon footprint of each scenario, the following Life Cycle Analysis (LCA) data for the electric components is used.

The carbon footprint for each kWh that comes from the grid is calculated as follows according to the Technical Directive 20701–1, of the Technical Chamber of Greece:

- 0.989kg$CO_2$eq/kWh is the average carbon footprint for primary energy that is produced from fossil fuels.
- 79.84% is the percentage of electricity that was produced from fossil fuels in 2021 in the Greek electricity Grid according to (Panos et al., 2022).
- 2.9 is the multiplier to convert consumed energy to primary energy.

$$Grid\ carbon\ footprint: 0.989 kgCO_2eq/kWh * 0.7984 * 2.9 \approx 2{,}2899\ kgCO_2eq/kWh \quad (10)$$

According to Tremeac & Meunier, the LCA of wind turbines produces a carbon footprint that ranges from 0.0158 kg$CO_2$eq/kWh up to 0.0464 kg$CO_2$eq/kWh. For the purposes of this thesis, the value of 0.040 kg$CO_2$eq/kWh is used.

According to Rapa et al., the electricity produced by photovoltaics has a carbon footprint of 0.0794 kg$CO_2$eq/kWh.

According to Chen et al., the carbon footprint of biomass gasification is 0.0839 kg$CO_2$eq/kWh.

With this data, the equation to calculate each scenario's carbon footprint (in kg$CO_2$eq/kWh) can be explained.

$$CF_{SX} = \%_{Grid} CF_{Grid} + \%_{PV} CF_{PV} + \%_{SG} CF_{SG} + \%_{WT} CF_{WT} \quad (11)$$

Where $CF_{SX}$ is the carbon footprint of scenario X, $\%_Y$ is the percentage of total energy that is provided by component Y, and $CF_Y$ is the carbon footprint of component Y in kg$CO_2$eq/kWh.

## 3.10. HOMER Calculations

After all the data has been imported, the HOMER program performs a set of calculations in order to produce the correct results for each component and as an extension, for each scenario.

### 3.10.1. Mathematical modelling of the PV component

In order to calculate the power output of the PV component of the system, the HOMER program uses the following equation:

$$P_{PV} = Y_{PV} f_{PV} \left( \frac{\bar{G}_T}{\bar{G}_{T,STC}} \right) [1 + a_P (T_c - T_{c,STC}) \quad (12)$$

Where:

STC: Standard Test Conditions (Radiation of 1kW/m$^2$, cell temperature of 25$^o$C, and no wind).

$Y_{PV}$ is the rated capacity of the PV array, which is its power output under standard test conditions as expressed in kW.

$f_{PV}$ is the PV derating factor expressed as a percentage (%)

$\bar{G}_T$ is the solar radiation incident on the PV array in the current time step as expressed in kW/m$^2$.

$\bar{G}_{T,STC}$ is the incident radiation at standard test conditions which is equal to 1 kW/m$^2$.

$a_P$ is the temperature coefficient of power as expressed in %/°C.

$T_c$ is the PV cell temperature in the current time step as expressed in °C.

$T_{c,STC}$ is the PV cell temperature under standard test conditions, which is equal to 25°C.

The PV cell temperature ($T_c$) is the temperature on the surface of the solar cell, which during the night is equal to the ambient temperature but during the day and especially in full sun, it can greatly exceed the ambient temperature.

First of all, an energy balance is defined for the PV array according to the following equation (Duffie & Beckman, 1991):

$$\tau \alpha G_T = \eta_c G_T + U_L (T_c - T_a) \quad (13)$$

where:

$\tau$ is the solar transmittance of any cover over the PV array expressed as a percentage (%).

$\alpha$ is the solar absorptance of the PV array expressed as a percentage (%).

$G_T$ is the solar radiation striking the PV array expressed in kW/m$^2$.

$\eta_c$ is the electrical conversion efficiency of the PV array expressed as a percentage (%).

$U_L$ is the coefficient of heat transfer to the surroundings expressed in kW/m$^2$°C.

$T_c$ is the PV cell temperature expressed in °C.

$T_a$ is the ambient temperature expressed in °C.

Solar transmittance of a surface is the fraction of the sun's radiation that is transmitted through the surface. According to Duffie & Beckman, for PVs this is equal to 0.9 or 90%.

The solar absorptance of a surface is the fraction of the sun's radiation that the surface absorbs. In the case of PVs, this value is set equal to 0.9 or 90% (Duffie & Beckman, 1991).

### 3.10.2. Mathematical modelling of the WT component

In each timestep, the HOMER program calculates the power output of the WT component using a three-step process.

First, it calculates the wind speed at the hub height according to the following equation:

$$U_{hub} = U_{anem} * \frac{\ln(z_{hub}/z_0)}{\ln(z_{anem}/z_0)} \quad (14)$$

Where:

$U_{hub}$ is the wind speed at the hub height of the wind turbine in m/s.

$U_{anem}$ is the wind speed at anemometer height in m/s.

$z_{hub}$ is the hub height of the wind turbine in m.

$z_{anem}$ is the anemometer height in m.

$z_0$ is the surface roughness length m.

$\ln(\ldots)$ is the natural logarithm.

In this case study, this calculation is not necessary because the hub height is the same as the anemometer height, and therefore the wind speed that is imported from the NASA POWER Project's data, is equal to the wind speed at the hub height.

When it has found the wind speed for that timestep, it refers to the power curve, to find the power output of the turbine for that wind speed.

Because power curves usually represent the turbine's performance under STP conditions, the HOMER program multiplies the value found from the power curve with the air density ratio, according to the following equation:

$$P_{WTG} = \left(\frac{\rho}{\rho_0}\right) \cdot P_{WTG,STP} \quad (15)$$

Where:

$P_{WTG}$ is the wind turbine power output in kW.

$P_{WTG,STP}$ is the wind turbine power output at standard temperature and pressure in kW.

$\rho$ is the actual air density in kg/m$^3$.

$\rho_0$ is the air density at standard temperature and pressure which is equal to 1.225 kg/m$^3$.

### 3.10.3. Mathematical modelling of the Converter component

The power output of the converter is calculated as follows:

$$P_{out} = P_{in}\eta_{inv} \quad (16)$$

Where:

$P_{out}$ is the power output on the AC side that is used by the electric load or sent to the grid.

$P_{in}$ is the power that is received by the converter from the PV arrays.

$\eta_{inv}$ is the conversion efficiency of the component.

### 3.10.4. Calculating the economic parameters of each scenario

In order to calculate the systems initial capital cost, the cost of all its components must be summed according to the following equation:

$$C_{cap} = C_{SG} + C_{WT} + C_{PV} \quad (17)$$

The cost of the converter is not added here because it is incorporated into the cost of the PV component.

Another important parameter is the annualized cost of a component, which is the cost that, if it were to occur equally in every year of the project lifetime, would give the same net present cost as the actual cash flow sequence associated with that component. To calculate it, the following equation is used:

$$C_{ann} = CRF\left(i, R_{proj}\right) * C_{NPC} \quad (18)$$

Where:

$C_{NPC}$ is the Net Present Cost in €.

$i$ is the annual real discount rate.

$R_{proj}$ is the project's lifetime in years.

$CRF(\dots)$ is a function returning the capital recovery factor.

The annual real discount rate is calculated as follows:

$$i = \frac{i' - f}{1 + f} \quad (19)$$

Where:

$i$ is the real discount rate, $f$ is the expected inflation rate, and $i'$ is the nominal discount rate or the rate at which you can borrow money.

The capital recovery factor is calculated according to the following equation:

$$CRF(i, N) = \frac{i(1+i)^N}{(1+i)^N - 1} \quad (20)$$

Where:

$i$ is the real discount rate.

$N$ is the number of years.

The LCOE, which is one of the most important points of comparison between scenarios, is calculated as follows:

$$LCOE = \frac{C_{NPC}}{E_{served}} \quad (21)$$

Where $E_{served}$ is the total electric load that has been served during the system's lifetime.

Some other equally important factors when comparing scenarios include the Return on Investment (ROI), the Payback Period (PP), and the Internal Rate of Return (IRR).

To calculate the Return on Investment, the following equation is used:

$$ROI = \frac{\sum_{I=0}^{R_{proj}} C_{i,ref} - C_i}{R_{proj}(C_{cap} - C_{cap,ref})} \quad (22)$$

Where:

$C_{i,ref}$ is the nominal annual cash flow for the base or reference system.

$C_i$ is the nominal annual cash flow for the current system.

$R_{proj}$ is the project's lifetime in years.

$C_{cap}$ is the capital cost of the current system.

$C_{cap,ref}$ is the capital cost of the base or reference system.

To calculate the IRR, the Net Present Value is set equal to zero, and thus the following equation is used:

$$NPV = 0 \Rightarrow NPV = \sum_{t=1}^{N} \frac{C_t}{(1 + IRR)^t} - C_{cap} = 0 \quad (23)$$

Where $C_t$ is the net cash inflow during the year t, and $C_{cap}$ is the initial capital investment.

Finally, the PP is calculated as follows:

$$PP = \frac{C_{cap}}{C_i} \quad (24)$$

Where $C_{cap}$ is the initial capital investment, and $C_i$ is the nominal annual cash flow for the current system.

## 3.11. Ranking the scenarios using the Technique for Order of Preference by Similarity to Ideal Solution (TOPSIS)

After the HOMER program has produced the results of the simulations, the TOPSIS was used to rank the scenarios according to 5 variables, each with its own significance.

The TOPSIS is a multi-criteria decision analysis approach invented by Ching-Lai Hwang and Yoon in 1981. It was later improved by Yoon in 1987 and Hwang, Lai, and Liu in 1993. The TOPSIS is founded on the premise that the preferred option should be the one with the lowest geometric distance from the positive ideal solution (PIS) and the one with the greatest geometric distance from the negative ideal solution (NIS). It is a compensatory aggregation approach that analyses a group of options by normalizing scores for each criterion and computing the geometric distance that each alternative has from the ideal alternative, which has the highest score in each criterion. TOPSIS method criterion weights can be determined using methods such as the Ordinal Priority Approach, Analytic Hierarchy Process. TOPSIS makes the premise that the criteria increase or decrease monotonically. In multi-criteria applications, normalisation is commonly essential since the parameters or criteria are frequently of discordant dimensions (Uzun Ozsahin et al., 2021).

In order to implement the TOPSIS, a number of steps must be followed as described below:

The first step is to construct an evaluation matrix with m choices and n criteria, with the intersection of each alternative and criteria provided as $x_{ij}$, yielding a matrix $(x_{ij})_{m\times n}$. Each criterion can have a positive impact on the ranking of the alternative in which case the maximization of this criterion is desired, or it can have a negative impact on the ranking of the alternative in which case the minimization of this criterion is of benefit.

The second step is to normalize $(x_{ij})_{m\times n}$ in order to create a new matrix. This is necessary to be able to compare the various criteria to each other because oftentimes their unit of measure may differ. This process is performed as follows:

$$R = (r_{ij})_{m\times n} \quad (25)$$

$$r_{ij} = \frac{x_{ij}}{\sqrt{\sum_{k=1}^{m} x_{kj}^2}}, \qquad i = 1,2,\dots,m, \quad j = 1,2,\dots,n \quad (26)$$

The third step is to assign a weight to each criterion and calculate the weighted normalized decision matrix $(t_{ij})$ as follows:

$$t_{ij} = r_{ij} \cdot w_{ij}, \quad i = 1,2,\dots,m, \quad j = 1,2,\dots,n \quad (27)$$

$w_j = W_j / \sum_{k=1}^{n} W_k, \quad j = 1,2,\dots,n$ (28) and $\sum_{i=1}^{n} w_i = 1$ and $W_j$ is the original weight given to the indicator $v_j, \ j = 1,2,\dots,n$

The fourth step is to find the best and the worst alternatives $A_b$ and $A_w$ or Positive Ideal Solution (PIS) and Negative Ideal Solution (NIS). To form the $A_b$, criteria with a positive impact are maximized while criteria with a negative impact are minimized. To form the $A_w$, the criteria that have a positive impact are minimized and the criteria that have a negative impact are maximized. The equations that describe this process are shown below:

$$A_w = \left[\left(\max\left(t_{ij}|i = 1, 2, \dots, m\right)|j \in J_-\right), \left(\min\left(t_{ij}|i = 1, 2, \dots, m\right)|j \in J_+\right)\right] \equiv [t_{wj}|j = 1, 2, \dots, n] \quad (29)$$

$$A_b = \left[\left(\min\left(t_{ij}|i = 1, 2, \dots, m\right)|j \in J_-\right), \left(\max\left(t_{ij}|i = 1, 2, \dots, m\right)|j \in J_+\right)\right] \equiv \left[t_{wj}\middle|j = 1, 2, \dots, n\right] \quad (30)$$

Where $J_+$ represents the criteria that have a positive impact while $J_-$ represents the criteria that have a negative impact.

The fifth step is to calculate the $L^2$-norm distance that the alternative $i$ has from the best alternative $A_b$ according to the following equation:

$$d_{ib} = \sqrt{\sum_{j=1}^{n}\left(t_{ij} - t_{bj}\right)^2}, \qquad i = 1, 2, \dots, m \quad (31)$$

And the $L^2$-norm distance that alternative $i$ has from the worst alternative $A_w$ according to the following equation:

$$d_{iw} = \sqrt{\sum_{j=1}^{n}\left(t_{ij} - t_{wj}\right)^2}, \qquad i = 1, 2, \dots, m \quad (32)$$

The sixth step is to calculate the similarity of the alternative to the best or worst alternative depending on whether the problem at hand is a negative or a positive optimization problem.

The similarity to the worst alternative is calculated according to the following equation:

$$s_{iw} = \frac{d_{iw}}{(d_{iw} + d_{ib})}, \qquad 0 \le s_{iw} \le 1, \quad i = 1, 2, \dots, m \quad (33)$$

While the similarity to the best alternative is calculated as:

$$s_{ib} = \frac{d_{ib}}{(d_{iw} + d_{ib})}, \qquad 0 \le s_{ib} \le 1, \quad i = 1, 2, \dots, m \quad (34)$$

And finally in the last step the alternatives are ranked based on the values of their similarity to the best and worst alternative.

In this case study the criteria that are used to rank the alternatives include the following parameters:

NPC, LCOE, Discounted Payback Period, Renewable Fraction, and Carbon Footprint.

The weights that are assigned to these criteria are as follows:

$$NPC = 0$$

$$LCOE = 0.35$$

$$Discounted\ Payback\ Period = 0.10$$

$$Renewable\ Fraction\ =\ 0.2$$

$$Carbon\ Footprint\ =\ 0.35.$$

## 3.12. Sensitivity analysis of the optimal scenario

The scenario that was ranked as the closest to the optimal solution by the TOPSIS method, is analysed for its sensitivity towards five important variables of the system.

The sensitivity variables that are used in this analysis are the following:

1) Average Biomass Price as measured in €/kg.
2) Biomass Availability as measured in kg/day.
3) Average Daily Electric Load as measured in kWh/day.
4) Electricity Rates as measured in €/kWh.
5) Solar Global Horizontal Irradiance (GHI) as measured in kWh/m$^2$/day.

The base case value for each one of these variables is multiplied by the following coefficients:

0.5, 0.7, 0.8, 0.9, 1 (original value), 1.1, 1.2, 1.3, 1.5

When the sensitivity variables are multiplied by these coefficients, the following values are produced:

Table 4: Values of sensitivity variables for the sensitivity analysis (in grey color are the original values of the simulation)

| Coefficient | Average Biomass Price (€/kg) | Biomass Availability (t/day) | Average Daily Electric Load (kWh/day) | Electricity Rates (€/kWh) | Solar GHI (kWh/m$^2$/day) |
|---|---|---|---|---|---|
| 0.5 | 0.5 | 0.325 | 553.705 | 0.158 | 2.520 |
| 0.7 | 0.7 | 0.455 | 775.187 | 0.221 | 3.528 |
| 0.8 | 0.8 | 0.520 | 885.928 | 0.253 | 4.032 |
| 0.9 | 0.9 | 0.585 | 996.669 | 0.285 | 4.536 |
| 1.0 | 1.0 | 0.650 | 1,107.410 | 0.316 | 5.040 |
| 1.1 | 1.1 | 0.715 | 1,218.151 | 0.348 | 5.544 |
| 1.2 | 1.2 | 0.780 | 1,328.892 | 0.379 | 6.048 |
| 1.3 | 1.3 | 0.845 | 1,439.633 | 0.411 | 6.552 |
| 1.5 | 1.5 | 0.975 | 1,661.115 | 0.474 | 7.560 |

A total of 40 sensitivity simulations are run excluding the original scenarios. For each sensitivity simulation, a graph showing the energy generation per renewable component in comparison to the electric load is presented. Similarly, graphs showing the LCOE and CF for each scenario are presented to observe how these variables change according to each sensitivity variables' value.

## 3.13. Assumptions made in this diploma thesis

1) The thermal energy that is produced from the SG component, originates only from the CHP Heat Recovery Ratio of the Generator which is equal to 25%. In reality, such systems of biomass gasification produce 2kWh of thermal energy for every kWh electrical energy.
2) For the sensitivity analysis of the electricity rates, the scheduled rates that are used in all other analyses, are replaced by simple rates which are stable for all days and hours. This is because the HOMER program does not support a sensitivity analysis of the electricity rates when using scheduled rates. The value of €0.316/kWh was calculated as the average among all 12 months, as billed by the electricity provider.

# 4. Results and Discussion

In order to simulate all possible scenarios, a total of 15 combinations of components are made, excluding the base case that only has the grid and the boiler as components. Each combination has a unique set of components which make up the system. A very important differentiating factor between scenarios, is the kind of biomass that is used in the syngas generator. This biomass can be one of the following three kinds as stated in the previous chapter. The first kind of biomass is extracted olive pomace, the second is broiler feathers and the third is a combination of olive pomace and broiler feathers at a weight ratio of 9:1, respectively.

When the HOMER software calculates each component's total capacity and its power output for every timestep, it optimizes for minimal NPC and, as an extension, COE.

The best 15 combinations of components and biomass fuels are presented below:

Table 5: Best combinations of components' capacity for each scenario alongside their NPC

| Scenario Number | SG (kW) | PV (kW) | WT (number) | NPC (million €) |
|---|---|---|---|---|
| **0** | 0 | 0 | 0 | 1.887 |
| **1** | 30 | 215 | 0 | 1.115 |
| **2** | 30 | 203 | 1 | 1.127 |
| **3** | 0 | 193 | 0 | 1.223 |
| **4** | 0 | 188 | 1 | 1.233 |
| **5** | 30 | 0 | 6 | 1.622 |
| **6** | 25 | 0 | 0 | 1.632 |

| | | | | |
|---|---|---|---|---|
| **7** | 0 | 0 | 25 | 1.784 |
| **8** | 3 | 228 | 0 | 1.186 |
| **9** | 3 | 225 | 1 | 1.197 |
| **10** | 2.5 | 0 | 6 | 1.820 |
| **11** | 2 | 0 | 0 | 1.846 |
| **12** | 30 | 212 | 0 | 1.138 |
| **13** | 25 | 211 | 1 | 1.152 |
| **14** | 35 | 0 | 0 | 1.637 |
| **15** | 35 | 0 | 2 | 1.638 |

It is apparent by studying Table 5, that PVs are more profitable than WTs because whenever PVs are part of the system, there is only one WT used. The maximum amount of wind turbines (6) is used whenever PVs are not available. Another interesting observation when comparing scenario 1 to scenario 3, is that it is more profitable to install a larger capacity PV in combination with an SG component than without one. This observation is also reaffirmed when comparing scenario 3 with scenario 8.

In scenarios 8, 9, 10 and 11, the capacity of the SG component is much lower when compared to the other scenarios that have an SG, because of the limited supply of feathers.

Table 6: Economic characteristics of the best scenarios

| Scenario Number | NPC (million €) | LCOE (€/kWh) | Change compared to base | Discounted PP (years) | IRR (%) |
|---|---|---|---|---|---|
| **0** | 1.887 | 0.316 | - | - | - |
| **1** | 1.115 | 0.135 | -57% | 5.07 | 22.90 |
| **2** | 1.127 | 0.139 | -56% | 5.20 | 22.40 |
| **3** | 1.223 | 0.157 | -50% | 3.68 | 30.60 |
| **4** | 1.233 | 0.159 | -50% | 3.90 | 29.10 |
| **5** | 1.622 | 0.268 | -15% | 8.03 | 15.20 |
| **6** | 1.632 | 0.270 | -15% | 4.77 | 24.30 |
| **7** | 1.784 | 0.272 | -14% | 16.98 | 7.70 |
| **8** | 1.186 | 0.141 | -55% | 4.15 | 27.50 |
| **9** | 1.197 | 0.142 | -55% | 4.39 | 26.10 |
| **10** | 1.820 | 0.304 | -4% | 11.80 | 10.80 |
| **11** | 1.846 | 0.309 | -2% | 2.70 | 41.20 |
| **12** | 1.138 | 0.139 | -56% | 5.17 | 22.60 |
| **13** | 1.152 | 0.140 | -56% | 5.18 | 22.50 |
| **14** | 1.637 | 0.271 | -14% | 6.25 | 19.00 |
| **15** | 1.638 | 0.271 | -14% | 7.22 | 16.70 |

Table 6 shows that while scenario 11 only has a very small decrease in the LCOE, it has the shortest discounted payback period of all scenarios. This is because the only component of the system that needs to be purchased, installed, and operated, is a 2

kW SG. It is also worth noting that scenario 7 which has 25 turbines and no other additional components, besides the grid and the boiler, has the longest discounted payback period. This is due to the very small wind potential in the study area. An interesting observation is that the scenario with the lowest LCOE does not have the highest IRR.

Table 7: Grid-related metrics for all scenarios

| Scenario Number | Net Energy Purchased (NEP) (kWh) | Grid/Energy Purchased (kWh) | Net Energy Purchased as % of total energy consumed |
|---|---|---|---|
| **0** | 404,203.00 | 404,203.1 | 100.00% |
| **1** | -71,227.64 | 55,337.82 | -17.62% |
| **2** | -61,357.24 | 69,268.77 | -15.18% |
| **3** | 120,232.80 | 220,261.8 | 29.75% |
| **4** | 121,822.57 | 219,626 | 30.14% |
| **5** | 156,814.07 | 158,884.8 | 38.80% |
| **6** | 198,314.60 | 154,373 | 49.06% |
| **7** | 239,234.00 | 278,051 | 59.19% |
| **8** | 50,442.50 | 55,337.82 | 12.48% |
| **9** | 48,177.60 | 69,268.77 | 11.92% |
| **10** | 346,376.51 | 158,884.8 | 85.69% |
| **11** | 387,191.10 | 154,373 | 95.79% |
| **12** | -64,271.38 | 55,337.82 | -15.90% |
| **13** | -53,147.63 | 69,268.77 | -13.15% |
| **14** | 158,884.80 | 158,884.8 | 39.31% |
| **15** | 154,369.46 | 154,373 | 38.19% |

In scenarios 1, 2, 12, 13, Table 7 shows that the net production of electricity from the added components (SG and PV for scenarios 1 and 12; and SG, PV and WT for scenarios 2 and 13) exceeds the demand by a substantial margin. Unfortunately, since there is a net-metering agreement in place, the company will not be compensated for this extra energy it provides to the grid. It is also worth noting that while in scenarios 2 and 9, the same amount of energy is purchased from the grid, the net energy purchased is vastly higher in scenario 9. This difference is due to the higher capacity of the SG component in scenario 2, which not only compensates for that scenario's lower PV capacity, but also exceeds it by a very large amount. The explanation for this difference in net energy purchased is the following:

Both systems operate in a similar fashion because of the presence of the same components (PVs, SGs and WTs) that produce power. However, at the timesteps where it would be more profitable to supply the demand using the SG component, the system in scenario 3 is at a disadvantage because of the limited supply of biomass fuel for the SG, which in turn limits this components capacity.

Table 8: Electrical energy production per component

| | **SG** | | **JA540** | | **WT 10kW** | |
|---|---|---|---|---|---|---|
| Scenario Number | Production (kWh) | % of total electricity production | Production (kWh/yr) | % of total electricity production | Production (kWh/yr) | % of total electricity production |
| 0 | 0 | 0.00% | 0 | 0.00% | 0 | 0.00% |
| 1 | 159,827 | 39.54% | 322,044.7 | 79.67% | 0 | 0.00% |
| 2 | 160,315.7 | 39.66% | 304,740.7 | 75.39% | 6,598.765 | 1.63% |
| 3 | 0 | 0.00% | 289,765.6 | 71.69% | 0 | 0.00% |
| 4 | 0 | 0.00% | 281,410 | 69.62% | 6,598.765 | 1.63% |
| 5 | 207,796.5 | 51.41% | 0 | 0.00% | 39,592.59 | 9.80% |
| 6 | 205,888.5 | 50.94% | 0 | 0.00% | 0 | 0.00% |
| 7 | 0 | 0.00% | 0 | 0.00% | 164,969 | 40.81% |
| 8 | 18,226.13 | 4.51% | 342,382.2 | 84.71% | 0 | 0.00% |
| 9 | 18,248.41 | 4.51% | 337,937.1 | 83.61% | 6,598.765 | 1.63% |
| 10 | 18,234 | 4.51% | 0 | 0.00% | 39,592.59 | 9.80% |
| 11 | 17,012 | 4.21% | 0 | 0.00% | 0 | 0.00% |
| 12 | 156,421.9 | 38.70% | 318,421 | 78.78% | 0 | 0.00% |
| 13 | 139,726.3 | 34.57% | 317,373.2 | 78.52% | 6,598.765 | 1.63% |
| 14 | 245,318.3 | 60.69% | 0 | 0.00% | 0 | 0.00% |
| 15 | 236,636.1 | 58.54% | 0 | 0.00% | 13,197.53 | 3.27% |

As expected from the SG component's capacity in scenario 8, 9, 10, and 11, its contribution towards meeting the electrical energy demand is very low (Table 8). It is apparent from Table 8 that the wind energy potential is very low in the study area since a 10kW turbine in scenarios 2, 4, 9 and 13, only produces 6,598.765 kWh, giving it a capacity factor of 7.53%. For comparison, the capacity factor of land-based wind turbines in the United States ranges from 24% to 56% and averages at 36% (Center for Sustainable Systems, 2022). Of course, the capacity factor of wind turbines in all scenarios is the same because the wind turbines and the wind potential are the same. It is worth noting that the SG component has the highest capacity factor of all components, in all scenarios that it is present. Its peak capacity factor is observed in

scenario 9 with a value equal to 69.4%. Finally, it is clear that the bulk of electrical energy is produced by the PV component whenever it is present in a scenario.

Table 9: Renewable fraction and carbon footprint for each scenario

| Scenario Number | Renewable Fraction | Carbon Footprint (kgCO2eq/kWh) |
|---|---|---|
| 0 | - | 2.290 |
| 1 | 117.62% | 0.308 |
| 2 | 115.18% | 0.363 |
| 3 | 70.25% | 1.034 |
| 4 | 69.86% | 1.035 |
| 5 | 61.20% | 0.942 |
| 6 | 50.94% | 1.029 |
| 7 | 40.81% | 1.452 |
| 8 | 87.52% | 0.374 |
| 9 | 88.08% | 0.433 |
| 10 | 14.31% | 1.693 |
| 11 | 4.21% | 2.071 |
| 12 | 115.90% | 0.311 |
| 13 | 113.15% | 0.367 |
| 14 | 60.69% | 0.951 |
| 15 | 61.81% | 0.925 |

In Table 9 it is worth noting that whenever the renewable fraction is less than 100%, the carbon footprint is significantly increased. This is because of the very small carbon footprint of renewable technology components of the system and the high percentage of fossil fuels used in the energy mix of the grid that results in a comparatively very high carbon footprint.

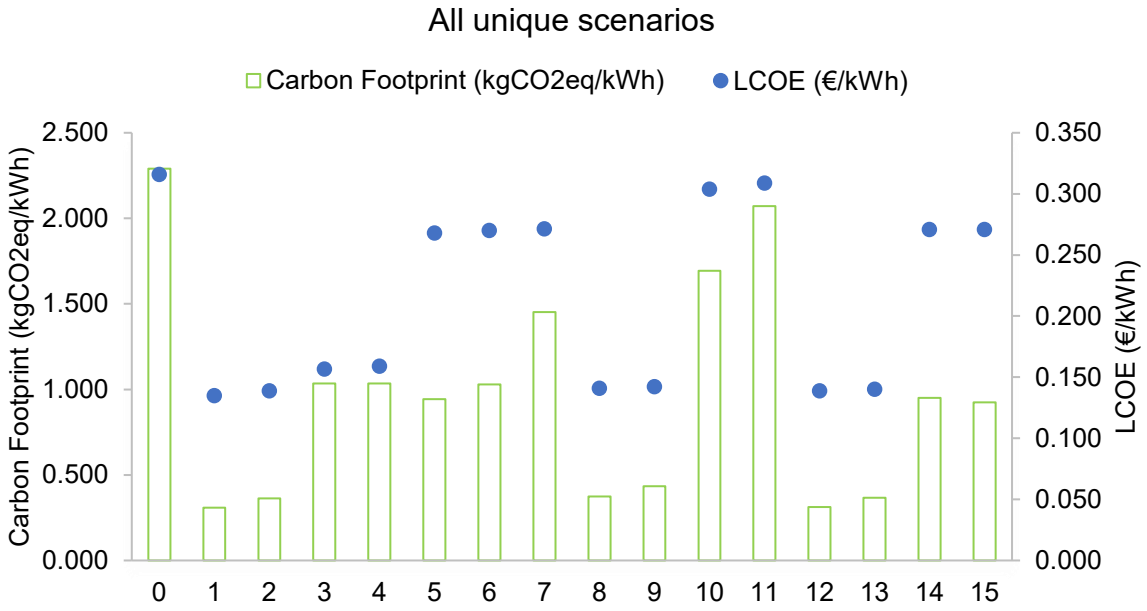


Figure 44: Chart depicting each scenario's LCOE and carbon footprint

It can clearly be seen in Figure 44 that the scenarios with the lowest LCOE also have the lowest carbon footprint. This is very convenient because it eliminates the conflict between profitability and protection of the environment. The 6 scenarios with the lowest LCOE and carbon footprint (1, 2, 8, 9, 12, 13) combine the SG with the PV and one WT in scenarios 2, 9 and 13. As expected, scenarios 10 and 11 have the highest carbon footprint and LCOE, after the base scenario, due to their low renewable fraction.

## 4.1. Analysis of the optimal scenarios among the examined cases

The optimal scenarios with regard to minimum NPC value among the sets of simulations that were run are 1, 8, and 12. As explained in the methodology chapter, a separate simulation was run where the only renewable energy component was a WT. This produces only one scenario with 25, 10kW wind turbines. However, its' LCOE is €0.272/kWh which is very high when compared to scenario 1 which has an LCOE equal to €0.135/kWh.

The optimal scenario in the case where the SG component is fuelled by Olive Pomace, is number 12 due to the lowest NPC it incurs on the business. If the SG component is fuelled by broiler feathers, the optimal scenario is number 8 since it has the lowest NPC. And finally, if the SG component is fuelled by the combination of olive pomace and feathers, the optimal scenario is number 1, which again, has the lowest NPC.

The scenario that has the lowest NPC of all, is scenario number 1 with an NPC equal to €1.115 million.

### 4.1.1. Analysis of the optimal scenario when the SG component uses Olive Pomace

The optimal scenario when the SG component uses olive pomace as fuel, is scenario number 12. The components that were included in the simulation of this scenario are

a 30kW SG, PVs with a total capacity of 212kW, the olive pomace boiler and the grid. In this scenario, the NPC is equal to €1.138 million and the LCOE is equal to €0.139/kWh, which represents a 56% reduction when compared to the base case. The discounted payback period in this scenario is 5.17 years, the IRR is 22.6%, and the renewable fraction is 115.9% which represent a negative value of net energy purchased from the grid. However, this does not mean that there is no energy purchased. In fact, a total of 55,337.82kWh are purchased. Furthermore, the SG component produced 38.7% of the total electrical energy demand, and the PV produced 78.78% thereof. The carbon footprint of this scenario is calculated as 0.311kg$CO_2$eq/kWh.

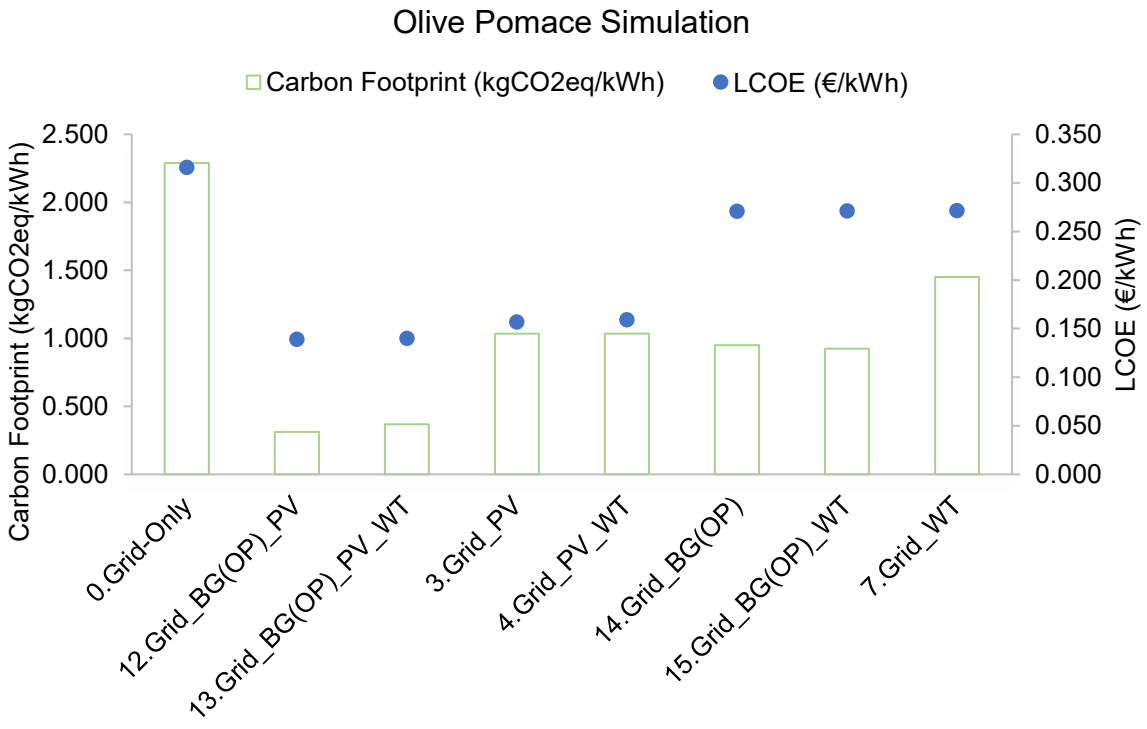


Figure 45: Simulated scenarios with olive pomace as fuel for the SG component

When observing Figure 45, it is clear that the trend of the carbon footprint is generally followed by the LCOE trend. However, it is notable that while the difference in carbon footprint between scenarios 13 and 3 is quite substantial, the value of the LCOE increases much less. The same observation can be made when comparing scenario 15 to scenario 7. On the other hand, when comparing scenario 4 to scenario 14, it can be observed that while there is only a small increase in the carbon footprint, there is a substantial increase in the LCOE.

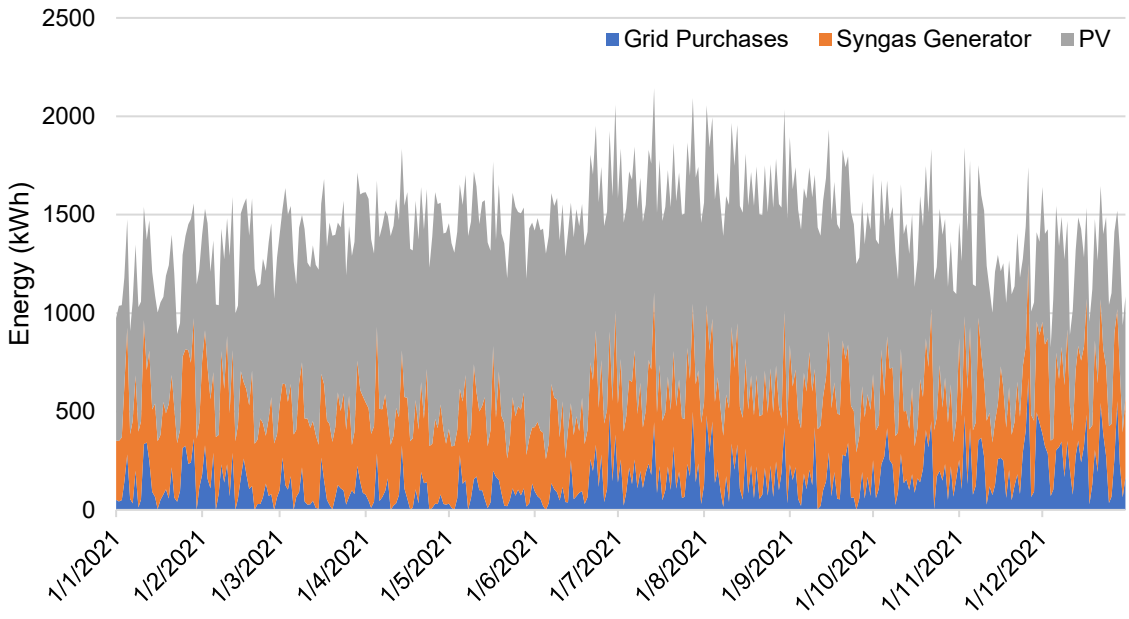


Figure 46: Daily electrical energy output per component in olive pomace scenario

Figure 46 shows that the electrical demand rises in the summer months, which is expected due to the high ambient temperature resulting in increased cooling needs for the poultry slaughterhouse and processing plant. This increased demand is satisfied primarily by the grid and the syngas generator. This is because despite the increased solar radiation and increased clearness index, the PV component performs at a lower efficiency rate due to its increased temperature as can be seen in Figure 47.

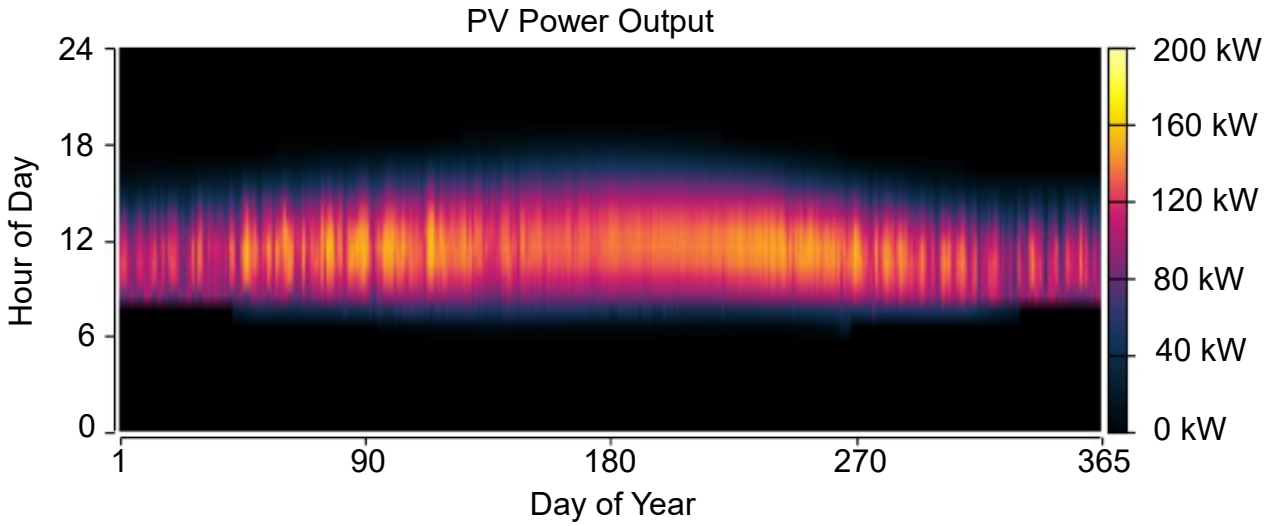


Figure 47: PV power output in olive pomace optimal scenario

It is interesting to note that Figure 47 shows that the peak of electrical energy production from the PV component is actually in the spring around March and April due to the lower ambient temperature. In Figure 48 it can be seen that this peak occurs on the 26$^{th}$ of April and the PV's generation for that day is 1,151.24kWh.

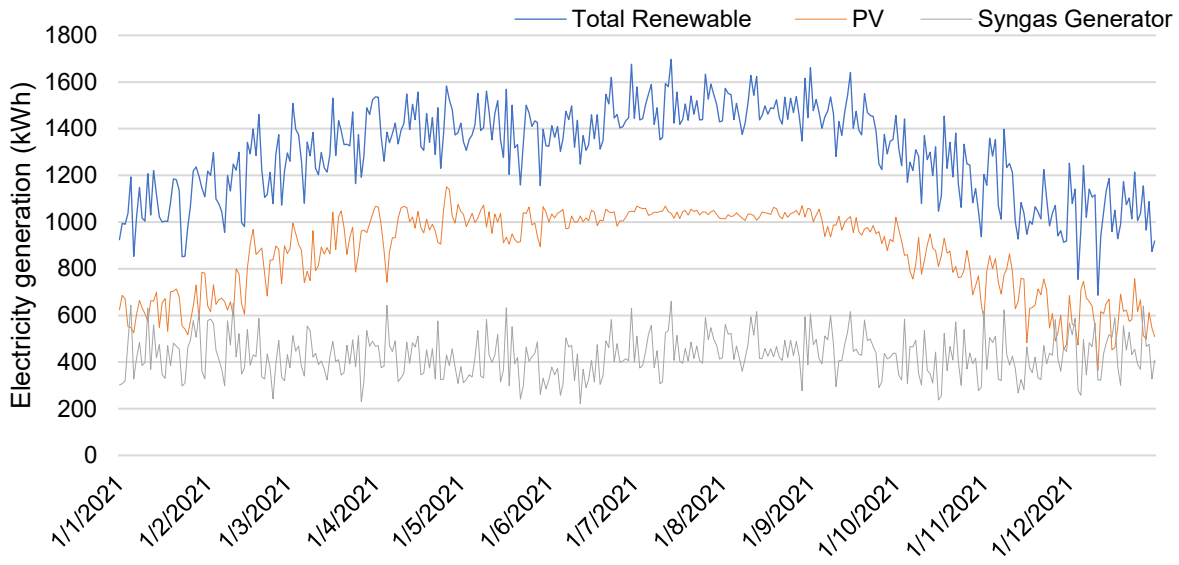


Figure 48: Total daily renewable electrical energy generation in olive pomace scenario

It is interesting to observe in Figure 48 that, during spring, autumn and winter, the electrical energy output of the PV oscillates much more compared to the summer months. This is explained by looking at Figure 47. Because some days during autumn, winter, and spring can be overcast while the next or previous day may be clear, a high degree of oscillation is to be expected. In the summer months however, this rapid change in weather is not as common, resulting in a smoother line.

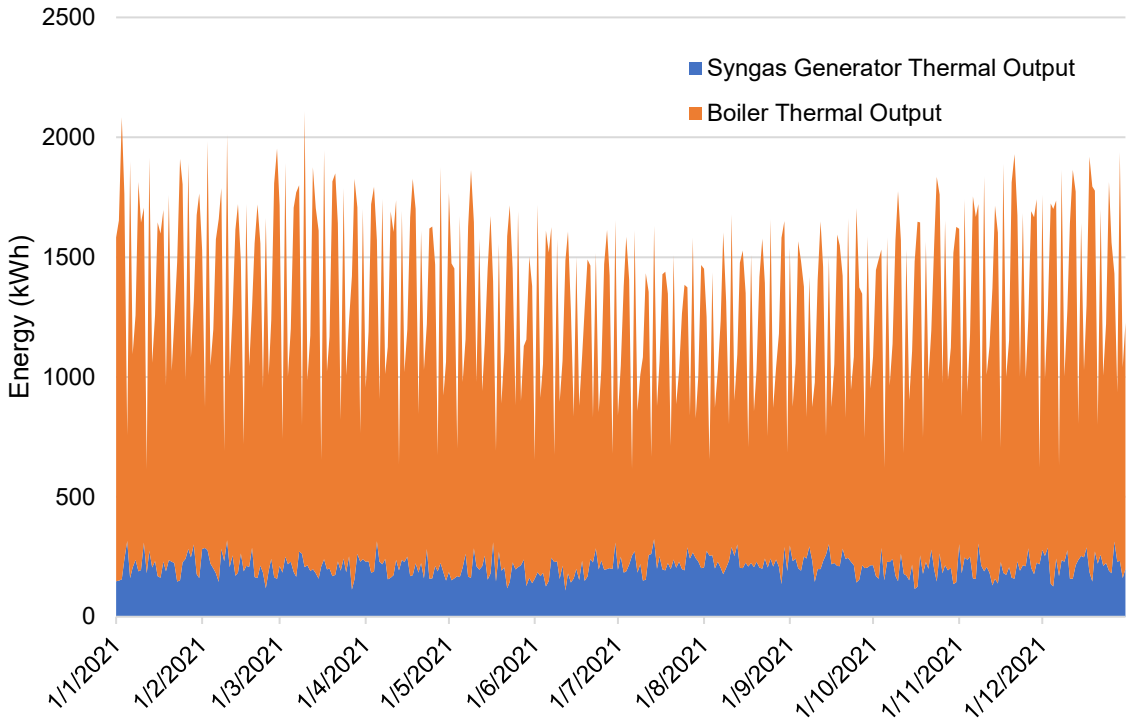


Figure 49: Daily thermal energy output per component in the olive pomace scenario

Due to the high thermal energy demand and the comparatively low thermal energy production from the SG component, as depicted in Figure 49, most of the thermal energy is produced by the boiler which burns extracted olive pomace. It is clear that in the summer months the thermal energy demand is lower. This is because of the greatly increased ambient temperature that the study area experiences during that season. It is also obvious that the thermal demand is characterized by spikes which can be attributed to the days that the slaughterhouse and the compound feed production plant work simultaneously.

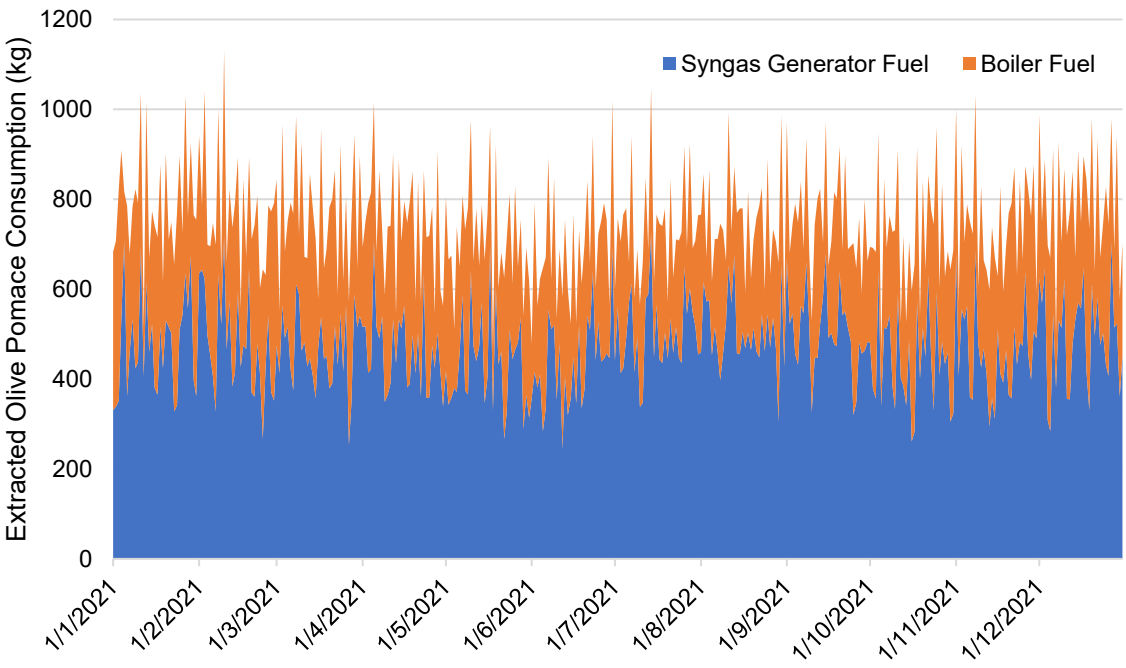


Figure 50: Daily consumption of extracted olive pomace in olive pomace scenario

However, when looking at Figure 50, it is clear that most of the extracted olive pomace is consumed by the SG component. This is explained by the fact that the SG component has a Heat Recovery Ratio of 25%, while the boiler has an efficiency equal to 85%.

### 4.1.2. Analysis of the optimal scenario when the SG component uses Feathers

The optimal scenario when the SG component uses feathers as fuel, is scenario number 8. The components that were included in the simulation of this scenario are a 3kW SG, PVs with a total capacity of 228kW, the olive pomace boiler and the grid. In this scenario, the NPC is equal to €1.186 million and the LCOE is equal to €0.141/kWh, which represents a 55% reduction when compared to the base case. The discounted payback period in this scenario is 4.15 years, the IRR is 27.5%, and the renewable fraction is 87.52%. The net energy purchased from the grid is equal to 50,442.50kWh while the total energy purchased from the grid 55,337.82kWh. Furthermore, the SG component produced 4.51% of the total electrical energy demand, and the PV produced 84.71% thereof. The carbon footprint of this scenario is calculated as 0.374kg$CO_2$eq/kWh.

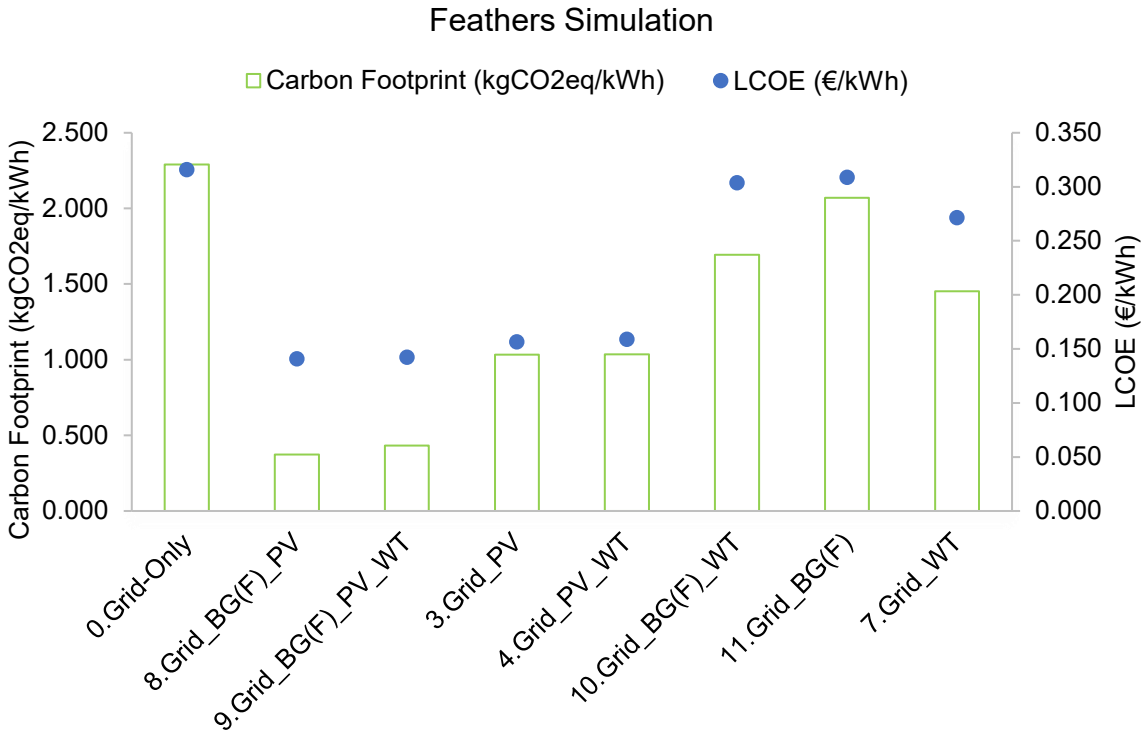


Figure 51: Simulated scenarios with feathers as fuel for the SG component

When observing Figure 51, it is clear that the trend of the carbon footprint is generally followed by the LCOE trend. However, it is notable that while the difference in carbon footprint between scenarios 9 and 3 is quite substantial, the value of the LCOE increases much less. It also notable that the values of the LCOE and carbon footprint in scenario 11 are almost the same as that of the base case. This is due to the very small contribution of electrical energy by the SG component (4.51%), and thus 95.49% has to be bought from the grid.

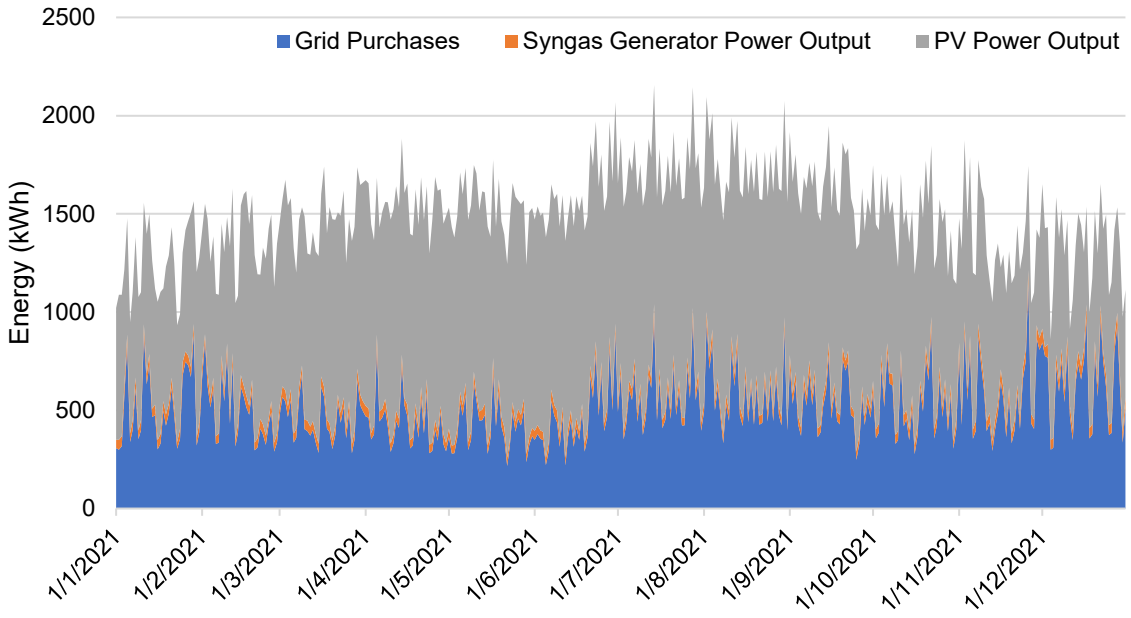


Figure 52: Daily electrical energy output per component in feather scenario

Figure 52 shows that the electrical demand rises in the summer months, which is expected due to the high ambient temperature resulting in increased cooling needs for the poultry slaughterhouse and processing plant. This increased demand is satisfied primarily by the grid and not the PV component. This is because despite the increased solar radiation and increased clearness index, the PV component performs at a lower efficiency rate due to its increased temperature as can be seen in Figure 53. The contribution of electrical energy from the syngas generator is minimal as confirmed by Figure 52 due to the limited availability of fuel.

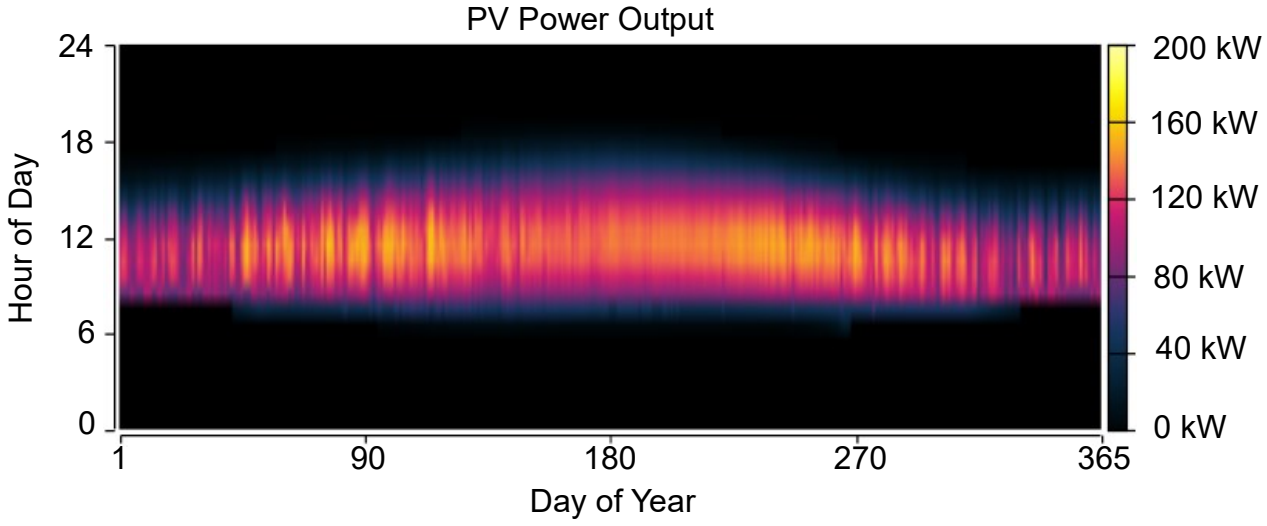


Figure 53: PV power output in olive pomace optimal scenario

It is interesting to note that Figure 53 shows that the peak of electrical energy production from the PV component is actually in the spring around March and April due to the lower ambient temperature.

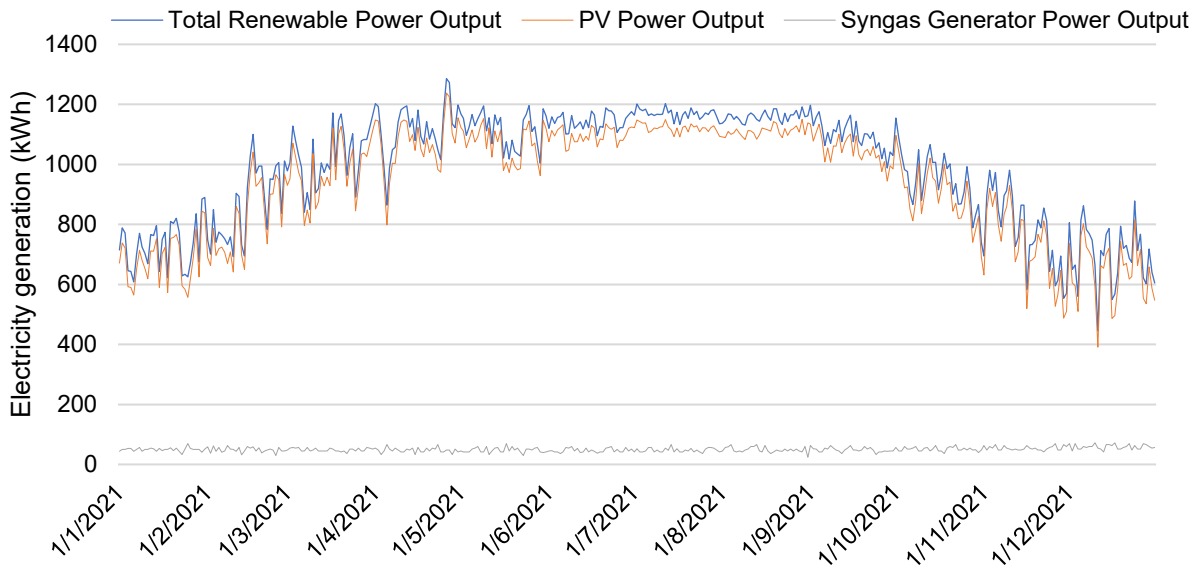


Figure 54: Daily renewable electrical energy generation in feather scenario

It is interesting to observe in Figure 54 that, during spring, autumn and winter, the total daily renewable electrical energy output oscillates much more compared to the summer months. This is explained by looking at Figure 53. Because some days during autumn, winter, and spring can be overcast while the next or previous day may be clear, a high degree of oscillation is to be expected. In the summer months however, this rapid change in weather is not as common, resulting in a smoother line.

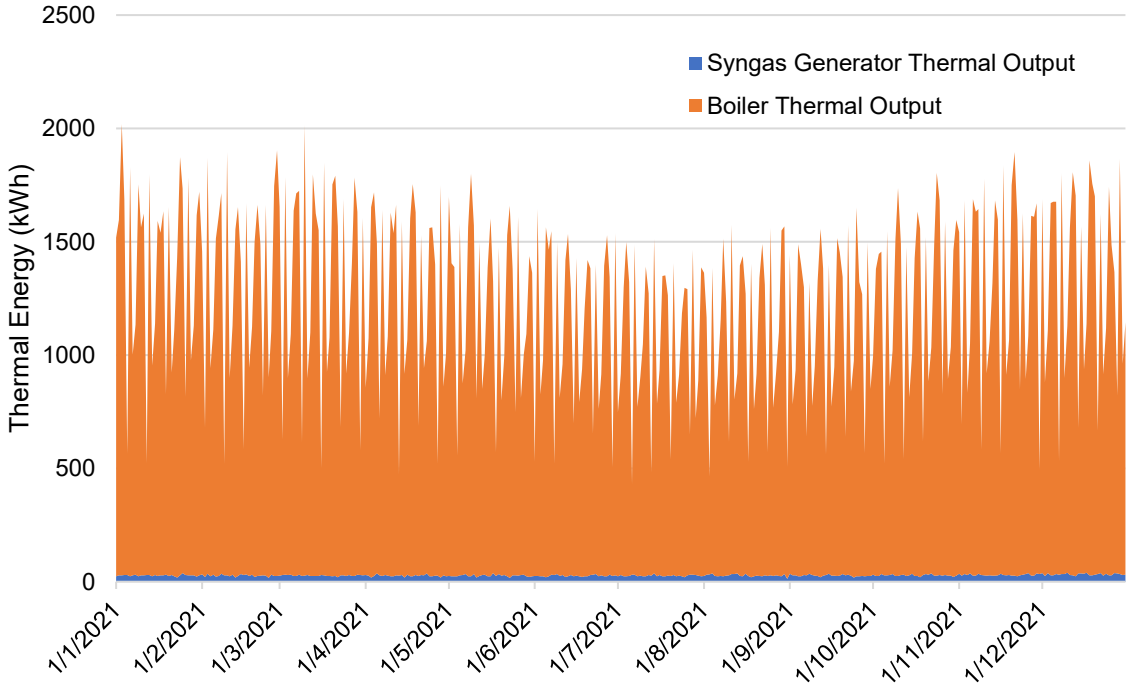


Figure 55: Daily thermal energy output per component in the feather scenario

Due to the high thermal energy demand and the extremely low thermal energy production from the SG component, as depicted in Figure 55, almost all of the thermal energy is produced by the boiler which burns extracted olive pomace. It is clear that in the summer months the thermal energy demand is lower. This is because of the greatly increased ambient temperature that the study area experiences during that season. It is also obvious that the thermal demand is characterized by spikes which can be attributed to the days that the slaughterhouse and the compound feed production plant work simultaneously.

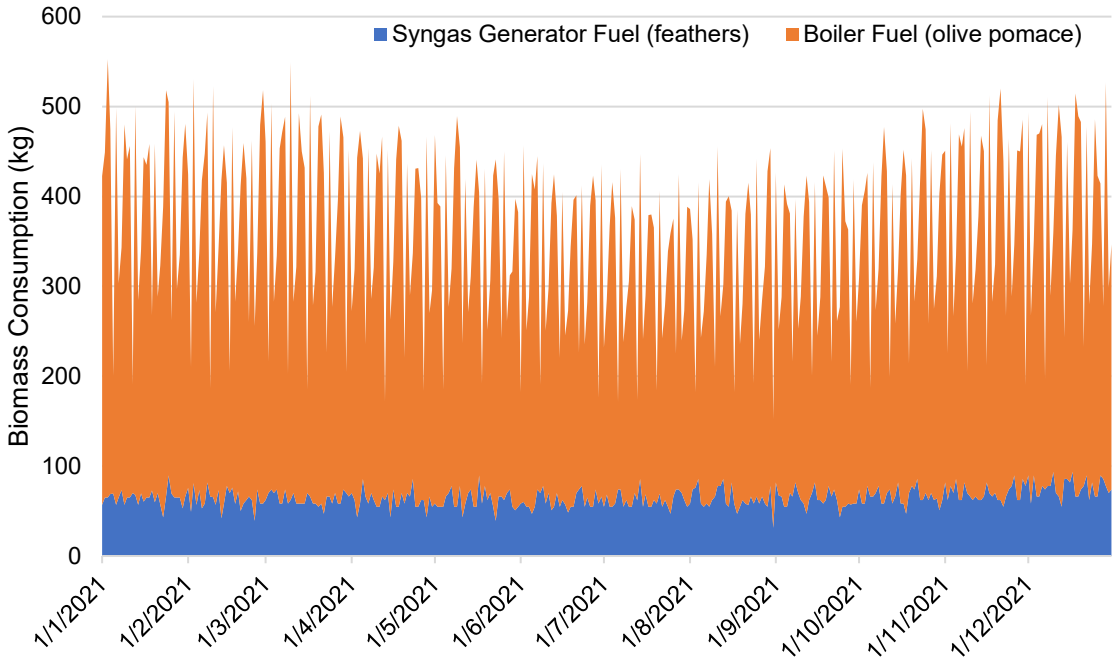


Figure 56: Daily consumption of extracted olive pomace and feathers

In this scenario the daily consumption of fuel in the SG component and the boiler are reversed (Figure 56). This is because of the decrease in thermal energy production of the SG component and the increase in the boiler's thermal energy production to cover the demand.

### 4.1.3. Analysis of the optimal scenario when the SG component uses Olive Pomace and Feathers combined

The optimal scenario when the SG component uses olive pomace and feathers combined at a weight ratio of 9:1 as fuel, is scenario number 1. The components that were included in the simulation of this scenario are a 30kW SG, PVs with a total capacity of 215kW, the olive pomace boiler and the grid. In this scenario, the NPC is equal to €1.115 million and the LCOE is equal to €0.135/kWh, which represents a 57% reduction when compared to the base case. The discounted payback period in this scenario is 5.07 years, the IRR is 22.9%, and the renewable fraction is 117.62% which represent a negative value of net energy purchased from the grid. However, this does not mean that there is no energy purchased. In fact, a total of 55,337.82kWh are purchased. Furthermore, the SG component produced 39.54% of the total electrical

energy demand, and the PV produced 79.67% thereof. The carbon footprint of this scenario is calculated as 0.308kg$CO_2$eq/kWh.

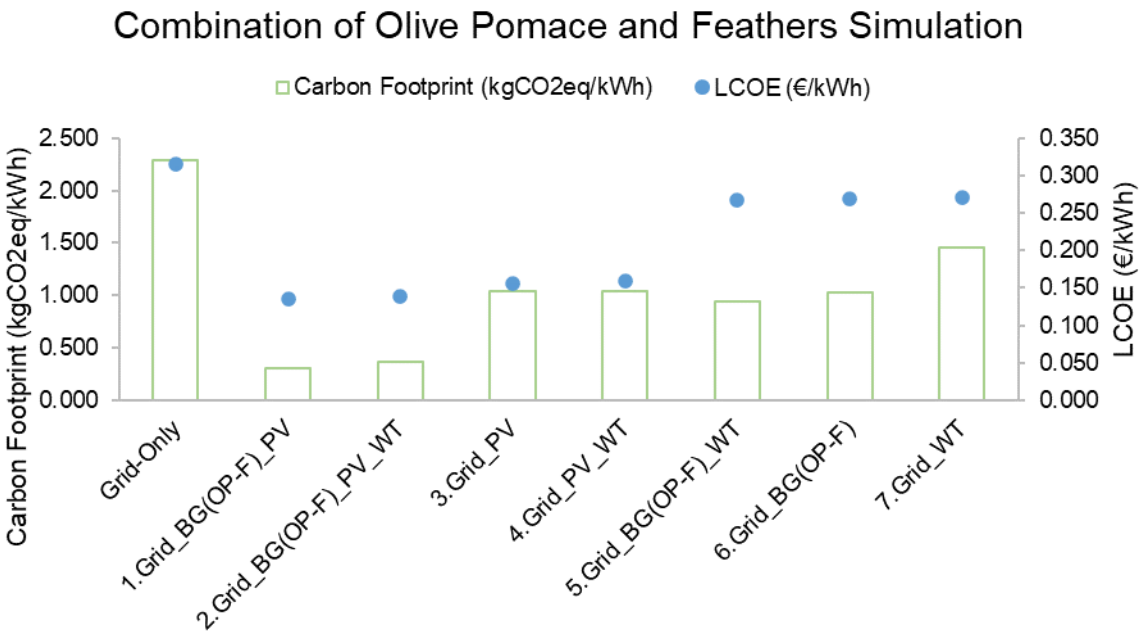


Figure 57: Simulated scenarios with a combination of olive pomace and feathers as fuel for the SG component

When observing Figure 57, it is clear that the trend of the carbon footprint is generally followed by the LCOE trend. However, it is notable that while the difference in carbon footprint between scenarios 2 and 3 is quite substantial, the value of the LCOE increases much less. Despite the steady and observable increase of the carbon footprint between scenarios 5, 6, and 7, their LCOE only increases marginally. On the other hand, when comparing scenario 4 to scenario 5, it can be observed that while there is only a small increase in the carbon footprint, there is a substantial increase in the LCOE.

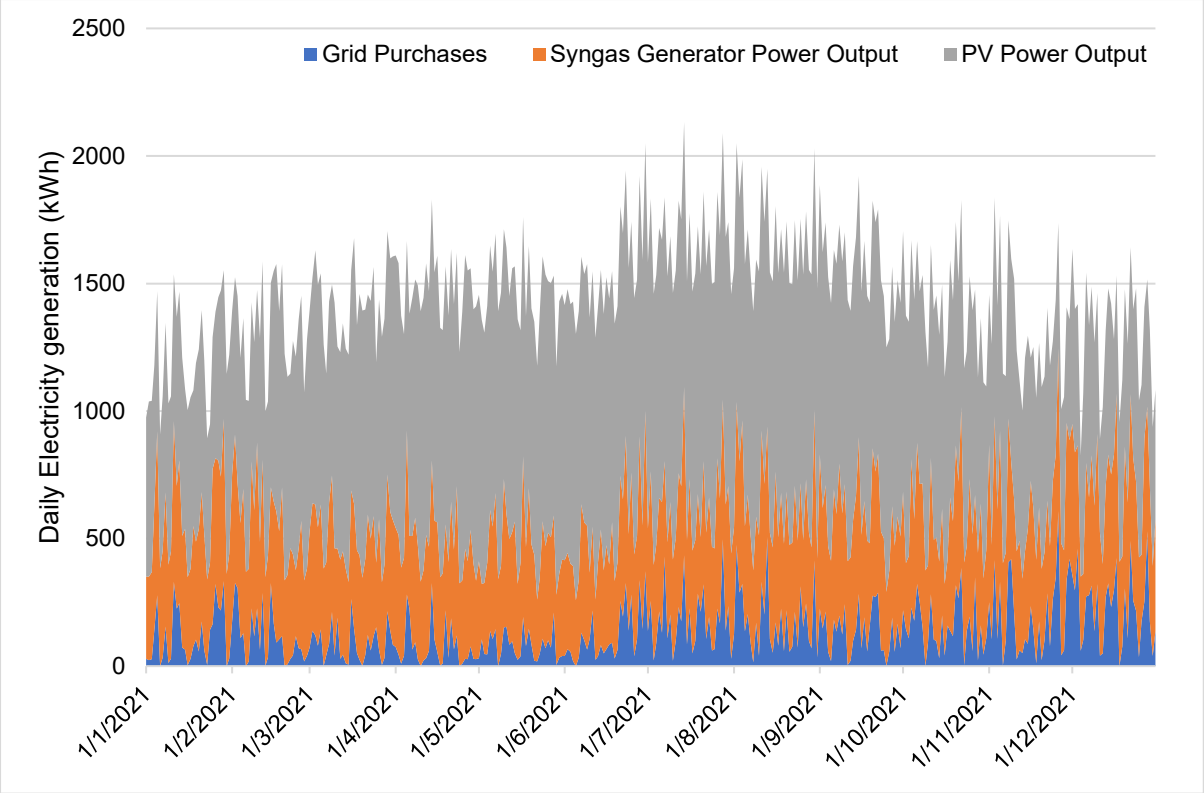


Figure 58: Daily electrical energy output per component in olive pomace-feather scenario

Figure 58 shows that the electrical demand rises in the summer months, which is expected due to the high ambient temperature resulting in increased cooling needs for the poultry slaughterhouse and processing plant. This increased demand is satisfied primarily by the grid and the syngas generator. This is because despite the increased solar radiation and increased clearness index, the PV component performs at a lower efficiency rate due to its increased temperature as can be seen in Figure 47.

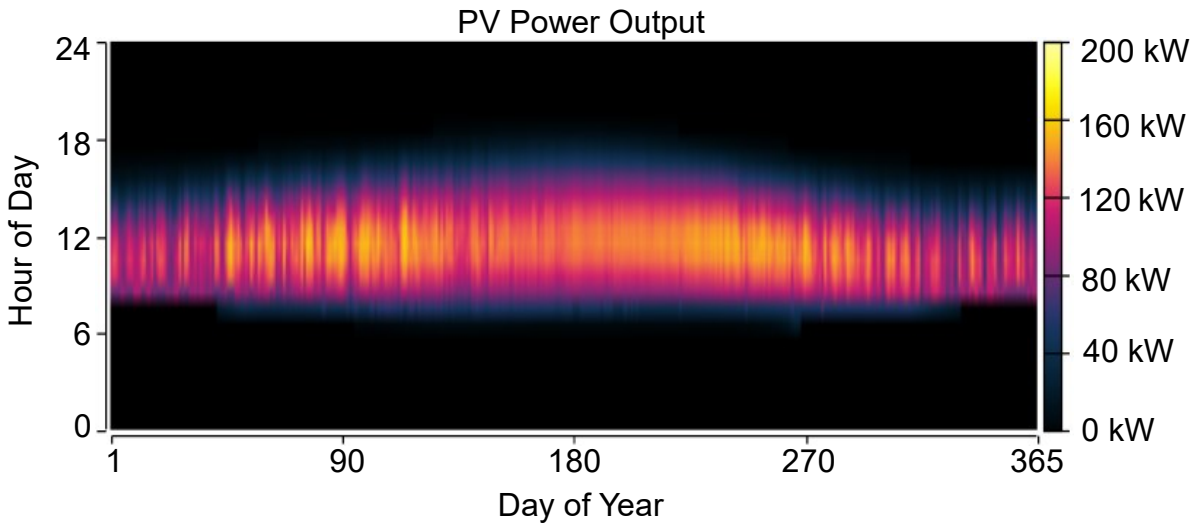


Figure 59: PV power output in olive pomace – feather optimal scenario

It is interesting to note that Figure 59 shows that the peak of electrical energy production from the PV component is actually in the spring around March and April due to the lower ambient temperature.

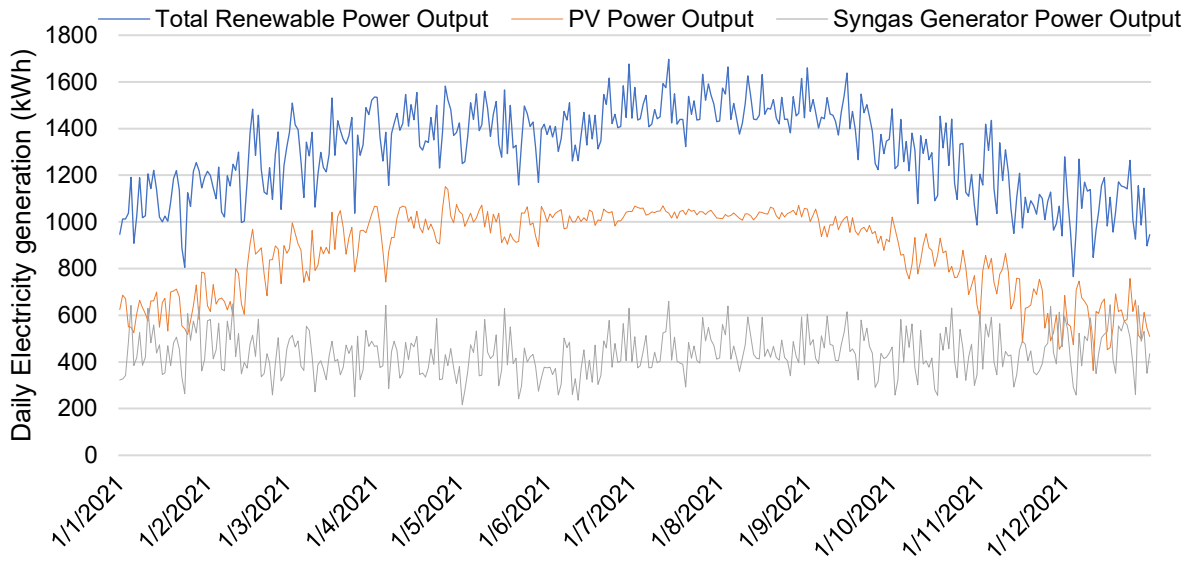


Figure 60: Daily renewable electrical energy output in olive pomace – feather scenario

It is interesting to observe in Figure 60 that, during spring, autumn and winter, the PV's daily renewable electrical energy output oscillates much more compared to the summer months. This is explained by looking at Figure 59. Because some days during autumn, winter, and spring can be overcast while the next or previous day may be clear, a high degree of oscillation is to be expected. In the summer months however, this rapid change in weather is not as common, resulting in a smoother line.

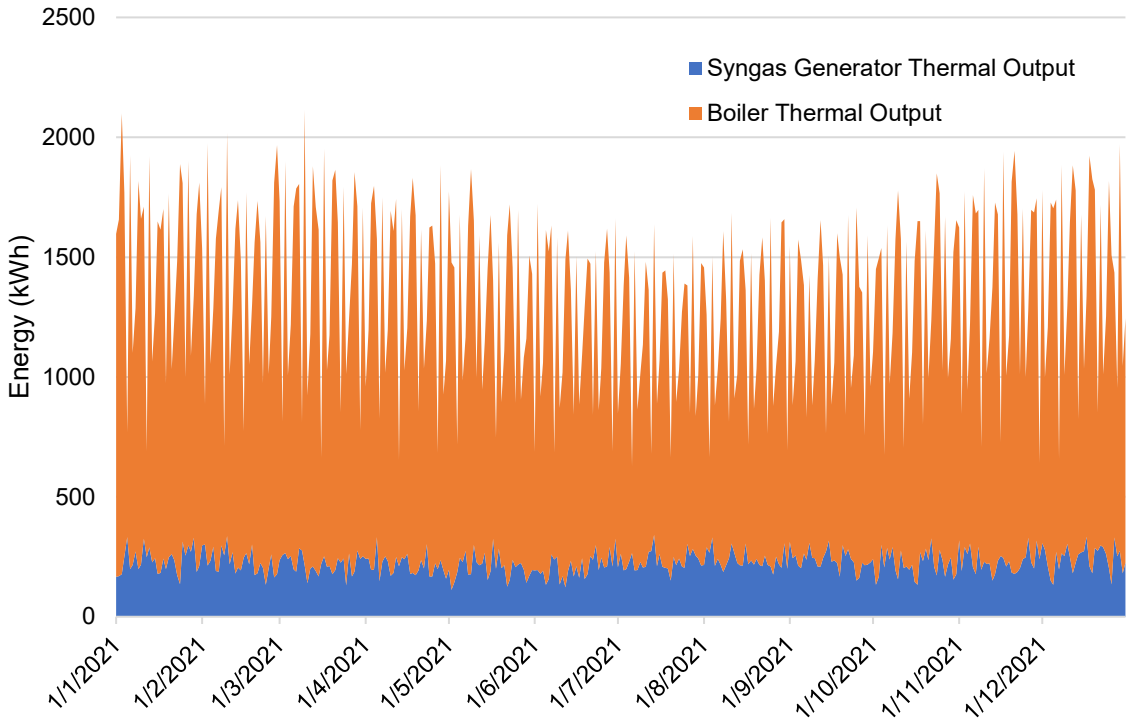


Figure 61: Daily thermal energy output per component in the olive pomace - feather scenario

Due to the high thermal energy demand and the comparatively low thermal energy production from the SG component, as depicted in Figure 61, most of the thermal energy is produced by the boiler which burns extracted olive pomace. It is clear that in the summer months the thermal energy demand is lower. This is because of the greatly increased ambient temperature that the study area experiences during that season. It is also obvious that the thermal demand is characterized by spikes which can be attributed to the days that the slaughterhouse and the compound feed production plant work simultaneously.

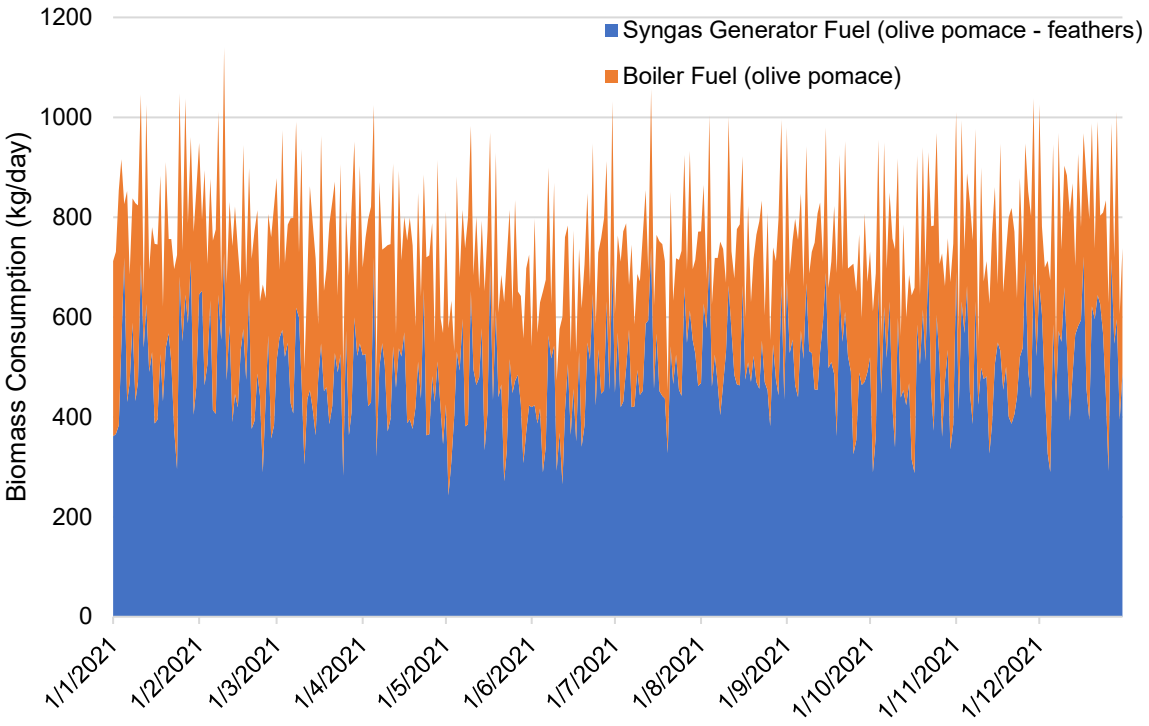


Figure 62: Daily consumption of extracted olive pomace and the combination of olive pomace with feathers in the olive pomace – feather scenario

However, when looking at Figure 62, it is clear that most of the biomass is consumed by the SG component. This is explained by the fact that the SG component has a Heat Recovery Ratio of 25%, while the boiler has an efficiency equal to 85%.

## 4.2. Optimal scenario selected by the Technique for Order of Preference by Similarity to Ideal Solution (TOPSIS)

As described in the methodology, the TOPSIS is implemented to evaluate the simulated scenarios according to 5 criteria, each with their own weight.

The results of this process are presented in Figure 63.

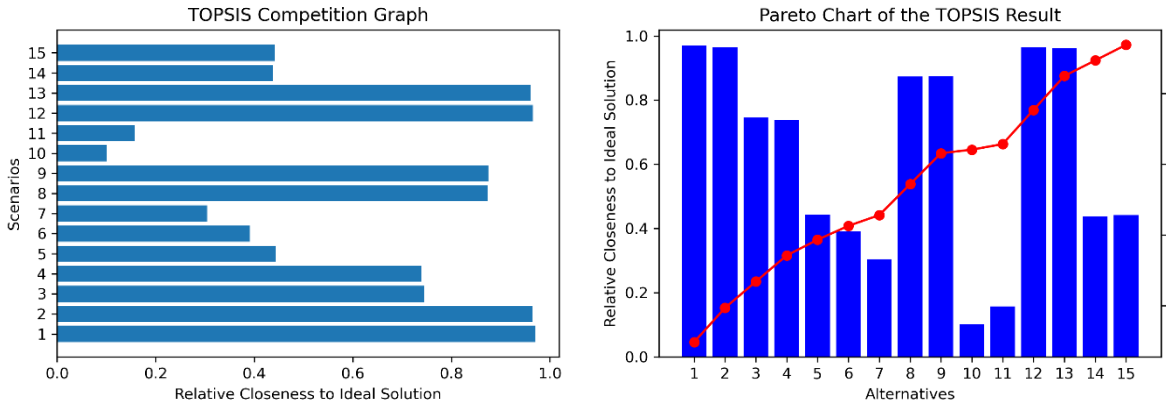

Figure 63: TOPSIS Competition Graph (left) and pareto chart of the TOPSIS result (right) for all scenarios

The ranking that the TOPSIS produced is seen in Table 10:

Table 10: Ranking of the scenarios according to descending closeness to ideal solution

| Scenario Number | Components |
|---|---|
| 1 | Grid_BG(OP-F)_PV |
| 12 | Grid_BG(OP)_PV |
| 2 | Grid_BG(OP-F)_PV_WT |
| 13 | Grid_BG(OP)_PV_WT |
| 9 | Grid_BG(F)_PV_WT |
| 8 | Grid_BG(F)_PV |
| 3 | Grid_PV |
| 4 | Grid_PV_WT |
| 5 | Grid_BG(OP-F)_WT |
| 15 | Grid_BG(OP)_WT |
| 14 | Grid_BG(OP) |
| 6 | Grid_BG(OP-F) |
| 7 | Grid_WT |
| 11 | Grid_BG(F) |
| 10 | Grid_BG(F)_WT |

## 4.3. Sensitivity Analysis

The sensitivity analysis' objective is to identify the parameters of the system which have the biggest impact on its profitability and carbon footprint value.

After performing this analysis, a number of graphs are produced in order to present the results in a more comprehensive manner. These graphs can be seen below.

Figure 64 shows that with regards to the extracted olive pomace price, the LCOE is affected almost linearly while the carbon footprint shows minimal change when the price is less than €0.1/kg. However, when the price exceeds that of the original scenario (€0.1/kg) the carbon footprint starts rising notably. This is because the SG component is already working at near-maximum capacity when operational and thus the drop in its fuel price is not able to raise its energy generation significantly. However, when its fuel becomes more expensive, the rise in carbon footprint is attributed to the increased amount of energy purchased from the grid since it is increasingly cheaper than the energy generated by the SG component. The steady rise in the LCOE is attributed to both the rise of the price of the extracted olive pomace as well as the rise of energy purchased from the grid.

Figure 64 also shows the change in LCOE and carbon footprint as the price of the energy purchased from the grid changes. There is a steep increase in the LCOE and a significant drop in the carbon footprint as the electricity rate changes from

€0.158/kWh to €0.221/kWh. This is because of the fact that when the electricity rate is €0.158/kWh, it is not economically viable to generate electricity with the SG component. As a result, all the electric load that is not served by the PV component, is served by the grid, resulting in a greatly increased carbon footprint.

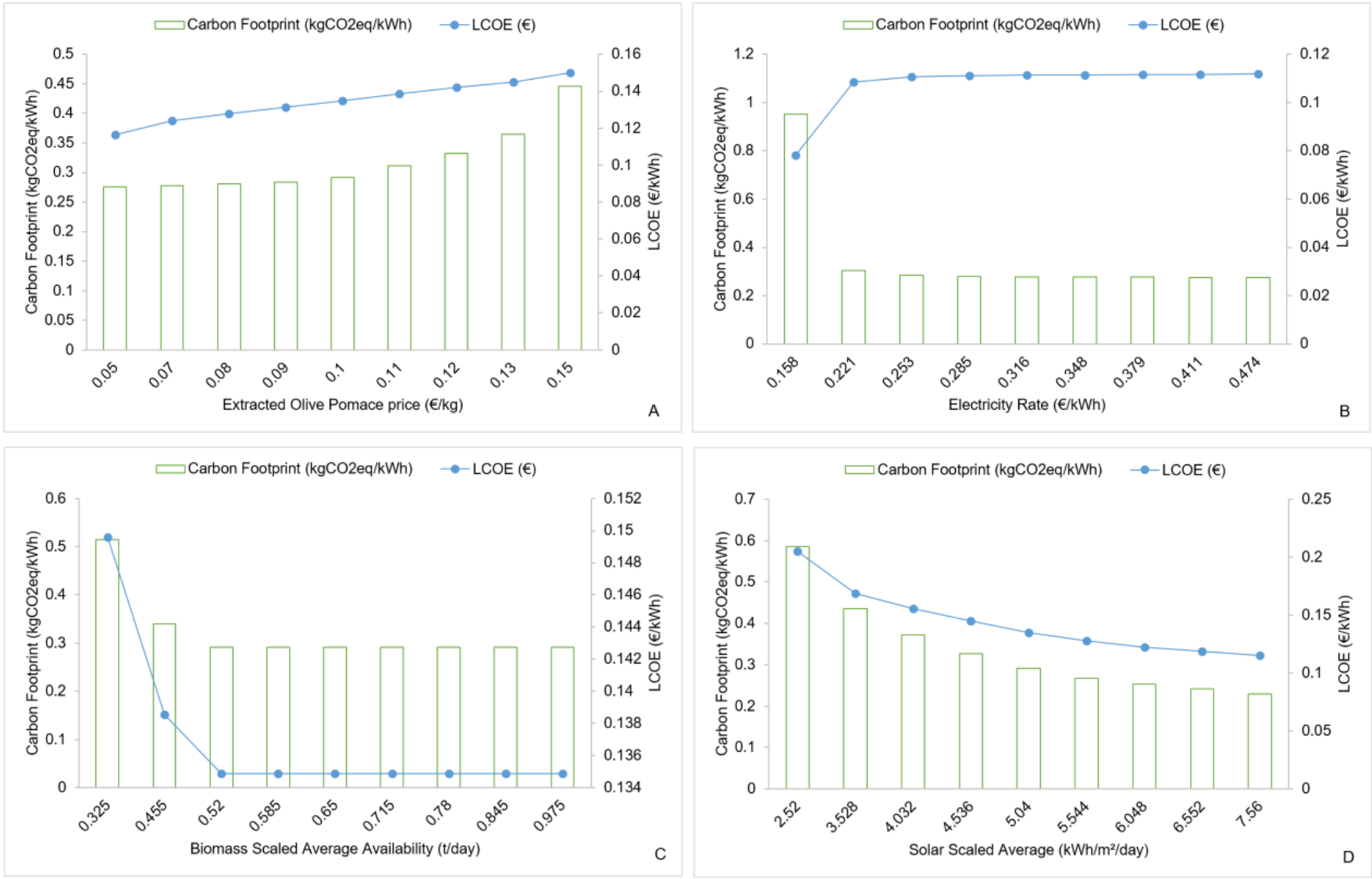


Figure 64: LCOE and CF values for four sensitivity variables

It is also apparent that when the electricity rate is €0.221/kWh or higher, the LCOE increases minimally and the carbon footprint decreases at an analogous minimal pace.

It is interesting to note the increase in the LCOE as the biomass availability falls below the 0.52t/day mark. This is due to the fact that the biomass quantity that is available is inadequate to fully utilize the SG's capacity and thus cover primarily the night-time electric load which cannot be covered by the PV component. This results in increased energy purchases from the grid to cover this load. Since the LCOE and carbon footprint remain stable when the biomass availability is 0.52t/day or higher, it can safely be concluded that any excess biomass quantities remain unused.

Figure 64 also shows that the LCOE and carbon footprint are significantly affected by the solar GHI. Both the LCOE and the carbon footprint decrease as the solar GHI increases, although the rate of their decrease diminishes despite the steady increase in solar GHI. This diminishing effect is explained by the fact that the increased solar GHI comes with increased cell temperature which in turn reduces the component's efficiency of transforming light into electrical energy.

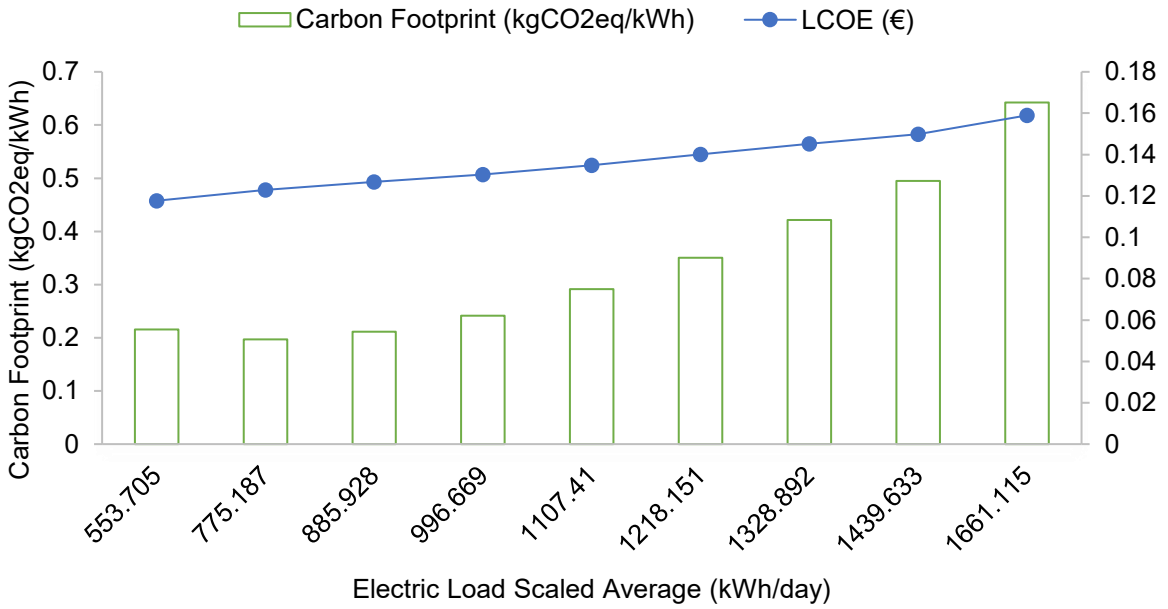


Figure 65: LCOE and CF values for changing electric load cases

The fifth parameter that is part of the sensitivity analysis, is that of the average electric load. In the case of this sensitivity variable, hourly data is still used but is scaled according to the daily average. The LCOE and CF values for this sensitivity variable simulation can be seen in Figure 65. It is interesting to note that the carbon footprint is slightly increased when the average daily electric load is equal to 553.705kWh/day. This is because the SG component has a minimum load ratio of 25% and is not dispatched to sell electricity back to the grid. This means that when the electric load drops below 7.5kW, the SG is unable to serve it, resulting in a slight increase in the energy purchased from the grid. As the average daily electric load increases beyond 775.187kWh/day the carbon footprint and LCOE also increase substantially. This is because the SG and PV components are increasingly unable to serve the electric load

resulting in an increase in energy purchased from the grid. It is also noteworthy that the carbon footprint increases at a much faster pace than the LCOE. This is explained by the fact that the difference in carbon footprint for energy from the grid and energy from the SG and PV is much larger than the difference in rate per kWh.

### 4.3.1. Biomass price sensitivity analysis

In the case of a changing average biomass price, the PV component's energy generation as well as the electric load are unaffected. There is a slight reduction in the SG component's energy generation because at increasingly more timesteps it is cheaper to purchase energy from the grid as the biomass price rises (

Figure 66). However, even at the highest price of €0.15/kg the SG's energy generation is significant especially in the summer months when the plant's electric load is the highest and electricity prices are also very high.

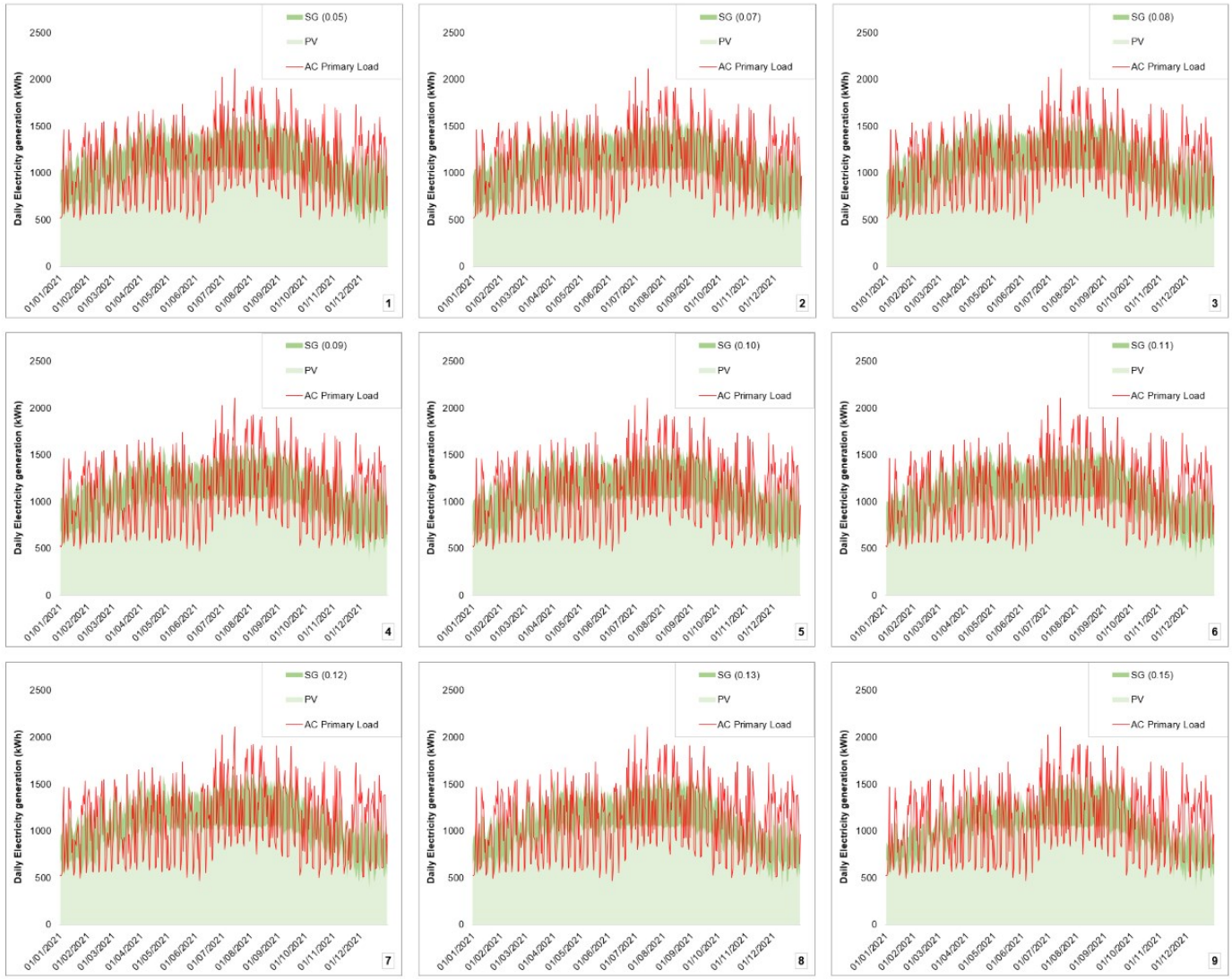


Figure 66: Daily energy generation of the SG and PV alongside the daily electric load for the average biomass price sensitivity analysis

### 4.3.2. Average electricity rates sensitivity analysis

In this case of a changing electricity rate, the unaffected parameters are again the PV energy generation and the electric load. It is noteworthy that when the electricity rate drops to €0.158/kWh, the SG is not used at all, since its energy generation cost is higher than that of the energy purchased from the grid.

In this case of a changing electricity rate, the unaffected parameters are again the PV energy generation and the electric load. It is noteworthy that when the electricity rate drops to €0.158/kWh, the SG is not used at all as seen in

Figure 67, since its energy generation cost is higher than that of the energy purchased from the grid. An unexpected result is that even though the electricity rate more than doubled between the €0.221/kWh case and the €0.474/kWh case, the SG component's total energy generation only increased by a mere 4.37%. In contrast to this rise in total energy generation, the mean electrical output of the SG decreases slightly as the electricity rates rise. When the rate is €0.221/kWh, the mean electrical output is 27.6kW and when the rate is €0.474/kWh, the mean electrical output is 26.6kW. The biggest difference in the operation of the SG can be found in the minimum electrical output which is 18.0kW when the rate is €0.221/kWh and 7.5kW when the rate is €0.474/kWh. This is due to the maintenance cost that is induced in accordance with the machine's operating hours, even if its electrical output is lowered.

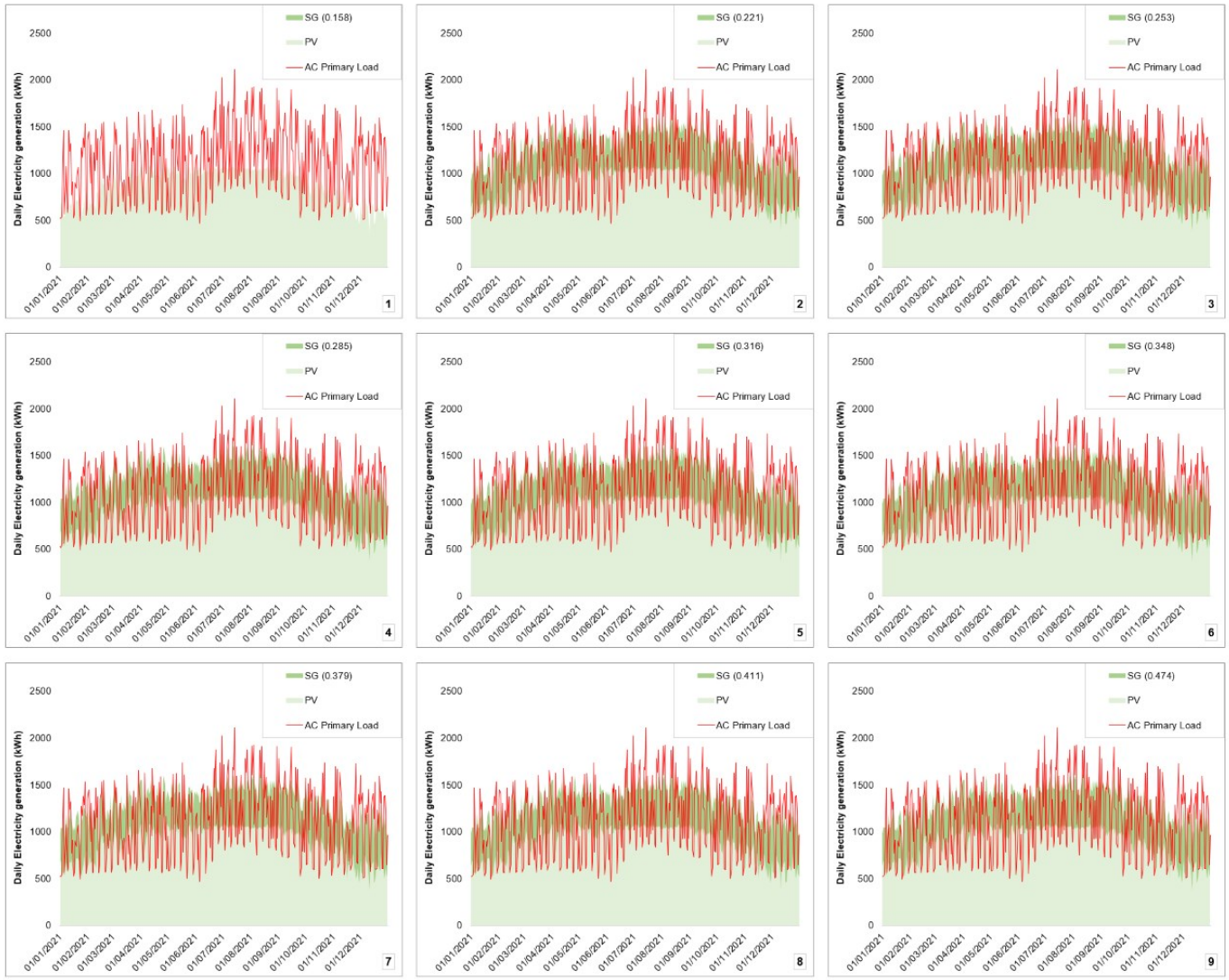


Figure 67: Daily energy generation of the SG and PV alongside the daily electric load for the average electricity rate sensitivity analysis

### 4.3.3. Biomass availability sensitivity analysis

By observing

Figure 68, it is clear that the biomass availability has to drop below 0.520t/day for there to be a significant drop in energy generation by the SG component. It is also notable that any biomass availability above 0.520 does not affect the SG's energy generation. This is because of the fact that the SG component is only used to serve the electric load and not to achieve zero net energy purchased from the grid. This has, as a result, that when the PV fully serves the electric load, the SG is not activated and thus mostly operates during night-time hours and other times at which the PV is unable to serve the load (for example on a cloudy day or when the load exceeds the PV's capacity). During night-time hours the SG is mostly able to cover the electric load and thus is usually not limited by the biomass availability.

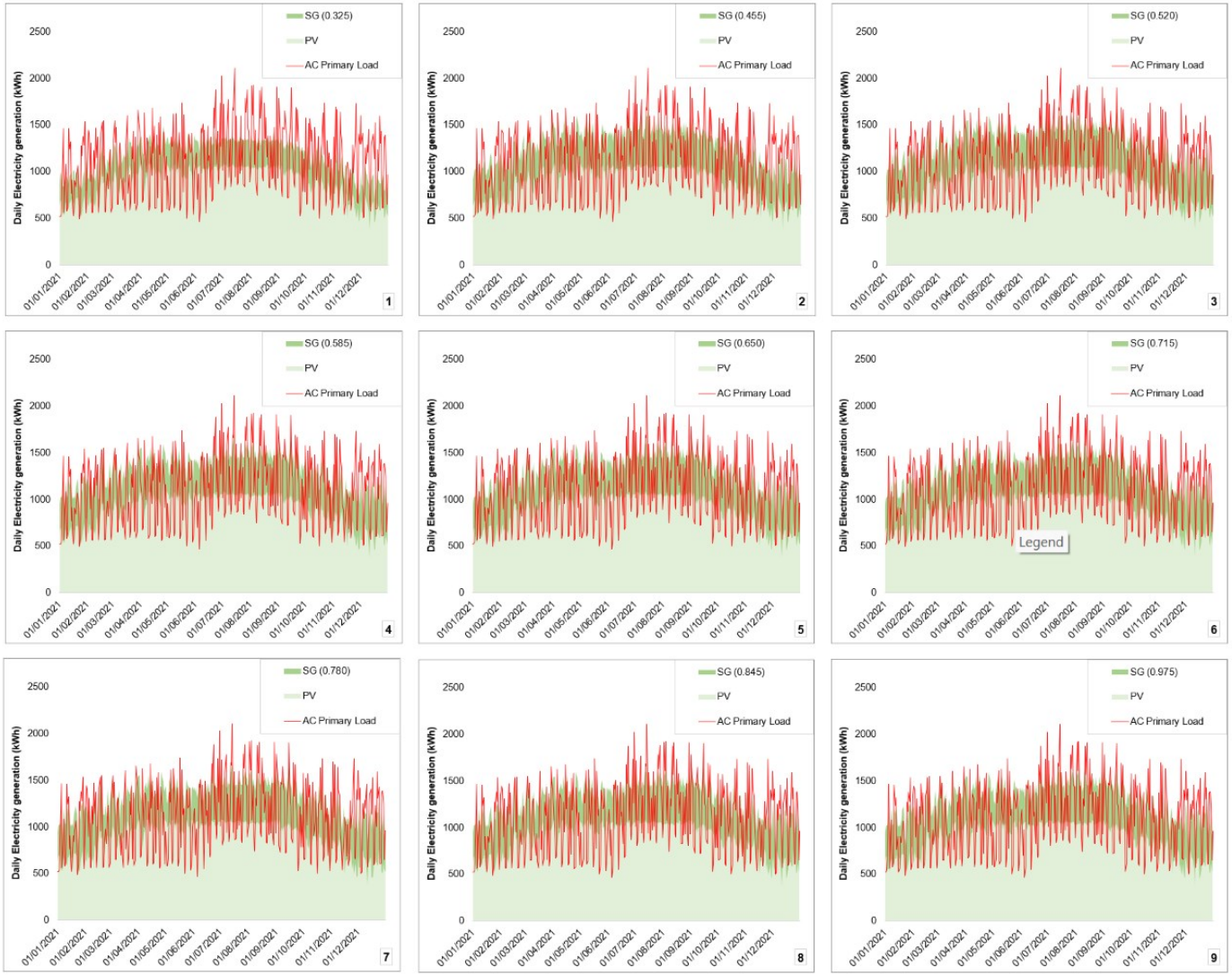


Figure 68: Daily energy generation of the SG and PV alongside the daily electric load for the average biomass availability sensitivity analysis

### 4.3.4. Solar GHI sensitivity analysis

Since the bulk of renewable energy is generated by the PV component, the results shown in

Figure 69 are to be expected. It is clear, that the renewable fraction is significantly reduced, as the solar GHI is decreased. It should come as no surprise that the SG component's energy generation greatly increases, especially during the day-time hours to serve the electric load that exceeds the PV's generation. It is noteworthy that the PV's energy generation reduction intensifies in the summer when compared to the spring, as the solar GHI increases. This is observable because when the solar GHI is 2.52kWh/$m^2$/day, the PV's energy generation creates a bell curve throughout the year. As the solar GHI increases, the top of the curve becomes flatter and when the solar GHI reaches the values of 6.55kWh/$m^2$/day and 7.56kWh/$m^2$/day, there is a clear downward dent in the summer months.

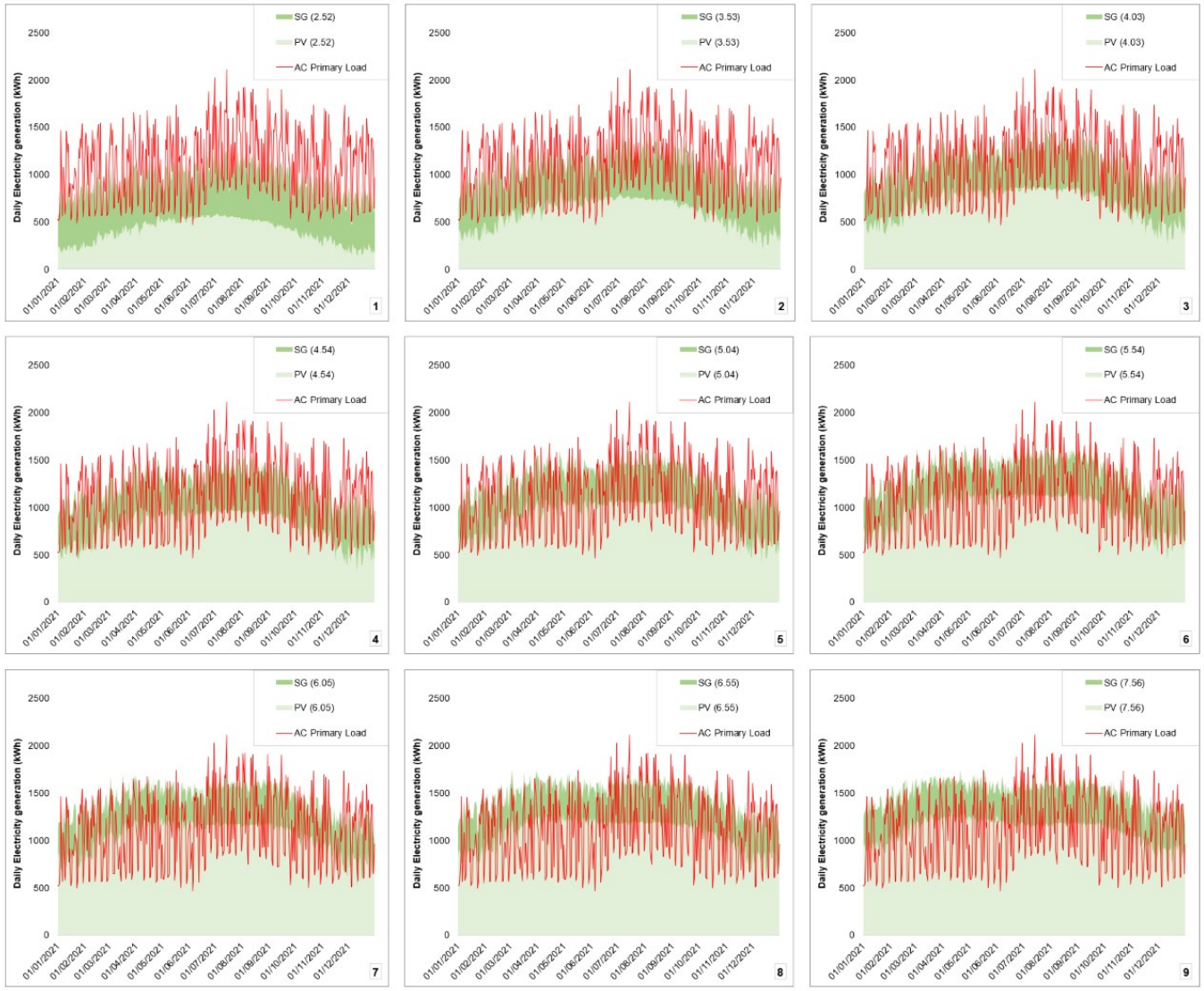


Figure 69: Daily energy generation of the SG and PV alongside the daily electric load for the solar GHI sensitivity analysis

### 4.3.5. Electric load sensitivity analysis

Figure 70 clearly shows that when the electric load has an average value in the range of 554-886kWh/day, the electrical energy generated by the PV and the SG far exceeds the electric load. Although the daily energy generation of the PV component suffices to serve the electric load in the case where the average is 554kWh/day, the SG is still generating a noteworthy percentage of the total electrical energy due to the night-time electric load which cannot be served by the PV. This load is quite high especially in the summer when the cooling needs are increased due to the high ambient temperature. It is also observed that the SG component's electrical energy generation keeps increasing as the average daily electric load increases, which means that the SG component is not operating at maximum capacity at all hours.

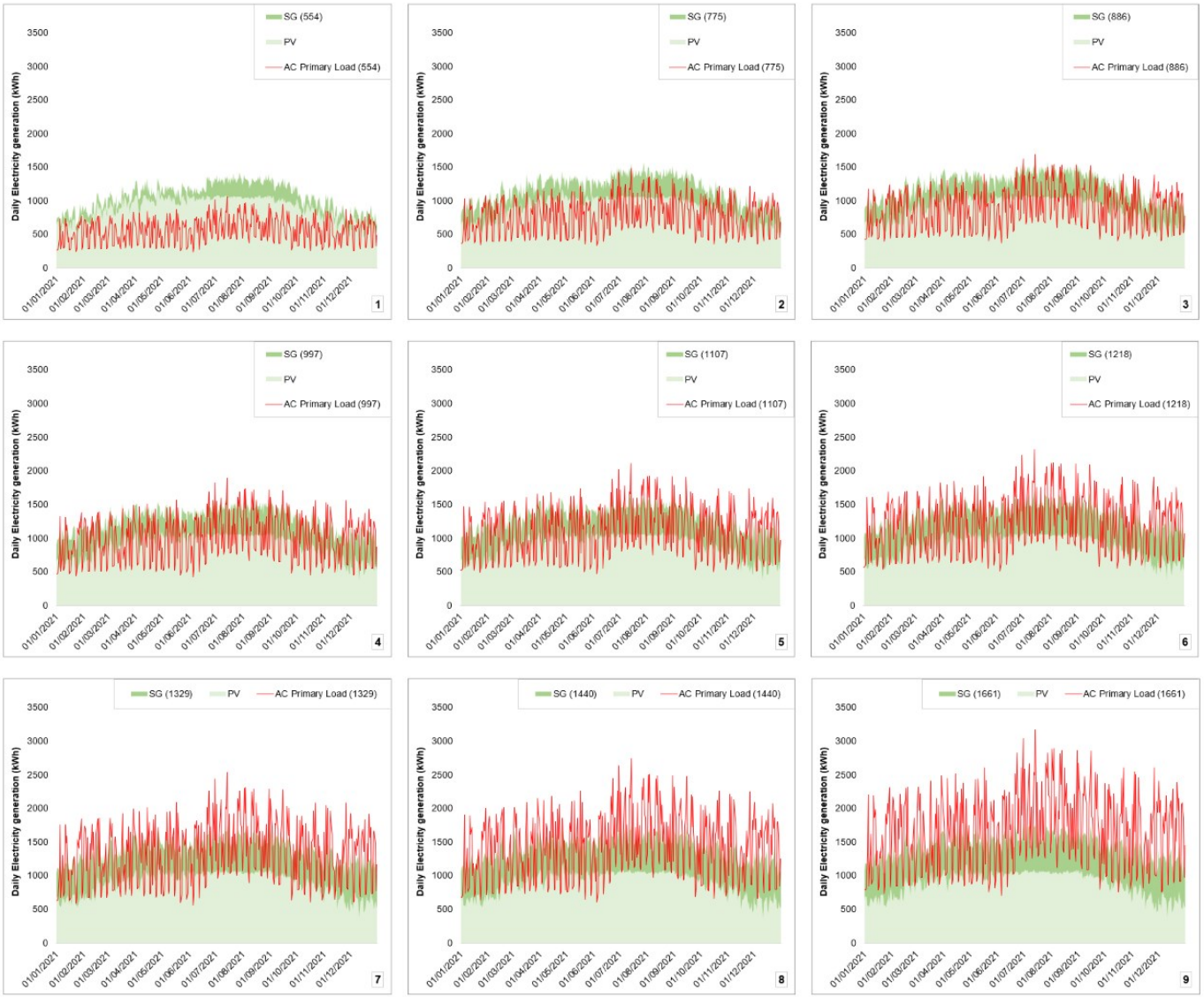


Figure 70: Daily energy generation of the SG and PV alongside the daily electric load for the electric load sensitivity analysis

## 4.4. Comparison with similar studies

A few similar studies that have been done in the past, are presented in Table 11.

Table 11: Similar studies and their results

| Study | RF (%) | LCOE |
|---|---|---|
| This study | 117.62 | 0.135 €/kWh |
| (Malik et al., 2022) | 82.00 | 0.099 $/kWh |
| (Al-Najjar et al., 2022) | 64.30 | 0.438 $/kWh |
| (Ji et al., 2022) | 73.00 | 0.103 $/kWh |
| (B. K. Das, Hassan, et al., 2021) | 100.00 | 0.195 $/kWh |
| (Singh & Basak, 2021) | 100.00 | 0.089 $/kWh |
| (Rajbongshi et al., 2017) | 89-100 | 0.145 $/kWh |
| (Bagheri et al., 2019) | 100.00 | 0.385 $/kWh |
| (Li et al., 2020) | 100.00 | 0.201 $/kWh |
| (Tiwary et al., 2019) | 83.5-85.2 | 0.222-0.245 £/kWh |
| (Jahangir & Cheraghi, 2020) | 100.00 | 0.128-0.223 $/kWh |

As is clearly shown in Table 11, the results of this study are well within the range of other similar studies that used biomass to power a generator with the exception of the renewable fraction. This is above all other studies because the net energy purchased from the grid has a negative value, meaning that the system sold more energy than it purchased. Unfortunately, LCA data was not used in these studies to calculate the actual carbon footprint of their energy generation methods, and as a result, a comparison with regard to that parameter is not possible. When observing the LCOE in this study, it can be seen that it has a moderate to low value. This is despite the fact that the price of extracted olive pomace has risen over 40% in the past couple of years. When looking in more detail at some of the studies in Table 11, it is notable how the study that Malik et al. conducted, has very similar outcomes. They proposed a system comprising of PVs and a syngas generator which uses pine needles from a nearby forest. However, the availability of these pine needles is higher, at 690 tons per year, while the availability of the combination of extracted olive pomace and feathers in this case is 237.25 tons per year. Another very important difference is the fact that the cost per ton of biomass in the study of Malik et al. is just $14.57 ≈ €13.69, which is very low in comparison to this study's biomass cost of €114.01 per ton.

# 5. Conclusions

The aim of this thesis is to analyse various systems and combinations thereof, which could serve the electrical and thermal load of a poultry slaughterhouse and compound feed production plant in Lakonia, Greece, in a more economically sustainable manner and at the same time reduce the carbon footprint of those plants.

The approach that is taken toward meeting those objectives is to assess the available renewable energy resources which are wind, solar and two kinds of biomass, and model various systems that integrate wind turbines, photovoltaics and a syngas generator in order to utilise these resources while adhering to the legislative and resource constraints. Fifteen distinct scenarios are evaluated for their performance on the above-mentioned parameters and the optimal scenario is chosen using the TOPSIS method.

With regard to the methodology that is used, first of all, a description of the study area is given with all of the relevant meteorological data, which enables the assessment of the renewable resources of wind and solar in the area. Then, a thorough analysis of the processes that take place in the case study's plants is presented and the electrical and thermal load consuming processes are identified. After this, the actual combined electric load of these plants is presented as sourced from the electricity provider in hourly timesteps for a full year (2021). Then, the thermal load is estimated according to the quantity of fuel that is used, alongside the personal knowledge of the author and the plant operators, in combination with the knowledge of the fuel's calorific value when burned in a conventional biomass boiler. The final part of the methodology includes the presentation of the scenarios that are simulated, the mathematical modelling of all utilised components of the system, the presentation of the TOPSIS method, the sensitivity analysis that is performed on the optimal scenario, as well as the assumptions that were made in this study.

After simulating all 15 distinct scenarios, three main categories of systems can be identified. These include systems in which the SG component uses:

1) Extracted olive pomace,
2) Broiler feathers,
3) A combination of extracted olive pomace and broiler feathers at a weight ratio of 9:1 respectively.

The optimal scenarios from these three categories are analysed in detail with hourly timestep heatmaps and daily energy generation per component graphs to present as much information as possible.

The optimal out of all scenarios was one where PVs, an SG, the grid and a biomass boiler were used. In this scenario, the biomass boiler burns extracted olive pomace and the SG burns syngas produced from a combination of extracted olive pomace and broiler feathers at a weight ratio of 9:1, respectively. This scenario produced remarkable results, slicing the LCOE by more than 50% and achieving an LCOE which is on the low end when compared to a lot of similar studies like the ones mentioned in Table 11.

## 5.1. Weaknesses of this study

The weaknesses that can be identified for this study are the following:

1) The available electric load data represents the combined load of the poultry slaughterhouse and the feed production plant and there are no distinct load profiles available.

2) The thermal load profile was crudely estimated with regard to its hourly distribution since the feed production plant's thermal load demand is unpredictable depending on the client's orders and the operator's discretion in choosing the hour of day that the feed is produced.
3) The real-time electricity rates, although available, were not used due to the fact that the HOMER program cannot support a net-metering scheme with real-time hourly rates.
4) In the sensitivity analysis of the optimal scenario, the electricity rates parameters could only be simulated in the form of a simple rate, meaning a rate that is stable throughout the 8760 hours of the year. This of course creates a significant difference between the actual energy cost and the simulated one, while also making the SG component unable to respond to hourly peaks in electricity rates.
5) The thermal energy that is produced by the SG component is not modelled accurately due to the inability of the HOMER program to take into account the heat that is generated in the production of syngas.

## 5.2. Opportunities and suggestions for future research

In the context of waste to energy, just like the utilisation of broiler feathers for fuel, sewage sludge and poultry litter could be used for the production of biogas which in turn could be used as fuel in an electricity generator. Other technologies that could be investigated are photovoltaics that also heat water via tubes that run through them. This is, in the author's opinion, a technology of high potential because it not only enhances the overall energy efficiency of the system through by capturing heat energy that would otherwise be lost; but through the capturing of this heat, reduces the panel's temperature, making it operate at a higher electrical efficiency, especially in high ambient temperatures.

# 6. Bibliography

## 6.1. Studies listed in the table of the literature review


1) (Furubayashi, 2022)
2) (Fioriti et al., 2020)
3) (Tiwary et al., 2019)
4) (Javed et al., 2021)
5) (Malik et al., 2022)
6) (Buller et al., 2022)
7) (Emrani et al., 2022)
8) (Bukar et al., 2020)
9) (Jahangir & Cheraghi, 2020)
10) (Murugaperumal et al., 2020)
11) (Ji et al., 2022)
12) (Kirim et al., 2022)

13)(Shezan et al., 2022)
14)(Demirci et al., 2022)
15)(Aziz et al., 2022)
16)(Hossein Jahangir et al., 2022)
17)(Cao et al., 2022)
18)(Hoseinzadeh & Astiaso Garcia, 2022)
19)(Akhtari & Baneshi, 2019)
20)(Qiblawey et al., 2022)
21)(Nasser et al., 2022)
22)(Chennaif et al., 2022)
23)(Chaurasia et al., 2022)
24)(Kaur et al., 2021)
25)(B. K. Das, Hassan, et al., 2021)
26)(Wang et al., 2021)
27)(Sifakis et al., 2021)
28)(Ribó-Pérez et al., 2021)
29)(B. K. Das, Tushar, et al., 2021)
30)(Ajiboye et al., 2022)
31)(Baruah et al., 2021)
32)(Eisapour et al., 2021)
33)(Malik et al., 2021)
34)(Fard et al., 2021)
35)(Al-Ghussain et al., 2021)
36)(Ali et al., 2021)
37)(Singh & Basak, 2021)
38)(Shboul et al., 2021)
39)(B. K. Das, Alotaibi, et al., 2021)
40)(Molyneaux et al., 2016)
41)(Rezk et al., 2019)
42)(R. Kumar & Channi, 2022)
43)(Seedahmed et al., 2022)
44)(Roy et al., 2022)
45)(Rajbongshi et al., 2017)
46)(Patel & Singal, 2016)
47)(Amutha & Rajini, 2016)
48)(Kusakana, 2016)
49)(Diab et al., 2016)
50)(Bagheri et al., 2019)
51)(Al-Buraiki & Al-Sharafi, 2021)
52)(Elkadeem et al., 2021)
53)(Luta & Raji, 2018)
54)(Odou et al., 2020)
55)(Wu et al., 2018)
56)(Liu et al., 2020)
57)(Habib et al., 2019)
58)(Duman & Güler, 2018)

59)(Grande et al., 2018)
60)(Al-Najjar et al., 2022)
61)(B. K. Das et al., 2022)
62)(Bhatt et al., 2022)
63)(Haghighat Mamaghani et al., 2016)
64)(Jung & Villaran, 2017)
65)(Ajlan et al., 2017)
66)(M. J. Khan et al., 2017)
67)(H. S. Das et al., 2017)
68)(M. Das et al., 2019)
69)(Diemuodeke et al., 2019)
70)(Hossain et al., 2017)
71)(Al-Sharafi et al., 2017)
72)(P. Das et al., 2022)
73)(Singh et al., 2017)
74)(Bentouba & Bourouis, 2016)
75)(Park & Kwon, 2016)
76)(Fazelpour et al., 2016)
77)(He et al., 2021)
78)(Mokhtara et al., 2021)
79)(Chade et al., 2015)
80)(Kalinci, 2015)
81)(Kim et al., 2014)
82)(Elmaadawy et al., 2020)
83)(Atallah et al., 2020)
84)(Padrón et al., 2019)
85)(Güler et al., 2013)
86)(Ashourian et al., 2013)
87)(Gebrehiwot et al., 2019)
88)(Fodhil et al., 2019)
89)(C. Xu et al., 2020)
90)(Peláez-Peláez et al., 2021)
91)(Salameh et al., 2021)
92)(Ahmad et al., 2018)
93)(Silva et al., 2013)
94)(Li et al., 2020)
95)(Dursun, 2012)
96)(Rasool et al., 2022)
97)(Yang et al., 2022)
98)(Li et al., 2022)
99)(Karakoulidis et al., 2011)
100) (Türkay & Telli, 2011)

## 6.2. Full Bibliography

Ahmad, J., Imran, M., Khalid, A., Iqbal, W., Ashraf, S. R., Adnan, M., Ali, S. F., & Khokhar, K. S. (2018). 93. Techno economic analysis of a wind-photovoltaic-biomass hybrid renewable energy system for rural electrification: A case study of

Kallar Kahar. *Energy*, *148*, 208–234. https://doi.org/10.1016/j.energy.2018.01.133

Ajiboye, A. A., Popoola, S. I., Adewuyi, O. B., Atayero, A. A., & Adebisi, B. (2022). 97. Data-driven optimal planning for hybrid renewable energy system management in smart campus: A case study. *Sustainable Energy Technologies and Assessments*, *52*. https://doi.org/10.1016/j.seta.2022.102189

Ajlan, A., Tan, C. W., & Abdilahi, A. M. (2017). 54. Assessment of environmental and economic perspectives for renewable-based hybrid power system in Yemen. In *Renewable and Sustainable Energy Reviews* (Vol. 75, pp. 559–570). Elsevier Ltd. https://doi.org/10.1016/j.rser.2016.11.024

Akbari, A., Vahidinasab, V., Arasteh, H., & Kazemi-Robati, E. (2022). Rural and residential microgrids: concepts, status quo, model, and application. *Residential Microgrids and Rural Electrifications*, 131–161. https://doi.org/10.1016/B978-0-323-90177-2.00007-4

Akhtari, M. R., & Baneshi, M. (2019). 95. Techno-economic assessment and optimization of a hybrid renewable co-supply of electricity, heat and hydrogen system to enhance performance by recovering excess electricity for a large energy consumer. *Energy Conversion and Management*, *188*, 131–141. https://doi.org/10.1016/j.enconman.2019.03.067

alamy.com. (2019). *Huge collection of brown chicken feathers. Plumage carpet background or texture. close-up chicken feather texture for background Stock Photo - Alamy*. https://www.alamy.com/huge-collection-of-brown-chicken-feathers-plumage-carpet-background-or-texture-close-up-chicken-feather-texture-for-background-image338686252.html

Al-Buraiki, A. S., & Al-Sharafi, A. (2021). 85. Technoeconomic analysis and optimization of hybrid solar/wind/battery systems for a standalone house integrated with electric vehicle in Saudi Arabia. *Energy Conversion and Management*, *250*. https://doi.org/10.1016/j.enconman.2021.114899

Al-Ghussain, L., Darwish Ahmad, A., Abubaker, A. M., & Mohamed, M. A. (2021). 32. An integrated photovoltaic/wind/biomass and hybrid energy storage systems towards 100% renewable energy microgrids in university campuses. *Sustainable Energy Technologies and Assessments*, *46*. https://doi.org/10.1016/j.seta.2021.101273

Ali, F., Ahmar, M., Jiang, Y., & AlAhmad, M. (2021). 33. A techno-economic assessment of hybrid energy systems in rural Pakistan. *Energy*, *215*. https://doi.org/10.1016/j.energy.2020.119103

Al-Najjar, H., El-Khozondar, H. J., Pfeifer, C., & al Afif, R. (2022). 8. Hybrid grid-tie electrification analysis of bio-shared renewable energy systems for domestic application. *Sustainable Cities and Society*, *77*. https://doi.org/10.1016/j.scs.2021.103538

Al-Sharafi, A., Sahin, A. Z., Ayar, T., & Yilbas, B. S. (2017). 58. Techno-economic analysis and optimization of solar and wind energy systems for power generation and hydrogen production in Saudi Arabia. In *Renewable and Sustainable Energy Reviews* (Vol. 69, pp. 33–49). Elsevier Ltd. https://doi.org/10.1016/j.rser.2016.11.157

Amelia, A. R., Irwan, Y. M., Safwati, I., Leow, W. Z., Mat, M. H., Shukor, M., Rahim, A., & Esa, S. M. (2019). *Technologies of solar tracking systems: A review*. https://doi.org/10.1088/1757-899X/767/1/012052

Amutha, W. M., & Rajini, V. (2016). 42. Cost benefit and technical analysis of rural electrification alternatives in southern India using HOMER. In *Renewable and Sustainable Energy Reviews* (Vol. 62, pp. 236–246). Elsevier Ltd. https://doi.org/10.1016/j.rser.2016.04.042

Anderson, R., Bayer, P. E., & Edwards, D. (2020). Climate change and the need for agricultural adaptation. In *Current Opinion in Plant Biology* (Vol. 56, pp. 197–202). Elsevier Ltd. https://doi.org/10.1016/j.pbi.2019.12.006

Arias, P.A., Bellouin, N., Coppola, E., Jones, R. G., Krinner, G., Marotzke, J., Naik, V., Palmer, M. D., Plattner, G.-K., Rogelj, J., Rojas, M., Sillmann, J., Storelvmo, T., Thorne, P. W., Trewin, B., & et al. (2021). Technical Summary. *Climate Change 2021: The Physical Science Basis. Contribution of Working Group I to the Sixth Assessment Report of the Intergovernmental Panel on Climate Change*. https://doi.org/10.1017/9781009157896.002

Arvelakis, S., Gehrmann, H., Beckmann, M., & Koukios, E. G. (2002). Effect of leaching on the ash behavior of olive residue during fluidized bed gasification. *Biomass and Bioenergy*, *22*(1), 55–69. https://doi.org/10.1016/S0961-9534(01)00059-9

Ashourian, M. H., Cherati, S. M., Mohd Zin, A. A., Niknam, N., Mokhtar, A. S., & Anwari, M. (2013). 67. Optimal green energy management for island resorts in Malaysia. *Renewable Energy*, *51*, 36–45. https://doi.org/10.1016/j.renene.2012.08.056

Atallah, M. O., Farahat, M. A., Lotfy, M. E., & Senjyu, T. (2020). 78. Operation of conventional and unconventional energy sources to drive a reverse osmosis desalination plant in Sinai Peninsula, Egypt. *Renewable Energy*, *145*, 141–152. https://doi.org/10.1016/j.renene.2019.05.138

Aydingakko, A., Mukhaini, M., & Jassasi, S. (2016, November). *Renewable Energy Potential in Middle East and Particularly Oman case*.

Aziz, A. S., Tajuddin, M. F. N., Zidane, T. E. K., Su, C. L., Alrubaie, A. J. K., & Alwazzan, M. J. (2022). 15. Techno-economic and environmental evaluation of PV/diesel/battery hybrid energy system using improved dispatch strategy. *Energy Reports*, *8*, 6794–6814. https://doi.org/10.1016/j.egyr.2022.05.021

Bagheri, M., Delbari, S. H., Pakzadmanesh, M., & Kennedy, C. A. (2019). 45. City-integrated renewable energy design for low-carbon and climate-resilient

communities. *Applied Energy*, *239*, 1212–1225. https://doi.org/10.1016/j.apenergy.2019.02.031

Bahnasawy, A., Ali, S. A., & El-Haddad, Z. (2014). *Energy of feed Related papers ENERGY CONSUMPT ION IN MANUFACT URING OF DIFFERENT T YPES OF FEEDS Oladipo Olat ubosun Role of feeding rat e in energy consumpt ion and mechanical propert ies for different t ypes of feed pell… ENERGY CONSUMPTION IN MANUFACTURING OF DIFFERENT TYPES OF FEEDS*.

Bain, R. L., & Broer, K. (2011). *3 Gasification*. https://doi.org/10.1002/9781119990840.ch3

Baruah, A., Basu, M., & Amuley, D. (2021). 28. Modeling of an autonomous hybrid renewable energy system for electrification of a township: A case study for Sikkim, India. *Renewable and Sustainable Energy Reviews*, *135*. https://doi.org/10.1016/j.rser.2020.110158

Bentouba, S., & Bourouis, M. (2016). 60. Feasibility study of a wind-photovoltaic hybrid power generation system for a remote area in the extreme south of Algeria. *Applied Thermal Engineering*, *99*, 713–719. https://doi.org/10.1016/j.applthermaleng.2015.12.014

Bereżnicka, J., & Pawlonka, T. (2018). MEAT CONSUMPTION AS AN INDICATOR OF ECONOMIC WELL-BEING — CASE STUDY OF A DEVELOPED AND DEVELOPING ECONOMY. *Acta Scientiarum Polonorum. Oeconomia*, *17*(2), 17–26. https://doi.org/10.22630/aspe.2018.17.2.17

Bhatt, A., Ongsakul, W., & Madhu M., N. (2022). 10. Optimal techno-economic feasibility study of net-zero carbon emission microgrid integrating second-life battery energy storage system. *Energy Conversion and Management*, *266*. https://doi.org/10.1016/j.enconman.2022.115825

*Biomass explained - U.S. Energy Information Administration (EIA)*. (2022). https://www.eia.gov/energyexplained/biomass/

Blanco, M. I. (2009). The economics of wind energy. *Renewable and Sustainable Energy Reviews*, *13*(6–7), 1372–1382. https://doi.org/10.1016/J.RSER.2008.09.004

Briam, R., Walker, M. E., & Masanet, E. (2015). A comparison of product-based energy intensity metrics for cheese and whey processing. *Journal of Food Engineering*, *151*, 25–33. https://doi.org/10.1016/J.JFOODENG.2014.11.011

Bukar, A. L., Tan, C. W., Yiew, L. K., Ayop, R., & Tan, W. S. (2020). 89. A rule-based energy management scheme for long-term optimal capacity planning of grid-independent microgrid optimized by multi-objective grasshopper optimization algorithm. *Energy Conversion and Management*, *221*. https://doi.org/10.1016/j.enconman.2020.113161

Buller, L. S., Sganzerla, W. G., Berni, M. D., Brignoli, S. C., & Forster-Carneiro, T. (2022). 6. Design and techno-economic analysis of a hybrid system for energy supply in a wastewater treatment plant: A decentralized energy strategy. *Journal*

*of Environmental Management*, *305*. https://doi.org/10.1016/j.jenvman.2021.114389

Campos, I., Pinheiro Valente, L. M., Matos, E., Marques, P., & Freire, F. (2020). Life-cycle assessment of animal feed ingredients: Poultry fat, poultry by-product meal and hydrolyzed feather meal. *Journal of Cleaner Production*, *252*. https://doi.org/10.1016/j.jclepro.2019.119845

Campoy, M., Gómez-Barea, A., Ollero, P., & Nilsson, S. (2014). Gasification of wastes in a pilot fluidized bed gasifier. *Fuel Processing Technology*, *121*, 63–69. https://doi.org/10.1016/j.fuproc.2013.12.019

Cao, Y., Bashiri Mousavi, S., & Ahmadi, P. (2022). 17. Techno-economic assessment of a biomass-driven liquid air energy storage (LAES) system for optimal operation with wind turbines. *Fuel*, *324*. https://doi.org/10.1016/j.fuel.2022.124495

Caresana, F. (2011). *Energy production from landfill biogas: An italian case*. https://doi.org/10.1016/j.biombioe.2011.08.002

Center for Sustainable Systems. (2022). “Wind Energy Factsheet.” Pub. No. CSS07. *University of Michigan*.

Chade, D., Miklis, T., & Dvorak, D. (2015). 63. Feasibility study of wind-to-hydrogen system for Arctic remote locations - Grimsey island case study. *Renewable Energy*, *76*, 204–211. https://doi.org/10.1016/j.renene.2014.11.023

Chaurasia, R., Gairola, S., & Pal, Y. (2022). 22. Technical, economic, and environmental performance comparison analysis of a hybrid renewable energy system based on power dispatch strategies. *Sustainable Energy Technologies and Assessments*, *53*. https://doi.org/10.1016/j.seta.2022.102787

Chen, A., & Sen, P. K. (2016, November 2). Advancement in battery technology: A state-of-the-art review. *IEEE Industry Application Society, 52nd Annual Meeting: IAS 2016*. https://doi.org/10.1109/IAS.2016.7731812

Chen, S., Feng, H., Zheng, J., Ye, J., Song, Y., Yang, H., & Zhou, M. (2020). Life Cycle Assessment and Economic Analysis of Biomass Energy Technology in China: A Brief Review. *Processes, MDPI*. https://doi.org/10.3390/pr8091112

Chennaif, M., Maaouane, M., Zahboune, H., Elhafyani, M., & Zouggar, S. (2022). 21. Tri-objective techno-economic sizing optimization of Off-grid and On-grid renewable energy systems using Electric system Cascade Extended analysis and system Advisor Model. *Applied Energy*, *305*. https://doi.org/10.1016/j.apenergy.2021.117844

Commission on Geopolitics of Energy Transformation, G. (2019). *A new world: The geopolitics of the energy transformation*. www.geopoliticsofrenewables.org

*Commission Regulation (EU) 2021/1372*, (2021). https://doi.org/10.2903/j.efsa.2018.5314

Corella, J., Toledo, J. M., & Padilla, R. (2004). Olivine or dolomite as in-bed additive in biomass gasification with air in a fluidized bed: Which is better? *Energy and Fuels*, *18*(3), 713–720. https://doi.org/10.1021/EF0340918/SUPPL_FILE/EF0340918SI20031201_062354.PDF

Crippa, M., Solazzo, E., Guizzardi, D., Monforti-Ferrario, F., Tubiello, F. N., & Leip, A. (2021). Food systems are responsible for a third of global anthropogenic GHG emissions. *Nature Food 2021 2:3*, *2*(3), 198–209. https://doi.org/10.1038/s43016-021-00225-9

Das, B. K., Alotaibi, M. A., Das, P., Islam, M. S., Das, S. K., & Hossain, M. A. (2021). 36. Feasibility and techno-economic analysis of stand-alone and grid-connected PV/Wind/Diesel/Batt hybrid energy system: A case study. *Energy Strategy Reviews*, *37*. https://doi.org/10.1016/j.esr.2021.100673

Das, B. K., Hassan, R., Islam, M. S., & Rezaei, M. (2022). 9. Influence of energy management strategies and storage devices on the techno-enviro-economic optimization of hybrid energy systems: A case study in Western Australia. *Journal of Energy Storage*, *51*. https://doi.org/10.1016/j.est.2022.104239

Das, B. K., Hassan, R., Tushar, M. S. H. K., Zaman, F., Hasan, M., & Das, P. (2021). 24. Techno-economic and environmental assessment of a hybrid renewable energy system using multi-objective genetic algorithm: A case study for remote Island in Bangladesh. *Energy Conversion and Management*, *230*. https://doi.org/10.1016/j.enconman.2020.113823

Das, B. K., Tushar, M. S. H. K., & Hassan, R. (2021). 96. Techno-economic optimisation of stand-alone hybrid renewable energy systems for concurrently meeting electric and heating demand. *Sustainable Cities and Society*, *68*. https://doi.org/10.1016/j.scs.2021.102763

Das, H. S., Tan, C. W., Yatim, A. H. M., & Lau, K. Y. (2017). 56. Feasibility analysis of hybrid photovoltaic/battery/fuel cell energy system for an indigenous residence in East Malaysia. In *Renewable and Sustainable Energy Reviews* (Vol. 76, pp. 1332–1347). Elsevier Ltd. https://doi.org/10.1016/j.rser.2017.01.174

Das, M., Singh, M. A. K., & Biswas, A. (2019). 94. Techno-economic optimization of an off-grid hybrid renewable energy system using metaheuristic optimization approaches – Case of a radio transmitter station in India. *Energy Conversion and Management*, *185*, 339–352. https://doi.org/10.1016/j.enconman.2019.01.107

Das, P., Das, B. K., Rahman, M., & Hassan, R. (2022). 75. Evaluating the prospect of utilizing excess energy and creating employments from a hybrid energy system meeting electricity and freshwater demands using multi-objective evolutionary algorithms. *Energy*, *238*. https://doi.org/10.1016/j.energy.2021.121860

Demirci, A., Akar, O., & Ozturk, Z. (2022). 14. Technical-environmental-economic evaluation of biomass-based hybrid power system with energy storage for rural electrification. *Renewable Energy*, *195*, 1202–1217. https://doi.org/10.1016/j.renene.2022.06.097

Department for Business Energy and Industrial Strategy. (2018). *DIGEST OF UNITED KINGDOM ENERGY STATISTICS 2018*. www.nationalarchives.gov.uk/doc/open-government-

Diab, F., Lan, H., Zhang, L., & Ali, S. (2016). 44. An environmentally friendly factory in Egypt based on hybrid photovoltaic/wind/diesel/battery system. *Journal of Cleaner Production*, *112*, 3884–3894. https://doi.org/10.1016/j.jclepro.2015.07.008

Diemuodeke, E. O., Addo, A., Oko, C. O. C., Mulugetta, Y., & Ojapah, M. M. (2019). 46. Optimal mapping of hybrid renewable energy systems for locations using multi-criteria decision-making algorithm. *Renewable Energy*, *134*, 461–477. https://doi.org/10.1016/j.renene.2018.11.055

Dudyński, M., Kwiatkowski, K., & Bajer, K. (2012). From feathers to syngas - Technologies and devices. *Waste Management*, *32*(4), 685–691. https://doi.org/10.1016/j.wasman.2011.11.017

Duffie, J., & Beckman, W. (1991). *Solar Engineering of Thermal Processes 2nd edition*. Wiley.

Duman, A. C., & Güler, Ö. (2018). 52. Techno-economic analysis of off-grid PV/wind/fuel cell hybrid system combinations with a comparison of regularly and seasonally occupied households. *Sustainable Cities and Society*, *42*, 107–126. https://doi.org/10.1016/j.scs.2018.06.029

Dursun, B. (2012). 69. Determination of the optimum hybrid renewable power generating systems for Kavakli campus of Kirklareli University, Turkey. In *Renewable and Sustainable Energy Reviews* (Vol. 16, Issue 8, pp. 6183–6190). https://doi.org/10.1016/j.rser.2012.07.017

Eisapour, A. H., Jafarpur, K., & Farjah, E. (2021). 29. Feasibility study of a smart hybrid renewable energy system to supply the electricity and heat demand of Eram Campus, Shiraz University; simulation, optimization, and sensitivity analysis. *Energy Conversion and Management*, *248*. https://doi.org/10.1016/j.enconman.2021.114779

Elkadeem, M. R., Kotb, K. M., Elmaadawy, K., Ullah, Z., Elmolla, E., Liu, B., Wang, S., Dán, A., & Sharshir, S. W. (2021). 86. Feasibility analysis and optimization of an energy-water-heat nexus supplied by an autonomous hybrid renewable power generation system: An empirical study on airport facilities. *Desalination*, *504*. https://doi.org/10.1016/j.desal.2021.114952

Elmaadawy, K., Kotb, K. M., Elkadeem, M. R., Sharshir, S. W., Dán, A., Moawad, A., & Liu, B. (2020). 77. Optimal sizing and techno-enviro-economic feasibility assessment of large-scale reverse osmosis desalination powered with hybrid renewable energy sources. *Energy Conversion and Management*, *224*. https://doi.org/10.1016/j.enconman.2020.113377

Emrani, A., Berrada, A., Arechkik, A., & Bakhouya, M. (2022). 7. Improved techno-economic optimization of an off-grid hybrid solar/wind/gravity energy storage

system based on performance indicators. *Journal of Energy Storage*, *49*. https://doi.org/10.1016/j.est.2022.104163

Eric Wilde. (2016). *Harvesting wind*. https://www.flickr.com/photos/dret/24110028330/

*EU imports of energy products - recent developments - Statistics Explained*. (2022). https://ec.europa.eu/eurostat/statistics-explained/index.php?title=EU_imports_of_energy_products_-_recent_developments&oldid=564016

FAO. (2017). *The future of food and agriculture-Trends and challenges*.

Fard, H. H., Tooryan, F., Dargahi, V., & Jin, S. (2021). 31. A cost-efficient sizing of grid-tied hybrid renewable energy system with different types of demands. *Sustainable Cities and Society*, *73*. https://doi.org/10.1016/j.scs.2021.103080

Fazelpour, F., Soltani, N., & Rosen, M. A. (2016). 62. Economic analysis of standalone hybrid energy systems for application in Tehran, Iran. *International Journal of Hydrogen Energy*, *41*(19), 7732–7743. https://doi.org/10.1016/j.ijhydene.2016.01.113

Fioriti, D., Pintus, S., Lutzemberger, G., & Poli, D. (2020). 82. Economic multi-objective approach to design off-grid microgrids: A support for business decision making. *Renewable Energy*, *159*, 693–704. https://doi.org/10.1016/j.renene.2020.05.154

Fodhil, F., Hamidat, A., & Nadjemi, O. (2019). 50. Potential, optimization and sensitivity analysis of photovoltaic-diesel-battery hybrid energy system for rural electrification in Algeria. *Energy*, *169*, 613–624. https://doi.org/10.1016/j.energy.2018.12.049

Furubayashi, T. (2022). 1. The role of biomass energy in a 100% renewable energy system for Akita prefecture, Japan. *Energy Storage and Saving*, *1*(3), 148–152. https://doi.org/10.1016/j.enss.2022.04.003

Gantz Andrea. (2022). *Mash or crumbled feed for layers? | WATTPoultry*. https://www.wattagnet.com/articles/18521-mash-or-crumbled-feed-for-layers

García-Ibañez, P., Cabanillas, A., & Sánchez, J. M. (2004). Gasification of leached orujillo (olive oil waste) in a pilot plant circulating fluidised bed reactor. Preliminary results. *Biomass and Bioenergy*, *27*(2), 183–194. https://doi.org/10.1016/j.biombioe.2003.11.007

Gebrehiwot, K., Mondal, M. A. H., Ringler, C., & Gebremeskel, A. G. (2019). 49. Optimization and cost-benefit assessment of hybrid power systems for off-grid rural electrification in Ethiopia. *Energy*, *177*, 234–246. https://doi.org/10.1016/j.energy.2019.04.095

Gómez-Barea, A., Arjona, R., & Ollero, P. (2005). Pilot-plant gasification of olive stone: A technical assessment. *Energy and Fuels*, *19*(2), 598–605. https://doi.org/10.1021/EF0498418/ASSET/IMAGES/LARGE/EF0498418F00010.JPEG

Grande, L. S. A., Yahyaoui, I., & Gómez, S. A. (2018). 53. Energetic, economic and environmental viability of off-grid PV-BESS for charging electric vehicles: Case study of Spain. *Sustainable Cities and Society*, *37*, 519–529. https://doi.org/10.1016/j.scs.2017.12.009

Grogg, K. (2005). *Harvesting the Wind: The Physics of Wind Turbines*. http://digitalcommons.carleton.edu/pacp/7

Guerrero-Lemus, R., & Martinez-Duart, J. M. (2012). *Renewable Energies and CO2*. https://doi.org/10.1007/978-1-4471-4385-7

Güler, Ö., Akdağ, S. A., & Dinçsoy, M. E. (2013). 66. Feasibility analysis of medium-sized hotel's electrical energy consumption with hybrid systems. *Sustainable Cities and Society*, *9*, 15–22. https://doi.org/10.1016/j.scs.2013.02.004

Habib, H. U. R., Wang, S., Elkadeem, M. R., & Elmorshedy, M. F. (2019). 51. Design Optimization and Model Predictive Control of a Standalone Hybrid Renewable Energy System: A Case Study on a Small Residential Load in Pakistan. *IEEE Access*, *7*, 117369–117390. https://doi.org/10.1109/ACCESS.2019.2936789

Hadas, A., & Kautsky, L. (1994). Feather meal, a semi-slow-release nitrogen fertilizer for organic farming. In *Fertilizer Research* (Vol. 38).

Haghighat Mamaghani, A., Avella Escandon, S. A., Najafi, B., Shirazi, A., & Rinaldi, F. (2016). 38. Techno-economic feasibility of photovoltaic, wind, diesel and hybrid electrification systems for off-grid rural electrification in Colombia. *Renewable Energy*, *97*, 293–305. https://doi.org/10.1016/j.renene.2016.05.086

He, W., Tao, L., Han, L., Sun, Y., Campana, E. pietro, & Yan, J. (2021). 87. Optimal analysis of a hybrid renewable power system for a remote island. *Renewable Energy*, *179*, 96–104. https://doi.org/10.1016/j.renene.2021.07.034

Hoseinzadeh, S., & Astiaso Garcia, D. (2022). 18. Techno-economic assessment of hybrid energy flexibility systems for islands' decarbonization: A case study in Italy. *Sustainable Energy Technologies and Assessments*, *51*. https://doi.org/10.1016/j.seta.2021.101929

Hossain, M., Mekhilef, S., & Olatomiwa, L. (2017). 57. Performance evaluation of a stand-alone PV-wind-diesel-battery hybrid system feasible for a large resort center in South China Sea, Malaysia. *Sustainable Cities and Society*, *28*, 358–366. https://doi.org/10.1016/j.scs.2016.10.008

Hossein Jahangir, M., Bazdar, E., & Kargarzadeh, A. (2022). 16. Techno-economic and environmental assessment of low carbon hybrid renewable electric systems for urban energy planning: Tehran-Iran. *City and Environment Interactions*, *16*. https://doi.org/10.1016/j.cacint.2022.100085

*How a battery works - Curious*. (2016). https://www.science.org.au/curious/technology-future/batteries

Hunt, J. D., Zakeri, B., Lopes, R., Barbosa, P. S. F., Nascimento, A., Castro, N. J. de, Brandão, R., Schneider, P. S., & Wada, Y. (2020). Existing and new

arrangements of pumped-hydro storage plants. *Renewable and Sustainable Energy Reviews*, *129*, 109914. https://doi.org/10.1016/J.RSER.2020.109914

hurstboiler.com. (2023). *Industrial Boiler Systems | Hurst Boiler*. https://www.hurstboiler.com/boilers

IEA. (2022). *A 10-Point Plan to Reduce the European Union's Reliance on Russian Natural Gas*. www.iea.org/t&c/

ILSR. (2015). *Net Metering – Institute for Local Self-Reliance*. https://ilsr.org/rule/net-metering/

*Industrial Symbiosis*. (2018).

(IPCC), I. P. on C. C. (2022). Changing Ocean, Marine Ecosystems, and Dependent Communities. In *The Ocean and Cryosphere in a Changing Climate* (pp. 447–588). Cambridge University Press. https://doi.org/10.1017/9781009157964.007

Jahangir, M. H., & Cheraghi, R. (2020). 90. Economic and environmental assessment of solar-wind-biomass hybrid renewable energy system supplying rural settlement load. *Sustainable Energy Technologies and Assessments*, *42*. https://doi.org/10.1016/j.seta.2020.100895

Javed, M. S., Ma, T., Jurasz, J., Canales, F. A., Lin, S., Ahmed, S., & Zhang, Y. (2021). 84. Economic analysis and optimization of a renewable energy based power supply system with different energy storages for a remote island. *Renewable Energy*, *164*, 1376–1394. https://doi.org/10.1016/j.renene.2020.10.063

Jekayinfa, S. O. (2007). *Energetic Analysis of Poultry Processing Operations*. http://ljs.academicdirect.org

Ji, L., Wu, Y., Liu, Y., Sun, L., Xie, Y., & Huang, G. (2022). 11. Optimizing design and performance assessment of a community-scale hybrid power system with distributed renewable energy and flexible demand response. *Sustainable Cities and Society*, *84*. https://doi.org/10.1016/j.scs.2022.104042

Jung, J., & Villaran, M. (2017). 39. Optimal planning and design of hybrid renewable energy systems for microgrids. In *Renewable and Sustainable Energy Reviews* (Vol. 75, pp. 180–191). Elsevier Ltd. https://doi.org/10.1016/j.rser.2016.10.061

Kalinci, Y. (2015). 64. Alternative energy scenarios for Bozcaada island, Turkey. In *Renewable and Sustainable Energy Reviews* (Vol. 45, pp. 468–480). Elsevier Ltd. https://doi.org/10.1016/j.rser.2015.02.001

Kalogirou, S. A., & Tripanagnostopoulos, Y. (2006). Hybrid PV/T solar systems for domestic hot water and electricity production. *Energy Conversion and Management*, *47*(18–19), 3368–3382. https://doi.org/10.1016/J.ENCONMAN.2006.01.012

Kandji, S. T., Verchot, L., & Mackensen, J. (2006). *Climate Change and Variability in the Southern Africa: Impacts and Adaptation Strategies in the Agricultural Sector*. www:http://www.worldagroforestrycentre.orgweb:www.unep.orgwww.unep.org

Karakoulidis, K., Mavridis, K., Bandekas, D. v., Adoniadis, P., Potolias, C., & Vordos, N. (2011). 70. Techno-economic analysis of a stand-alone hybrid photovoltaic-diesel-battery-fuel cell power system. *Renewable Energy*, *36*(8), 2238–2244. https://doi.org/10.1016/j.renene.2010.12.003

Karouzos. (2022). *Ηλεκτροπαραγωγή από Βιομάζα με τεχνολογία αεροποίησης syngas*. https://www.karouzos.gr/index-3-3.php

Karwacka, M., Ciurzyńska, A., Lenart, A., & Janowicz, M. (2020). Sustainable Development in the Agri-Food Sector in Terms of the Carbon Footprint: A Review. *Sustainability 2020, Vol. 12, Page 6463*, *12*(16), 6463. https://doi.org/10.3390/SU12166463

Kaur, H., Gupta, S., & Dhingra, A. (2021). 23. Analysis of hybrid solar biomass power plant for generation of electric power. *Materials Today: Proceedings*, *48*, 1134–1140. https://doi.org/10.1016/j.matpr.2021.08.080

Khan, M. J., Yadav, A. K., & Mathew, L. (2017). 55. Techno economic feasibility analysis of different combinations of PV-Wind-Diesel-Battery hybrid system for telecommunication applications in different cities of Punjab, India. In *Renewable and Sustainable Energy Reviews* (Vol. 76, pp. 577–607). Elsevier Ltd. https://doi.org/10.1016/j.rser.2017.03.076

Khan, T., Yu, M., & Waseem, M. (2022). Review on recent optimization strategies for hybrid renewable energy system with hydrogen technologies: State of the art, trends and future directions. *International Journal of Hydrogen Energy*, *47*(60), 25155–25201. https://doi.org/10.1016/J.IJHYDENE.2022.05.263

Khandelwal, S., Parwez, S., & Mehra, M. (2022). Climate change: effects on health and nutrition. *Reference Module in Food Science*. https://doi.org/10.1016/B978-0-12-821848-8.00131-1

Kim, H., Baek, S., Park, E., & Chang, H. J. (2014). 65. Optimal green energy management in Jeju, South Korea - On-grid and off-grid electrification. *Renewable Energy*, *69*, 123–133. https://doi.org/10.1016/j.renene.2014.03.004

Kirim, Y., Sadikoglu, H., & Melikoglu, M. (2022). 12. Technical and economic analysis of biogas and solar photovoltaic (PV) hybrid renewable energy system for dairy cattle barns. *Renewable Energy*, *188*, 873–889. https://doi.org/10.1016/j.renene.2022.02.082

Kolawole, O. D., Motsholapheko, M. R., Ngwenya, B. N., Thakadu, O., Mmopelwa, G., & Kgathi, D. L. (2016). Climate variability and rural livelihoods: How households perceive and adapt to climatic shocks in the Okavango Delta, Botswana. *Weather, Climate, and Society*, *8*(2), 131–145. https://doi.org/10.1175/WCAS-D-15-0019.1

Kumar, A., Schei, T., Ahenkorah, A., Rodriguez, R. C., Devernay, J.-M., Freitas, M., Hall, D., Killingtveit, Å., Liu, Z., Branche, E., Burkhardt, J., Descloux, S., Heath, G., Seelos, K., Morejon, C. D., & Krug, T. (2011). Hydropower. In *Renewable Energy Sources and Climate Change Mitigation* (pp. 437–496). Cambridge University Press. https://doi.org/10.1017/CBO9781139151153.009

Kumar, R., & Channi, H. K. (2022). 2. A PV-Biomass off-grid hybrid renewable energy system (HRES) for rural electrification: Design, optimization and techno-economic-environmental analysis. *Journal of Cleaner Production*, *349*. https://doi.org/10.1016/j.jclepro.2022.131347

Kumar Singla, M., Nijhawan, P., & Singh Oberoi, A. (2020). *Hydrogen fuel and fuel cell technology for cleaner future: a review*. https://doi.org/10.1007/s11356-020-12231-8/Published

Kusakana, K. (2016). 43. Optimal scheduling for distributed hybrid system with pumped hydro storage. *Energy Conversion and Management*, *111*, 253–260. https://doi.org/10.1016/j.enconman.2015.12.081

Kweku, D., Bismark, O., Maxwell, A., Desmond, K., Danso, K., Oti-Mensah, E., Quachie, A., & Adormaa, B. (2018). Greenhouse Effect: Greenhouse Gases and Their Impact on Global Warming. *Journal of Scientific Research and Reports*, *17*(6), 1–9. https://doi.org/10.9734/jsrr/2017/39630

Kwiatkowski, K., Krzysztoforski, J., Bajer, K., & Dudyński, M. (2012). *Gasification of feathers for energy production-a case study*. https://doi.org/10.5071/20thEUBCE2012-4BV.3.2

Kwiatkowski, K., Krzysztoforski, J., Bajer, K., & Dudyński, M. (2013). Bioenergy from feathers gasification - Efficiency and performance analysis. *Biomass and Bioenergy*, *59*, 402–411. https://doi.org/10.1016/j.biombioe.2013.07.013

Ladha-Sabur, A., Bakalis, S., Fryer, P. J., & Lopez-Quiroga, E. (2019). Mapping energy consumption in food manufacturing. *Trends in Food Science & Technology*, *86*, 270–280. https://doi.org/10.1016/J.TIFS.2019.02.034

Le, T. H., Le, A. T., & Le, H. C. (2021). The historic oil price fluctuation during the Covid-19 pandemic: What are the causes? *Research in International Business and Finance*, *58*, 101489. https://doi.org/10.1016/J.RIBAF.2021.101489

Li, J., Liu, P., & Li, Z. (2020). 76. Optimal design and techno-economic analysis of a solar-wind-biomass off-grid hybrid power system for remote rural electrification: A case study of west China. *Energy*, *208*. https://doi.org/10.1016/j.energy.2020.118387

Li, J., Liu, P., & Li, Z. (2022). 100. Optimal design of a hybrid renewable energy system with grid connection and comparison of techno-economic performances with an off-grid system: A case study of West China. *Computers and Chemical Engineering*, *159*. https://doi.org/10.1016/j.compchemeng.2022.107657

Liu, J., Wang, M., Peng, J., Chen, X., Cao, S., & Yang, H. (2020). 81. Techno-economic design optimization of hybrid renewable energy applications for high-rise residential buildings. *Energy Conversion and Management*, *213*. https://doi.org/10.1016/j.enconman.2020.112868

Luta, D. N., & Raji, A. K. (2018). 47. Decision-making between a grid extension and a rural renewable off-grid system with hydrogen generation. *International Journal of*

*Hydrogen Energy*, *43*(20), 9535–9548. https://doi.org/10.1016/j.ijhydene.2018.04.032

Malik, P., Awasthi, M., & Sinha, S. (2021). 30. Techno-economic and environmental analysis of biomass-based hybrid energy systems: A case study of a Western Himalayan state in India. *Sustainable Energy Technologies and Assessments*, *45*. https://doi.org/10.1016/j.seta.2021.101189

Malik, P., Awasthi, M., & Sinha, S. (2022). 5. A techno-economic investigation of grid integrated hybrid renewable energy systems. *Sustainable Energy Technologies and Assessments*, *51*. https://doi.org/10.1016/j.seta.2022.101976

Mccracken, K. J. (2002). *Effects of physical processing on the nutritive value of poultry diets*.

messinialive.gr. (2019). *ΚΛΗΜΗΣ: Ευρωπαϊκό Παράδειγμα Κυκλικής Οικονομίας! - Messinia Live*. https://www.messinialive.gr/klimis-evropaiko-paradeigma-kyklikis-oikonomias/

*Methane emissions*. (2022). https://energy.ec.europa.eu/topics/oil-gas-and-coal/methane-emissions_en

Mézes, L., & Tamás, J. (2015). Feather Waste Recycling for Biogas Production. *Waste and Biomass Valorization*, *6*. https://doi.org/10.1007/s12649-015-9427-7

*Mitigation of Climate Change Climate Change 2022 Working Group III contribution to the Sixth Assessment Report of the Intergovernmental Panel on Climate Change*. (2022). https://www.ipcc.ch/site/assets/uploads/2018/05/uncertainty-guidance-note.pdf.

Mokhtara, C., Negrou, B., Settou, N., Settou, B., & Samy, M. M. (2021). 88. Design optimization of off-grid Hybrid Renewable Energy Systems considering the effects of building energy performance and climate change: Case study of Algeria. *Energy*, *219*. https://doi.org/10.1016/j.energy.2020.119605

Molyneaux, L., Wagner, L., & Foster, J. (2016). 37. Rural electrification in India: Galilee Basin coal versus decentralised renewable energy micro grids. *Renewable Energy*, *89*, 422–436. https://doi.org/10.1016/j.renene.2015.12.002

*Most efficient solar panels 2022 — Clean Energy Reviews*. (2022). https://www.cleanenergyreviews.info/blog/most-efficient-solar-panels

Murugaperumal, K., Srinivasn, S., & Satya Prasad, G. R. K. D. (2020). 91. Optimum design of hybrid renewable energy system through load forecasting and different operating strategies for rural electrification. *Sustainable Energy Technologies and Assessments*, *37*. https://doi.org/10.1016/j.seta.2019.100613

Nasser, M., Megahed, T. F., Ookawara, S., & Hassan, H. (2022). 20. Techno-economic assessment of clean hydrogen production and storage using hybrid renewable energy system of PV/Wind under different climatic conditions. *Sustainable Energy Technologies and Assessments*, *52*. https://doi.org/10.1016/j.seta.2022.102195

Odou, O. D. T., Bhandari, R., & Adamou, R. (2020). 48. Hybrid off-grid renewable power system for sustainable rural electrification in Benin. *Renewable Energy*, *145*, 1266–1279. https://doi.org/10.1016/j.renene.2019.06.032

Padrón, I., Avila, D., Marichal, G. N., & Rodríguez, J. A. (2019). 79. Assessment of Hybrid Renewable Energy Systems to supplied energy to Autonomous Desalination Systems in two islands of the Canary Archipelago. *Renewable and Sustainable Energy Reviews*, *101*, 221–230. https://doi.org/10.1016/j.rser.2018.11.009

Panos, E., Densing, M., & Volkart, K. (2022). Energy. *Our World in Data*, *9*, 28–49. https://doi.org/10.1016/j.esr.2015.11.003

Park, E., & Kwon, S. J. (2016). 61. Towards a Sustainable Island: Independent optimal renewable power generation systems at Gadeokdo Island in South Korea. *Sustainable Cities and Society*, *23*, 114–118. https://doi.org/10.1016/j.scs.2016.02.017

Patel, A. M., & Singal, S. K. (2016). *41. LCC Analysis for Economic Feasibility of Rural Electrification by Hybrid Energy Systems*. www.sciencedirect.comwww.materialstoday.com/proceedings2214-7853

Pathumnakul, S., & Piewthongngam, K. (2010). How soaring agricultural prices will impact the way we do feed business. *Revista Brasileira De Zootecnia-Brazilian Journal of Animal Science - REV BRAS ZOOTECN*, *39*. https://doi.org/10.1590/S1516-35982010001300053

Peláez-Peláez, S., Colmenar-Santos, A., Pérez-Molina, C., Rosales, A. E., & Rosales-Asensio, E. (2021). 73. Techno-economic analysis of a heat and power combination system based on hybrid photovoltaic-fuel cell systems using hydrogen as an energy vector. *Energy*, *224*. https://doi.org/10.1016/j.energy.2021.120110

pelletizermill.com. (2023). *How To Mix Chicken Feed : 4 Best Chicken Feed Ingredients*. https://www.pelletizermill.com/blog/how-to-mix-chicken-feed-for-layers/

Poore, J., & Nemecek, T. (2018). Reducing food's environmental impacts through producers and consumers. *Science*, *360*(6392), 987–992. https://doi.org/10.1126/SCIENCE.AAQ0216/SUPPL_FILE/AAQ0216_DATAS2.XLS

Poullikkas, A., Kourtis, G., & Hadjipaschalis, I. (2013). A review of net metering mechanism for electricity renewable energy sources. In *Journal homepage: www.IJEE.IEEFoundation.org ISSN* (Vol. 4, Issue 6). Online. www.IJEE.IEEFoundation.org

*POWER | Data Access Viewer*. (2022). https://power.larc.nasa.gov/data-access-viewer/

Pye, S., Dobbins, A., Baffert, C., Brajković, J., Deane, P., & de Miglio, R. (2017). Energy Poverty Across the EU: Analysis of Policies and Measures. *Europe's*

*Energy Transition: Insights for Policy Making*, 261–280. https://doi.org/10.1016/B978-0-12-809806-6.00030-4

Qiblawey, Y., Alassi, A., Zain ul Abideen, M., & Bañales, S. (2022). 19. Techno-economic assessment of increasing the renewable energy supply in the Canary Islands: The case of Tenerife and Gran Canaria. *Energy Policy*, *162*. https://doi.org/10.1016/j.enpol.2022.112791

Rajbongshi, R., Borgohain, D., & Mahapatra, S. (2017). 40. Optimization of PV-biomass-diesel and grid base hybrid energy systems for rural electrification by using HOMER. *Energy*, *126*, 461–474. https://doi.org/10.1016/j.energy.2017.03.056

Ramírez, C. A., Patel, M., & Blok, K. (2006). How much energy to process one pound of meat? A comparison of energy use and specific energy consumption in the meat industry of four European countries. *Energy*, *31*(12), 2047–2063. https://doi.org/10.1016/J.ENERGY.2005.08.007

Rapa, M., Gobbi, L., & Ruggieri, R. (2020). Environmental and Economic Sustainability of Electric Vehicles: Life Cycle Assessment and Life Cycle Costing Evaluation of Electricity Sources. *Energies 2020, Vol. 13, Page 6292*, *13*(23), 6292. https://doi.org/10.3390/EN13236292

Rasool, M. H., Perwez, U., Qadir, Z., & Ali, S. M. H. (2022). 98. Scenario-based techno-reliability optimization of an off-grid hybrid renewable energy system: A multi-city study framework. *Sustainable Energy Technologies and Assessments*, *53*. https://doi.org/10.1016/j.seta.2022.102411

Renewable Energy Agency, I. (2012). *RENEWABLE ENERGY TECHNOLOGIES: COST ANALYSIS SERIES Volume 1: Power Sector Acknowledgement*. www.irena.org/Publications

Renewable Energy Agency, I. (2022). *RENEWABLE ENERGY STATISTICS 2022 STATISTIQUES D'ÉNERGIE RENOUVELABLE 2022 ESTADÍSTICAS DE ENERGÍA RENOVABLE 2022 About IRENA*. www.irena.org

Rezk, H., Abdelkareem, M. A., & Ghenai, C. (2019). 92. Performance evaluation and optimal design of stand-alone solar PV-battery system for irrigation in isolated regions: A case study in Al Minya (Egypt). *Sustainable Energy Technologies and Assessments*, *36*. https://doi.org/10.1016/j.seta.2019.100556

Ribó-Pérez, D., Herraiz-Cañete, Á., Alfonso-Solar, D., Vargas-Salgado, C., & Gómez-Navarro, T. (2021). 27. Modelling biomass gasifiers in hybrid renewable energy microgrids; a complete procedure for enabling gasifiers simulation in HOMER. *Renewable Energy*, *174*, 501–512. https://doi.org/10.1016/j.renene.2021.04.083

Roy, D., Hassan, R., & Das, B. K. (2022). 4. A hybrid renewable-based solution to electricity and freshwater problems in the off-grid Sundarbans region of India: Optimum sizing and socio-enviro-economic evaluation. *Journal of Cleaner Production*, *372*. https://doi.org/10.1016/j.jclepro.2022.133761

Salameh, T., Abdelkareem, M. A., Olabi, A. G., Sayed, E. T., Al-Chaderchi, M., & Rezk, H. (2021). 74. Integrated standalone hybrid solar PV, fuel cell and diesel generator power system for battery or supercapacitor storage systems in Khorfakkan, United Arab Emirates. *International Journal of Hydrogen Energy*, *46*(8), 6014–6027. https://doi.org/10.1016/j.ijhydene.2020.08.153

schmid-energy.ch. (2023). *Industrial Systems / Underfeed stoker firing system UTSK*. https://www.schmid-energy.ch/inhalt.aspx?groupnr=2794&nid=2794&lang=en

Seedahmed, M. M. A., Ramli, M. A. M., Bouchekara, H. R. E. H., Shahriar, M. S., Milyani, A. H., & Rawa, M. (2022). 3. A techno-economic analysis of a hybrid energy system for the electrification of a remote cluster in western Saudi Arabia. *Alexandria Engineering Journal*, *61*(7), 5183–5202. https://doi.org/10.1016/j.aej.2021.10.041

Shboul, B., AL-Arfi, I., Michailos, S., Ingham, D., AL-Zoubi, O. H., Ma, L., Hughes, K., & Pourkashanian, M. (2021). 35. Design and Techno-economic assessment of a new hybrid system of a solar dish Stirling engine instegrated with a horizontal axis wind turbine for microgrid power generation. *Energy Conversion and Management*, *245*. https://doi.org/10.1016/j.enconman.2021.114587

Shezan, S. A., Ishraque, M. F., Muyeen, S. M., Abu-Siada, A., Saidur, R., Ali, M. M., & Rashid, M. M. (2022). 13. Selection of the best dispatch strategy considering techno-economic and system stability analysis with optimal sizing. *Energy Strategy Reviews*, *43*. https://doi.org/10.1016/j.esr.2022.100923

Sifakis, N., Konidakis, S., & Tsoutsos, T. (2021). 26. Hybrid renewable energy system optimum design and smart dispatch for nearly Zero Energy Ports. *Journal of Cleaner Production*, *310*. https://doi.org/10.1016/j.jclepro.2021.127397

Silva, S. B., Severino, M. M., & de Oliveira, M. A. G. (2013). 68. A stand-alone hybrid photovoltaic, fuel cell and battery system: A case study of Tocantins, Brazil. *Renewable Energy*, *57*, 384–389. https://doi.org/10.1016/j.renene.2013.02.004

Singh, A., Baredar, P., & Gupta, B. (2017). 59. Techno-economic feasibility analysis of hydrogen fuel cell and solar photovoltaic hybrid renewable energy system for academic research building. *Energy Conversion and Management*, *145*, 398–414. https://doi.org/10.1016/j.enconman.2017.05.014

Singh, A., & Basak, P. (2021). 34. Conceptualization and techno-economic evaluation of microgrid based on PV/Biomass in Indian scenario. *Journal of Cleaner Production*, *317*. https://doi.org/10.1016/j.jclepro.2021.128378

Singh Brar, J., Singh, K., Zondlo, J., & Wang, J. (2013). Co-Gasification of Coal and Hardwood Pellets: A Case Study. *American Journal of Biomass and Bioenergy*, *2*(1), 25–40. https://doi.org/10.7726/ajbb.2013.1005

Sowah, A. N. A., Owusu, K., Yankson, P. W. K., & Quansah, E. (2020). Effects of socio-cultural norms on smallholder adaptation to climate change in Nkoranza South municipality, Ghana. *Https://Doi.Org/10.1080/09614524.2020.1829550*, *31*(2), 161–173. https://doi.org/10.1080/09614524.2020.1829550

Steffen, B., Beuse, M., Tautorat, P., & Schmidt, T. S. (2020). Experience Curves for Operations and Maintenance Costs of Renewable Energy Technologies. *Joule*, *4*(2), 359–375. https://doi.org/10.1016/J.JOULE.2019.11.012

Taghizadeh-Hesary, F., Rasoulinezhad, E., & Yoshino, N. (2019). Energy and Food Security: Linkages through Price Volatility. *Energy Policy*, *128*, 796–806. https://doi.org/10.1016/J.ENPOL.2018.12.043

*Technical directive 20701–1: National Specifications of Parameters for Calculating the Energy Performance of Buildings and the Issue of the Energy Performance Certificate*, (2017) (testimony of Technical Chamber of Greece).

*Technology | Highview Power*. (2022). https://highviewpower.com/technology/

*THE 17 GOALS | Sustainable Development*. (n.d.). Retrieved November 2, 2022, from https://sdgs.un.org/goals

Tiwary, A., Spasova, S., & Williams, I. D. (2019). 83. A community-scale hybrid energy system integrating biomass for localised solid waste and renewable energy solution: Evaluations in UK and Bulgaria. *Renewable Energy*, *139*, 960–967. https://doi.org/10.1016/j.renene.2019.02.129

*Too Much Oil: How a Barrel Came to Be Worth Less Than Nothing - The New York Times*. (2020). https://www.nytimes.com/2020/04/20/business/oil-prices.html

Tremeac, B., & Meunier, F. (2009). Life cycle analysis of 4.5 MW and 250 W wind turbines. *Renewable and Sustainable Energy Reviews*, *13*(8), 2104–2110. https://doi.org/10.1016/J.RSER.2009.01.001

Türkay, B. E., & Telli, A. Y. (2011). 71. Economic analysis of standalone and grid connected hybrid energy systems. *Renewable Energy*, *36*(7), 1931–1943. https://doi.org/10.1016/j.renene.2010.12.007

*Use of hydrogen - U.S. Energy Information Administration (EIA)*. (2022). https://www.eia.gov/energyexplained/hydrogen/use-of-hydrogen.php

Usman, M. R. (2022). Hydrogen storage methods: Review and current status. In *Renewable and Sustainable Energy Reviews* (Vol. 167). Elsevier Ltd. https://doi.org/10.1016/j.rser.2022.112743

Uzun Ozsahin, Hüseyin Gökçekuş, Berna Uzun, & James LaMoreaux. (2021). *Professional Practice in Earth Sciences Application of Multi-Criteria Decision Analysis in Environmental and Civil Engineering*. http://www.springer.com/series/11926

Wang, F., Xu, J., Liu, L., Yin, G., Wang, J., & Yan, J. (2021). 25. Optimal design and operation of hybrid renewable energy system for drinking water treatment. *Energy*, *219*. https://doi.org/10.1016/j.energy.2020.119673

*What Is a Solar Tracker and Is It Worth the Investment?* (2022). https://www.solarreviews.com/blog/are-solar-axis-trackers-worth-the-additional-investment

Wongngam, W., Mitani, T., Katayama, S., Nakamura, S., & Yongsawatdigul, J. (2020). Production and characterization of chicken blood hydrolysate with antihypertensive properties. *Poultry Science*, *99*(10), 5163–5174. https://doi.org/10.1016/J.PSJ.2020.07.006

World Bank. (2021). *Concentrating Solar Power: Clean Power on Demand 24/7.* www.worldbank.org

*World Energy Outlook 2022 – Analysis - IEA*. (2022). https://www.iea.org/reports/world-energy-outlook-2022

*World Market for Wind Power Saw Another Record Year in 2021: 97,3 Gigawatt of New Capacity Added - World Wind Energy Association*. (2022). https://wwindea.org/world-market-for-wind-power-saw-another-record-year-in-2021-973-gigawatt-of-new-capacity-added/

Wu, B., Maleki, A., Pourfayaz, F., & Rosen, M. A. (2018). 80. Optimal design of stand-alone reverse osmosis desalination driven by a photovoltaic and diesel generator hybrid system. *Solar Energy*, *163*, 91–103. https://doi.org/10.1016/j.solener.2018.01.016

Xu, C., Ke, Y., Li, Y., Chu, H., & Wu, Y. (2020). 72. Data-driven configuration optimization of an off-grid wind/PV/hydrogen system based on modified NSGA-II and CRITIC-TOPSIS. *Energy Conversion and Management*, *215*. https://doi.org/10.1016/j.enconman.2020.112892

Xu, T., & Flapper, J. (2011). Reduce energy use and greenhouse gas emissions from global dairy processing facilities. *Energy Policy*, *39*(1), 234–247. https://doi.org/10.1016/J.ENPOL.2010.09.037

Xu, Z., Chau, S. N., Chen, X., Zhang, J., Li, Y., Dietz, T., Wang, J., Winkler, J. A., Fan, F., Huang, B., Li, S., Wu, S., Herzberger, A., Tang, Y., Hong, D., Li, Y., & Liu, J. (2020). Assessing progress towards sustainable development over space and time. *Nature*, *577*(7788), 74–78. https://doi.org/10.1038/s41586-019-1846-3

Yang, J., Yang, Z., & Duan, Y. (2022). 99. Capacity optimization and feasibility assessment of solar-wind hybrid renewable energy systems in China. *Journal of Cleaner Production*, *368*. https://doi.org/10.1016/j.jclepro.2022.133139

Yanık, D. K. (2017). Alternative to traditional olive pomace oil extraction systems: Microwave-assisted solvent extraction of oil from wet olive pomace. *LWT*, *77*, 45–51. https://doi.org/10.1016/J.LWT.2016.11.020